Universidade Nova de Lisboa

Instituto de Higiene e Medicina Tropical

Trypanosoma brucei peptidase inhibitors.

Immunolocalization, secretion and potential use as targets for therapy

Raquel de Sá da Silva Laires

DISSERTAÇÃO PARA A OBTENÇÃO DO GRAU DE DOUTOR EM CIÊNCIAS BIOMÉDICAS,
ESPECIALIDADE DE BIOLOGIA CELULAR E MOLECULAR

(JULHO, 2012)

Universidade Nova de Lisboa

Insituto de Higiene e Medicina Tropical

Thesis: *Trypanosoma brucei* peptidase inhibitors. Immunolocalization, secretion and potential use as targets for therapy

Author: Raquel de Sá da Silva Laires

Supervisor: Doctor Carlos Novo, IHMT, UNL

Co-supervisor: Professor Jeremy C. Mottram, (University of Glasgow)

Tutorial Committee:

Doctor Carlos Novo (IHMT, UNL)
Doctor Luís Távora Tavira (IHMT, UNL)
Professor Jorge Atouguia (IHMT, UNL)

Dissertation presented to obtain a PhD degree in Biomedical Sciences, speciality Celular and Molecular Biology and was supervised by Doctor Carlos Novo, Professor Jeremy C. Mottram and Doctor Luís Távora Tavira. Financial support was provided by Fundação para a Ciência e Tecnologia (FCT) with a PhD fellowship grant (SFRH/BD/32110/2006) under POCI 2010 program.

Universidade Nova de Lisboa

Insituto de Higiene e Medicina Tropical

Título da Tese: Inibidores de peptidases de *Trypanosoma brucei*. Imunolocalização, secreção e potencial uso como alvo terapêutico

Autor: Raquel de Sá da Silva Laires

Orientador: Investigador Doutor Carlos Novo, IHMT, UNL

Co orientador: Professor Doutor Jeremy C. Mottram, (Universidade de Glasgow)

Comissão Tutorial:

Investigador Doutor Carlos Novo (IHMT, UNL)
Investigador Doutor Luís Távora Tavira (IHMT, UNL)
Professor Doutor Jorge Atouguia (IHMT, UNL)

Dissertação apresentada para cumprimento dos requisitos necessários à obtenção do grau de Doutor em Ciências Biomédicas, Especialidade de Biologia Celular e Molecular, realizada sob a orientação científica do Investigador Doutor Carlos Novo, do Professor Doutor Jeremy C. Mottram e do Investigador Doutor Luís Távora Tavira.

Apoio financeiro da FCT com a bolsa de doutoramento SFRH/BD/32110/2006 ao abrigo do Programa Operacional Ciência e Inovação 2010 (POCI 2010) do III Quadro Comunitário de Apoio (2000-2006)

Dedico esta tese,

Ao meu pai e à minha mãe que sempre me encorajaram a ir mais longe
Ao Zé que esteve sempre ao meu lado nesta longa caminhada
Ao Henrique, a luz dos meus olhos, por quem eu aspiro sempre mais

"Há um tempo em que é preciso abandonar as roupas usadas, que já tem a forma do nosso corpo, e esquecer os nossos caminhos, que nos levam sempre aos mesmos lugares. É o tempo da travessia: e, se não ousarmos fazê-la, teremos ficado, para sempre, à margem de nós mesmos."

Fernando Pessoa (1888-1935)

Para o meu filho Henrique uma importante lição,
To my son Henrique, a valuable lesson,

"Sejam quais forem os resultados, com êxito ou não, o importante é que no final cada um possa dizer: 'fiz o que pude'"

"Whether our efforts are, or not, favored by life, let us be able to say, when we come near the great goal, 'I have done what I could'"

Louis Pasteur (1822-1895)

Acknowledgements

This journey wouldn't be possible without the support, scientific or moral, from several people to whom I am truly grateful.

To begin with, I would like to thank my supervisor, Dr. Carlos Novo for his constant support, guidance and friendship that made it easier to overcome all the obstacles inherent to such journey and added so much to my experience over the past 5 years.

I would also like to thank my co-supervisor, Prof. Jeremy C. Mottram for the opportunity to work in his lab in Glasgow and whose guidance and scientific support were valuable assets to my thesis.

Working in the "Mottram Lab" was definitely an amazing experience and I would like to express my gratitude to all the people that welcomed me and contributed for the success of my "Glasgow experience", not only with scientific help but also with their friendship. Particularly, I would like to thank Elaine, Will, Daniela, Jim Scott, Nathaniel, Elmarie, Esther, Herbert, Tatiana, Alana and also Corinna, Tansy, Sophie and Glynn from the Hammarton group. It has been a pleasure to meet you all and I will sure be missing you.

To all the people that worked with me in the former UTPAM, Tiago, Bé, Sofia, Ângela, Maria, Ana Maria, Ana Domingos, Fernando; and the ones I met more recently in IHMT, Cátia, Pedro, Ana, Tiago, Isabel, Idalécia and so many others; thank you for all the support. You were all very important to the success of my PhD.

To my dear friend Rubina, a special thanks. You are partially responsible for my PhD. If it wasn't for I wouldn't have met all the people mentioned above. Thank you for being there for me, for your friendship and for caring.

Another special thanks to Sandra: for the companionship, for the rides home, for the pregnancy experience that we shared together and for being such an angel. You are a very special friend.

Finally thanks to my “Maria” Cristina. She was my lab colleague, my roommate, my friend, my support when I was feeling down, my “clown” when I needed a laughter, my “sister” when we were away. Our times in Glasgow will never be forgotten and the Welcome Centre will never be the same!!!!

Gostava de agradecer a todos os meus amigos fora da esfera laboratorial. Não vou mencionar nomes porque são tantas as pessoas que corria o risco de me esquecer de alguém. Neste aspecto sou uma mulher rica, rica em boas amizades de pessoas que me acompanham há anos e sabem a luta que tem sido este meu percurso. Todos foram determinantes para o meu sucesso, cada um à sua maneira e a todos, um muito obrigado.

À minha irmã Claúdia e aos meus sobrinhos Andreia e Rodrigo que me acompanham sempre e que são para mim um motivo de orgulho. Obrigado por todo o amor e carinho!

Aos meus pais que sempre me encorajaram a seguir este caminho; que me apoiaram em todas as decisões; que me estimularam para ir sempre mais além; que me educaram para ser uma pessoa responsável e com valores; que fizeram de mim a pessoa que sou hoje e que desejo ser sempre!

Finalmente, agradeço ao meu marido, meu namorado e amigo de longa data, Zé. Com ele eu partilhei a desilusão de não entrar para o curso que inicialmente pretendia, com ele brindei ao sucesso da conclusão da licenciatura, com ele sofri a saudade pela distância que nos separou quando o doutoramento me levou para Glasgow, com ele fui feliz no dia 21 de junho de 2008 e ainda mais feliz no dia 14 de dezembro de 2010 quando o nosso filho tão desejado veio a este mundo, com ele brindo agora ao sucesso da conclusão do doutoramento. A ele agradeço a eterna paciência, o companheirismo, o amor e a amizade que ao longo destes 16 anos têm feito de mim uma mulher plena de felicidade.

Abstract

***Trypanosoma brucei* peptidase inhibitors. Immunolocalization, secretion and potential use as targets for therapy**

Raquel de Sá da Silva Laires

Keywords: *Trypanosoma brucei*, ISP1, ISP2, flagellum, flagellar pocket, endocytosis, host-parasite interactions, monoclonal antibodies.

Peptidases are involved in several biological functions playing an important role in the pathogenicity of many parasitic infections. In mammals, one way in which the activity of these peptidases is controlled is by interaction with natural inhibitors, such as cystatins and serpins. In trypanosomatids, the genes encoding for endogenous inhibitors homologous to mammalian cystatins and serpins, are absent. Ecotin is an *Escherichia coli* protein capable of inhibiting a wide range of serine peptidases from S1A family such as trypsin. Ecotin orthologues can be found in a restricted range of bacterial pathogens and also in trypanosomatid parasitic protozoa. In *Trypanosoma brucei* two proteins of 19.7 kDa and 17.8 kDa were identified as ecotin-like inhibitors and given the generic name of Inhibitors of Serine Peptidases (ISP). The absence of peptidases predicted to be sensitive to the action of ISPs in *T. brucei* suggests that these inhibitors are targeting the host's serine peptidases, although their exact biological role was unknown. *T. brucei* mutant cell lines deficient in ISP1 (Δ*isp1*), ISP2 (Δ*isp2*) and both ISPs (Δ*isp1/2*) were successfully generated by targeted gene disruption. This was confirmed using monoclonal antibodies generated specifically against ISP1 and ISP2 that recognize the target protein in wild type and re-expressor cell lysates but not in the respective mutant cell line. The effect of ISP deletion in the parasites was determined both in culture and in mice *in vivo*. The deletion of *ISP* genes individually was shown to have no effect on the parasites *in vitro* or *in vivo*. However, different results were obtained for the simultaneous deletion of *ISP1* and *ISP2*. Although Δ*isp1/2* parasites have normal growth and morphology in culture, they exhibit a motility defect and are characterized by the accumulation of small vesicles outside the flagellar pocket consistent with an endocytosis/exocytosis defect. Furthermore, immunofluorescence shows that both ISPs are localized in the cytosol and in small punctuated structures near the flagellar pocket region. These data suggests that ISPs have an intracellular function independent of their inhibitory activity and probably associated with the flagellar pocket. The biological role of ISP1 and ISP2 in the host-parasite interaction was also evaluated by infecting mice with Δ*isp1/2* parasites. Parasitemia monitoring shows that the deletion of both *ISPs* results in prolonged host survival with reduced or undetectable parasite loads, suggesting an important role for these inhibitors in the parasite's survival. In contrast with recent findings of ISPs function in *Leishmania*, that assigns different biological roles to ISP1 and ISP2, the present study reveals some functional redundancy of ISPs in *T. brucei*, with both inhibitors being required for the parasite to infect the mammalian host efficiently. Finally, immuno-protection studies were made, to assess the potential of ISPs as targets for therapy. Immunization with recombinant ISPs and treatment with antibodies specific against ISP1 and ISP2 had no protective or neutralizing effect on *T. brucei* infected mice, revealing that these inhibitors are poor candidates for an anti-disease vaccine or for antibody-based therapy.

Resumo

Inibidores de peptidases de *Trypanosoma brucei*. Imunolocalização, secreção e potencial uso como alvo terapêutico

Raquel de Sá da Silva Laires

Palavras-chave: *Trypanosoma brucei*, ISP1, ISP2, flagelo, bolsa flagelar, endocitose, interacções parasita-hospedeiro, anticorpos monoclonais.

As peptidases encontram-se envolvidas em diversas funções biológicas possuindo um papel importante na patogenicidade de várias infecções parasitárias. Em mamíferos, a actividade peptidica é controlada por inibidores endógenos, como as cistatinas e as serpinas. Os genes que codificam para inibidores homólogos às cistatinas e serpinas de mamíferos, encontram-se ausentes do genoma de tripanossomatídeos. A ecotina é uma proteína de *Escherichia coli*, capaz de inibir uma grande variedade de peptidases serínicas da família S1A, tais como a tripsina. Existem duas proteínas do tipo da ecotina em *T. brucei*, ISP1 e ISP2. A ausência de peptidases sensíveis à acção dos ISPs no genoma de *Trypanosoma brucei*, sugere que estes tenham como alvo as peptidases serínicas do hospedeiro. Linhas celulares de *T. brucei* deficientes em ISP1 (*Δisp1*), ISP2 (*Δisp2*) e em ambos os ISPs (Δ*isp1/2*) foram produzidas com sucesso e a ausência dos inibidores comprovada com o uso de anticorpos monoclonais específicos contra o ISP1 e o ISP2, que reconhecem a proteina alvo em extractos de proteína total de parasitas selvagens mas não em extractos de parasitas mutantes. O efeito da ausência dos ISPs nas células foi avaliado *in vitro* e *in vivo*, verificando-se que a delecção individual de cada ISP não produz qualquer efeito nos parasitas que revelam um crescimento normal em cultura e padrões de infectividade em murganhos idênticos aos de parasitas selvagens. Em contraste, os parasitas Δ*isp1/2*, embora possuam um crescimento normal *in vitro* com ausência de alterações morfológicas grosseiras, são caracterizados por um alteração na mobilidade e pela acumulação de micro-vesiculas na região da bolsa flagelar, consistente com um defeito no processo de endocitose/exocitose. Adicionalmente, por imunofluorescência foi possível localizar os ISPs no citoplasma e na perto da bolsa flagelar. Em conjunto, estes dados sugerem uma função intracelular, independente da actividade inibitória dos ISPs e provavelmente associada ao flagelo ou à bolsa flagelar. O papel biológico dos ISPs na interação parasita-hospedeiro foi também avaliada através da infecção de murganhos com os parasitas Δ*isp1/2*.A monitorização da infecção demonstrou que a deleção de ambos os inibidores resulta em sobrevivência prolongada dos murganhos com cargas parasitárias reduzidas, sugerindo que os ISPs possuem um papel importante na sobrevivência do parasita. Em contraste com os resultados obtidos em *Leishmania* que atribuem diferentes funções a ISP1 e ISP2, este estudo sugere que existe uma redundância funcional dos mesmos em *T. brucei*, sendo necessária a presença de ambos para que o parasita estabeleça eficientemente a infecção no hospedeiro mamifero. Foram também realizados estudos de imuno-protecção em murganhos de modo a determinar o potencial dos ISPs como alvos terapêuticos. A imunização com ISP recombinante e o tratamento com anticorpos específicos contra ISP1 e ISP2 não produzem qualquer efeito protector ou neutralizante da infecção de murganhos, sugerindo que estes inibidores não constituem bons candidatos para o desenvolvimento de uma vacina ou terapia baseada em anticorpos.

Abbreviations

Amp	Ampicillin
AP	Alkaline phosphatase
Asp	Aspartic acid
bp	Base pair
BSA	Bovine serum albumin
BSD	Blasticidin
BSF	Bloodstream form
CATT	Card agglutination test for trypanosomiasis
CDKs	Cyclin-dependent kinases
CIP	Calf intestinal alkaline phosphatase
CP	Cysteine peptidase
CR3	Complement type-3 receptor
DABCO	4-diazabicyclo[2.2.2]octane
DAPI	4,6-diamidino-2-phenylindole
DMEM	Dulbecco's Modified Eagle Medium
DMSO	Dimethyl sulfoxide
DNA	Deoxyribonucleic acid
DTT	Dithiothreitol
EDTA	Ethylene diamine tetra acetic acid
ELISA	Fnzyme-linked immunoabsorbent assay
FAZ	flagellum attachment zone
FBS	Fetal bovine serum
FC	flagella connector
FCS	Fetal calf serum
GPI	Glycosylphosphatidylinositol
GST	Glutathione *S*-transferase
HAT	Hypoxanthine-aminopterin-thymidine
HGPRT	Hypoxanthineguanidinephosphoribosyltransferase
His	Histidine
HRP	Horseradish peroxidase

HT	Hipozanthine-thymidine
HYG	Hygromycin B
ICP	Inhibitor of cysteine peptidase
IFA	Indirect immunofluorescence antibody
IFT	Intraflagellar transport
IPTG	Isopropyl-β-D-thiogalactopyranoside
ISP1	Inhibitor of serine peptidase 1
ISP2	Inhibitor of serine peptidase 2
K	Kinetoplast
Kan	Kanamycin
Kb	Kilo base
kDa	Kilo Dalton
kDNA	Kinetoplastid DNA
LB	Luria bertani
μ	Micro
m	Milli
M	Molar
MAb's	Monoclonal antibodies
MBP	Maltose binding protein
N	Nucleus
NE	Neutrophil elastase
NEO	Neomycin
NETs	Neutrophil Extracellular Trap
OD	Optical density
OH	Hydroxyl
OPB	Oligopeptidase B
ORF	Open reading frame
PAC	Puromycin
PBS	Phosphate buffered saline
PCF	Procyclic form
PCR	Polymerase chain reaction
PEG	Polyethylene glycol
PFR	Paraflagellar rod

PHLEO	Phleomycin
POP	Prolyl oligopeptidase
RNA	Ribonucleic acid
RNAi	Ribonucleic acid interference
SDS-PAGE	sodium dodecyl sulphate polyacrylamide gel electrophoresis
SEM	Scanning electron microscopy
Ser	Serine
SH	Sulphydryl
SPF	Specific pathogen free
T	Threonine
TBS	Tris buffered saline
TTBS	Tween Tris buffered saline
TLR4	Toll like receptor 4
UTR	Untranslated region
UV	Ultra violet
V	Volts
VSG	Variant surface glycoproteins
v/v	Volume to volume
w/v	Weight to volume
WHO	World Health Organization

Table of Contents

Index of Figures

Index of Tables

Chapter 1

Introduction

1.1 Human African Trypanosomiasis

1.1.1 Epidemiology

African trypanosomiasis is a family of parasitic diseases affecting both humans and animals. It is caused by a flagellated protozoan parasite of the genus *Trypanosoma* that lives and multiplies extracellularly in the blood and tissue fluid of its mammalian hosts. The parasite is transmitted by the blood feeding tsetse fly (*Glossina sp*.) and the geographical distribution of trypanosomiasis in Africa is directly linked to the vector's suitable habitat, comprising a total of 10 million km^2 of territory, between latitude 14° North and 29° South, from the southern edge of the Sahara and the north of Kalahari deserts, one third of Africa's landscape (Brun *et al*., 2010, Barrett *et al*., 2003).

Trypanosoma brucei is divided in 3 subspecies, *T. brucei gambiense* and *T. brucei rhodesiense* causing the human form of the disease in West and East Africa, respectively and *T. brucei brucei* that, along with *T. congolense*, *T. evansi* and *T. vivax*, causes the animal form of African trypanosomiasis, also known as Nagana, a Zulu word meaning powerless/useless. Although these parasites cause relatively mild infections in wild animals, they cause a more severe form of the disease, often fatal in domestic animals. The symptoms begin with fever, eye discharge, oedema and anaemia and as the illness progresses, animals became more and more weak until paralysis and death eventually occur (Brun *et al*., 2010).

Domestic and wild animals can also be infected by *T. brucei gambiense* and *T. brucei rhodesiense.* Animals do not develop the disease when infected with these trypanosome species but they have a major epidemiological importance, acting as carriers or reservoirs of the infection (Figure 1.1).

T. brucei rhodesiense infection, which is a zoonosis, is usually transmitted from animals to man, with livestock and game animals (mainly antelopes) being the primary reservoir. *T. brucei gambiense* infection, which is considered an anthroponotic infection, is mainly transmitted from man to man and the reservoir is almost exclusively the human. Pigs and some wild animals can act as second reservoir and occasionally

transmission can occur directly from animals to humans, which is believed to be one of the causes of the long term maintenance of the disease in endemic areas (Malvy and Chappuis, 2011).

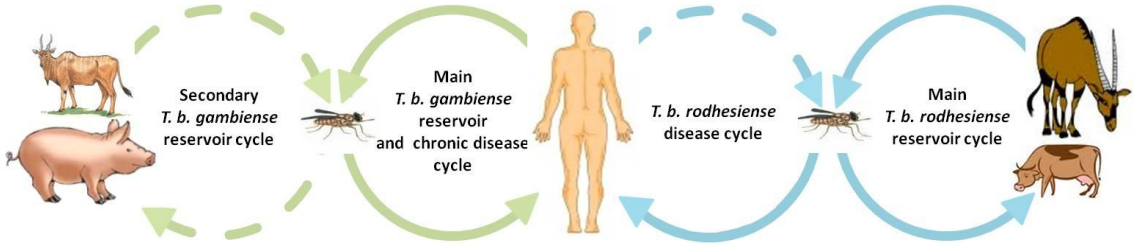

Figure 1.1 – Human african trypanosomiasis (HAT) transmission cycle.

T. b. gambiense transmission is mostly human-to-human (anthroponotic infection) and transmission from domestic animals to human occurs occasionally. *T. b. rhodesiense* infection in humans is transmitted mainly between game animals (zoonotic infection) and sometimes between animals and humans. Adapted from (Simarro *et al*., 2011).

Human African Trypanosomiasis (HAT), also known as sleeping sickness disease is one of the "neglected diseases", a group of diseases that includes schistosomiasis, visceral leishmaniasis and Chagas disease. This group of diseases is responsible for the death of hundreds of thousands of people in underdeveloped tropical regions. Nevertheless, current treatment of these diseases is often considered inadequate and ineffective and until recently the pharmaceutical industry as shown little interest in developing new drugs (Kennedy, 2008).

Human African trypanosomiasis is a potential fatal disease that affects mainly rural populations in 36 countries of sub-Saharan Africa (Figure 1.2). Along the past century, the prevalence has changed dramatically and three major epidemics have been reported. The first one affected equatorial Africa between 1896 and 1906 and killed an estimated 800,000 people (Brun *et al*., 2010, Steverding, 2008). A second major epidemic occurred between 1920 and 1940 and was controlled by the effort of mobile teams that organized active surveillance programs, screening millions of people at risk (Barrett, 2006).

By the 1960s the disease was almost eradicated thanks to the highly effective surveillance programs (Kennedy, 2008). However, the incidence of the disease re-

emerged in the 1990s due to the collapse of the surveillance and control programs allied to civil conflicts in some of the most endemic countries, such as Angola, Uganda, Democratic Republic of Congo and Sudan (Brun *et al*., 2010, Stuart *et al*., 2008, Kennedy, 2008, Stuart *et al*., 2005). By that time, 40,000 cases were reported but an estimated number of 300,000 cases remained undiagnosed and therefore untreated (Simarro *et al*., 2011)(http://www.who.int/mediacentre/factsheets/fs259/en/).

In 2005, surveillance was reinforced and the number of reported cases decreased significantly. However, these numbers are known to be uncertain as a result of under-reporting, once that African Trypanosomiasis affects mainly remote rural populations with little or no access to health facilities (Brun *et al*., 2010).

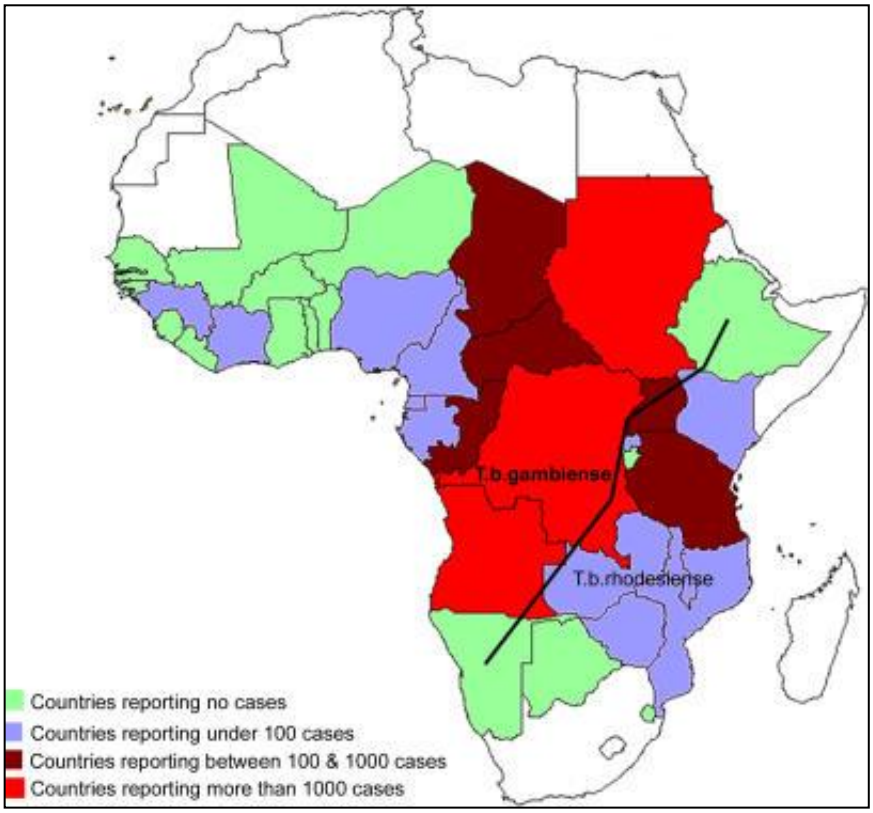

Figure 1.2 – Geographical distribution of HAT and epidemiological status of the disease in the last decade.

Geographic distribution of HAT is directly related with the tsetse fly population in the area. *T. b. gambiense* is transmitted by riverine tsetse flies from the *palpalis* group in West Africa and *T. b. rhodesiense* is transmitted by tsetse flies from the *morsitans* group (Simarro *et al*., 2011).

Around 50 million people live now in HAT transmission areas and although the number of new cases per year reported to WHO has dropped below 10,000 *(Simarro et al*., 2011), thousands of HAT cases may remain unreported or undiagnosed especially in remote areas. HAT is part of a list of disabling conditions caused by parasitic and bacterial infections that affect the world's poorest populations, often referred to as Tropical Neglected Diseases (Hotez *et al*., 2007) and along Animal African Trypanosomiasis, it is responsible for severe annual economic and human losses, causing a great socioeconomic effect on the affected populations, impairing development in sub-Saharan Africa (Brun *et al*., 2010, Antoine-Moussiaux *et al*., 2009, Kennedy, 2008, Hotez *et al*., 2007).

1.1.2 Clinical features

There are two different forms of sleeping sickness disease, the chronic form is transmitted by *T. brucei gambiense* in central and western Africa and the acute form of the disease is caused by *T. brucei rhodesiense* in East and South Africa (Brun *et al*., 2010, Kennedy, 2008).

In both forms, the disease appears in two stages and culminates in coma and death if left untreated. After the tsetse fly bite, parasites proliferate and spread to lymph nodes, reaching patient's bloodstream, causing the first stage of the disease, the hemolymphatic stage. This early stage of the disease is characterized by non specific symptoms, such as intermittent fever, headache, pruritus, weight loss, fatigue, joint pain, lymphadenopathy, hepatosplenomegaly and is frequently misdiagnosed. At this stage, parasites can be detected in blood, lymph or tissue aspirates but are usually bellow detection levels, especially when the patient is infected with *T. brucei gambiense* (Stuart *et al*., 2008, Barrett *et al*., 2003).

The second stage of sleeping sickness disease is also called meningo-encephalitic stage and it begins when parasites cross the blood brain barrier and invade the central nervous system, causing a number of neurological disturbances. As the disease progresses, headaches become more severe and sleep disorders appear, mainly

caused by dysregulation of the circadian rhythm (Stuart *et al*., 2008). Various severe neurological symptoms, such as psychiatric and mental features, motor and sensory disturbances and visual involvement accompany sleep disorders leading invariably to death in the absence of treatment (Kennedy, 2008).

T. brucei gambiense infection has a progressive course with an estimated average duration of 3 years, evenly divided between the two stages, whereas *T. brucei rhodesiense* infection results in patient's death within weeks or months (Checchi *et al*., 2008, Odiit *et al*., 1997).

1.1.3 Diagnosis

Diagnosis of HAT is divided in three distinct steps: screening, diagnostic confirmation and staging. Screening for potential infection is sometimes difficult, once the clinical features of the disease are not specific enough and lead to misdiagnose. The card agglutination test for trypanosomiasis (CATT) is considered the most efficient and best adapted screening method to use in endemic areas. It is a fast serological test that allows the screening of hundreds of individuals daily. However, it is only available for *T. brucei gambiense* infections (Brun *et al*., 2010).

Diagnostic confirmation of trypanosomiasis is ideally done by microscopic identification of trypanosomes in peripheral blood samples or lymph node aspirates. This diagnostic approach is easier in *rhodesiense* infections due to the high parasitemia that generally persists in contrast with *gambiense* infections, where parasitemia tends to be irregular and low (Kennedy, 2008). Detection of parasite DNA by PCR techniques might be of valuable use in the future, as more sensitive approach, but existing tests need further standardization and validation (Brun *et al*., 2010).

Once the course of treatment is defined according to the stage of the disease, it is important to establish precisely whether the central nervous system is affected. For that, cerebrospinal fluid is examined by lumbar puncture for parasite detection or elevated white blood cells and IgM levels (Brun *et al*., 2010, Stuart *et al*., 2008, Chappuis *et al*., 2005).

The diagnostic approach for *T. brucei rhodesiense* infection is significantly different from the gambiense. There is no suitable serological screening method comparable to the CATT test used for *T. brucei gambiense* detection and the screening in the field is based mainly on clinical history and existing symptoms. As the two species do not co-exist in the same geographical areas, except in Uganda, the detection of parasites on blood samples has been enough to differentiate between the chronic and acute form of the disease. Nevertheless, there is evidence that this natural separation can be disrupted, as it has been shown that *T. brucei rhodesiense* is being carried by the movement of infected animals in Uganda towards areas of endemic gambiense form of the disease. The overlap of the chronic and acute forms of the disease can therefore represent a major problem for the control and treatment of HAT (Chappuis *et al*., 2005, Welburn and Odiit, 2002, Welburn *et al*., 2001).

1.1.4 Treatment, control and potential targets for therapy

Current drug therapy for HAT is highly unsatisfactory and relies on four licensed drugs, all of which show numerous adverse effects and limited efficacy. Suramin and pentamidine are used for first stage treatment of HAT caused by *T. brucei rhodesiense* and *T. brucei gambiense*, respectively. Both drugs have moderate side-effects and high efficacy, but only when administered early in the disease progression. Melarsoprol is effective against second stage disease caused by both *T. brucei rhodesiense* and *T. brucei gambiense* but it is highly toxic, resulting in severe adverse reactions and causing death to 5% of all patients receiving treatment (Brun *et al*., 2010, Stuart *et al*., 2008, Kennedy, 2008). Eflornithine is the only new drug for the treatment of HAT developed in the past 50 years (Brun *et al*., 2010). It is only effective against infections with *T. brucei gambiense* and it has been increasingly used as an alternative therapy, once the treatment with melarsoprol has shown increased failure due to drug resistance (Stuart *et al*., 2008, Kennedy, 2008). Nifurtimox, a drug licensed for use against Chaga's disease has limited efficacy against second stage HAT but has been used combined with eflornithine, to shorten and simplify the treatment (Priotto *et al*., 2009, Priotto et al., 2007, Chappuis, 2007).

Due to the high toxicity of the available drugs and the absence of vaccines against trypanosome infection, the only preventive measure that seems adequate is the reduction of the tsetse fly bites by disruption of the man/fly contact, but the main control strategies are the reduction of the disease reservoir and the control of the tsetse fly vector. In *T. brucei gambiense* infections, the most significant reservoir is the human, so the main control strategy is surveillance, population screening and treatment of infected individuals to reduce the reservoir. As the reduction of reservoir is very difficult in *T. brucei rhodesiense* infections, due to the high variety of animal hosts that can act as a reservoir, the main strategy in use is the vector control, usually done with traps or screens combined with insecticides and fly attracting odors (Brun *et al*., 2010, Kennedy, 2008).

Despite being one of the most neglected diseases in Africa, extensive research has been conducted. The sequencing of the genome (Berriman *et al*., 2005) and the use of powerful molecular biology techniques (Alsford *et al*., 2011, Clayton *et al*., 2005, Ngô *et al*., 1998) have given new insights on the parasite biology and allowed the identification of new potential targets for therapy, such as the glucose metabolism and the glycosome (Nowicki *et al*., 2008, Verlinde *et al*., 2001), the pentose phosphate pathway (Barrett, 1997), the thiol metabolism (Schlecker *et al*., 2005, Schmidt and Krauth-Siegel, 2002), the lipid and sterol metabolism (Paul *et al*., 2001, Buckner *et al*., 2000, Yokoyama *et al*., 1998), cell signaling and differentiation, protein degradation and peptidase inhibitors (Santos *et al.*, 2007, Caffrey *et al.*, 2000, Troeberg *et al.*, 1999), membrane architecture, transporters and drug entry, regulation of nuclear gene expression, kinetoplastid and RNA editing, among others (Kennedy, 2008, Barrett *et al*., 2003).

1.2 *Trypanosoma brucei*

African trypanosomes are protozoan parasites belonging to the family of Trypanosomatids, order Kinetoplastida (Field and Carrington, 2009). Although they have the cellular organization of eukaryotic cells, these parasites are characterized by the development of some unusual features and organelles, such as the presence of a

distinct DNA containing region in their single large mitochondrion, the kinetoplast (Stuart *et al*., 2008). As they exhibit rich and diverse cell biology, kinetoplastid parasites in general and *Trypanosoma brucei* in particular, provide an excellent means for studying and understanding many of the intriguing aspects of its cell biology, such as cell structure and morphology, organelle positioning, cell division and protein trafficking within the cell (Matthews, 2005, Gull, 2001).

1.2.1 *T. brucei* life cycle

T. brucei has a complex life cycle, in which the parasite must adapt to completely different and often hostile environments when transmitted between its mammalian host and arthropod vector or when travelling trough different compartments within the tsetse fly. During its life cycle, the trypanosome undergoes multiple changes in its cell biology, revealing numerous developmental forms, primary metabolism differences and gene expression changes, enabling the parasite to survive and escape the host's immune system (Field and Carrington, 2009, Matthews, 2005).

During its developmental cycle, the trypanosome makes a series of transitions, colonizing 3 major environments: the mammalian bloodstream, the tsetse fly midgut and the tsetse fly salivary gland, alternating between proliferative stages and non-proliferative stages (Figure 1.3) (Stuart *et al*., 2008, Gull, 2001, Vickerman, 1985).

1.2.1.1 Development of *T. brucei* in the mammalian host

T. brucei is transmitted to the mammalian host by the tsetse fly during a blood meal. After the bite, metacyclic parasites are transmitted to the mammal, causing a local inflammatory reaction and forming a lesion at the site of the bite, a chancre.

From this chancre, trypanosomes enter the bloodstream and lymph nodes where they multiply by binary fission and proliferate as slender trypomastigotes (Vickerman, 1985).

As trypanosomes live extracellularly in the bloodstream, they undergo antigenic variation to evade the host's immune system. The immune system's evasion requires the sequential expression of distinct variant surface glycoproteins (VSGs) linked to the membrane's surface by a glycosylphosphatidylinositol (GPI) anchor (Cross, 1975). Once the VSG coat is recognized by the host's immune system and a specific antibody is raised, activating the complement, the parasitemia starts to decrease. However, a small number of trypanosomes survive by expressing a different VSG coat and thus escaping the immune system (Vickerman, 1978). This periodical switching of VSG coat and consequential evasion of the host's immune system causes the cyclical waves of parasitemia characteristic of the chronic form of Human African Trypanosomiasis (Fenn and Matthews, 2007).

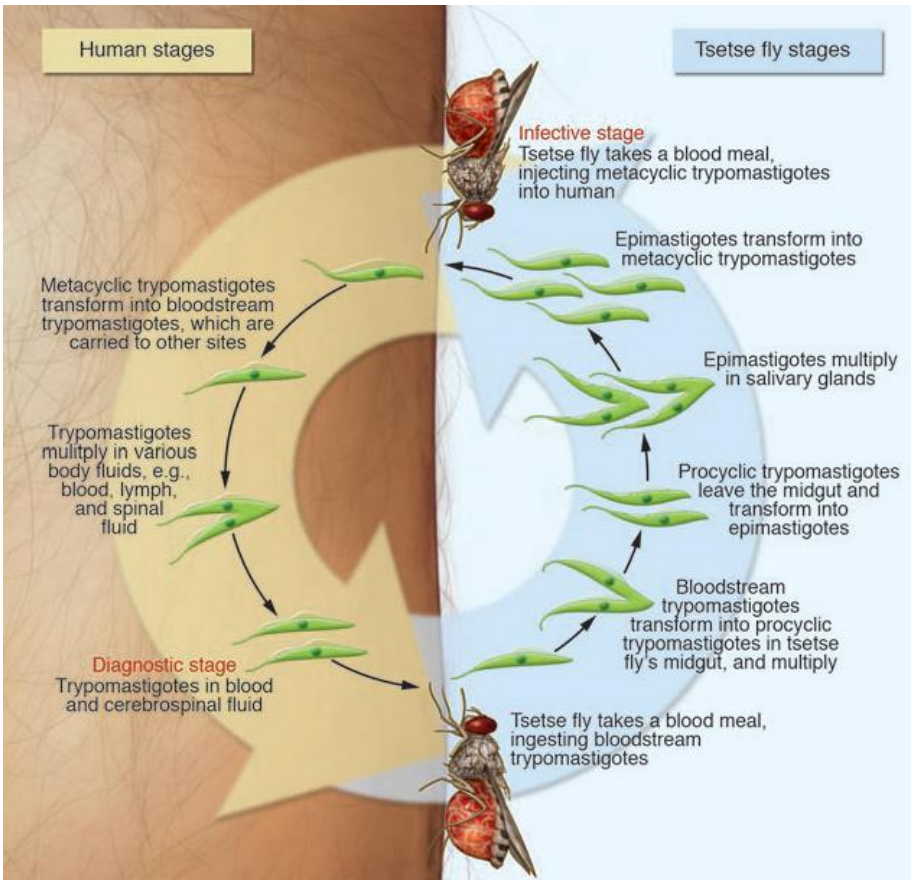

Figure 1.3 – *Trypanosoma brucei* life cycle.

Diagram showing the developmental stages of *T. brucei* found in the bloodstream of mammal hosts and in the midgut and salivary glands of the insect host (Stuart *et al.*, 2008).

Dividing slender parasites are found in ascending parasitemia while non-dividing stumpy trypomastigotes can be observed when the parasitemia goes into remission (Fenn and Matthews, 2007, Vickerman, 1985). As the number of parasites increases, short stumpy trypomastigotes replace slender ones after proliferation in the mammalian bloodstream. This differentiation appears to be induced by a molecule secreted by the parasite, referred to as Stumpy Induction Factor, and may serve two purposes. First it limits the number of parasites in the blood, increasing host's survival and maximizes the probability of disease transmission. Second, it ensures the coordination of morphological changes needed for the efficient transmission to the tsetse fly providing the continuation of the parasite's life cycle (Matthews, 2005, Vassella *et al*., 1997).

When accumulated, the Stumpy Induction Factor triggers cell cycle arrest in G1 phase and the mitochondrial respiratory chain is activated, preparing the cell to glucose limited environment and pre-adapting the parasite for the drastic changes of environmental conditions and for efficient transmission to the tsetse fly vector (Vassella *et al*., 1997, Priest and Hajduk, 1994).

1.2.1.2 Development of *T. brucei* in the tsetse fly vector

The trypanosome initially establishes in the tsetse fly midgut after a blood meal, before migrating to the salivary glands (Matthews, 2005). When the fly feeds from a mammalian host, the infected blood contains both long slender and short stumpy parasites. The transformation of this pleomorphic population of mammalian bloodstream forms of *T. brucei* to procyclic forms must rapidly occur to ensure parasite's survival in the vector (Ziegelbauer *et al*., 1990).

While the replicating slender forms of the parasite are killed by proteases, the non proliferating stumpy forms that are pre-adapted for life in the fly must rapidly undergo structural and metabolic transformation to insect stage cells (procyclic form) in the gut lumen (Roditi and Lehane, 2008, Hu and Aksoy, 2006).

The procyclic form (PCF) of *T. brucei* is extremely different from its mammalian counterpart: it uses proline as energy source instead of glucose, shows a different morphology and cell architecture and several changes in gene expression (Matthews and Gull, 1994).

After the differentiation of bloodstream forms into procyclic forms begins, the VSG coat is lost and replaced by a new surface protein coat, a procyclin coat resistant to tsetse fly midgut proteases (Matthews and Gull, 1994, Ziegelbauer *et al*., 1990). As approximately 99% of the parasites present in the ingested blood are eliminated by the fly, the trypanosome establishment in the midgut starts from a very small population of fully differentiated procyclic cells (Van Den Abbeele *et al*., 1999, Ziegelbauer *et al*., 1990).

That small population of PCF cells grows vigorously and as colonization progresses, from the posterior to the anterior midgut, parasites start to elongate and long trypomastigotes (mesocyclic trypomastigotes) can be found near the proventriculus, in the ectoperitrophic space in the anterior midgut. These cells invade the proventriculus lumen and migrate to the foregut and proboscis, where they undergo a complex differentiation to short epimastigotes (Roditi and Lehane, 2008, Van Den Abbeele *et al*., 1999).

To complete its life cycle, the parasite must colonize the tsetse fly salivary gland in order to generate metacyclic forms, infective for mammals. In the proventriculus, the long trypomastigote cells replicate their nuclear DNA and reposition their kinetoplast and basal body originating long epimastigote form parasites.

These cells undergo asymmetric division, generating short epimastigotes, presumed to be the ones colonizing the tsetse fly salivary gland and long epimastigotes whose fate is unknown.

Due to its small flagella, short epimastigotes have reduced motility and resemble the attached epimastigotes in the salivary gland. However, their inefficient flagella make it impossible for them to swim from the proboscis to the salivary gland, trough the hypopharynx. It is then proposed that the cells reaching the salivary gland are the asymmetrically dividing epimastigotes, which drive themselves using the flagellum of the long daughter cell (Roditi and Lehane, 2008).

Once in the salivary gland, these cells complete their division and the short epimastigotes are now able to attach to the wall and continue their development into mature metacyclic trypomastigote forms, infective for mammals (Roditi and Lehane, 2008).

1.2.2 *T. brucei* cell biology

Although *T. brucei* exists in two different developmental forms, perfectly adapted to survive in each of its hosts, both BSF and PCF parasites exhibit a similar morphology characterized by a cell body with a vermiform shape with tapered ends and a single flagellum emerging from the basal body, near the posterior end of the cell through a specialized plasma membrane invagination, the flagellar pocket (Figure 1.4) (Field and Carrington, 2009, Ralston *et al*., 2009).

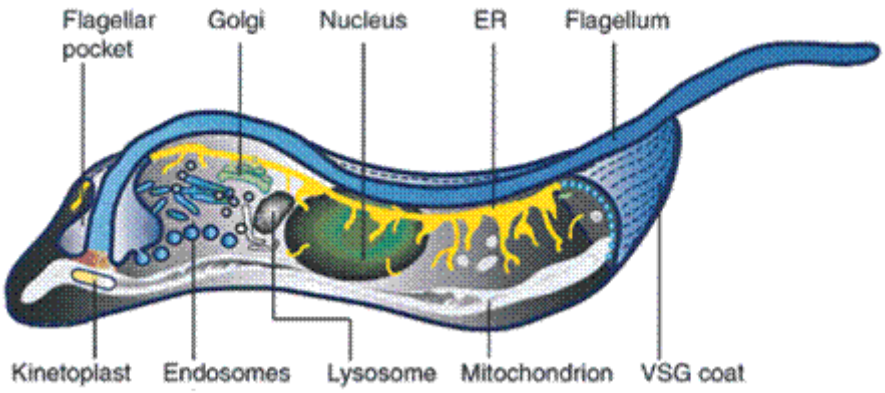

Figure 1.4 – The basic structure of *T. brucei*.

Schematic representation of *T. brucei*'s cell morphology, showing the parasite's major organelles and their organization within the cell (Grünfelder *et al*., 2003).

The flagellum of trypanosomes has several important functions, some of them essential for the parasite's pathogenicity. Trypanosomes use the flagellum to move, driving themselves with the flagellum leading, forming waves from tip to base and not from base to tip as observed in the majority of flagellated cells (Bastin *et al*., 2000).

In addition to its role in the parasite's motility, the flagellum is essential for host-parasite interaction, once it is required for the attachment to epithelial cells in the tsetse fly salivary gland (Vaughan, 2010). The flagellum is also critical for cellular morphogenesis (Kohl *et al*., 2003, Moreira-Leite *et al*., 2001), organelle inheritance and positioning and cell division (Ralston *et al*., 2006, Kohl *et al*., 2003). Finally, the flagellum could be involved in cell signaling and sensory functions (Vaughan, 2010).

Electron microscopy analysis of the flagellum reveals the presence of many conventional flagellar structures, such as the axoneme and some electron dense particles resembling IFT particles, but also of unusual extra-axonemal structures such as the paraflagellar rod (PFR) and the flagellum attachment zone (FAZ) and the flagella connector (FC), unique to trypanosomes and a few related protozoa (Ralston *et al*., 2009, Kohl and Bastin, 2005, Landfear and Ignatushchenko, 2001).

The axoneme presents the typical 9+2 microtubule arrangement, with the 9 outer doublets surrounding a central pair of singlet microtubules (Ralston *et al*., 2009, Kohl and Bastin, 2005). It also possesses all the conventional components of other eukaryotic axonemes such as the inner and outer dynein arms, the radial spokes connecting the outer doublets to the central pair, the nexin links associated with the outer doublets and the projections from each central pair microtubules connecting them to one another, revealing a high structural degree of conservation (Kohl and Bastin, 2005, Bastin *et al*., 2000).

The paraflagellar rod existence is restricted to kinetoplastids, euglenoids and dinoflagellates (Bastin *et al*., 1998). It can be detected alongside the axoneme once the flagellum exits from the flagellar pocket, running until the flagellum tip (Ralston *et al*., 2009). This structure is divided in 3 distinct regions, the proximal, intermediate and distal domains, with the proximal domain of the PFR being tightly connected to doublets 4 and 7 of the axoneme (Kohl and Bastin, 2005). Although its function remains unknown, PFR seems to be essential for flagellum and cell motility in trypanosomes and (Bastin *et al*., 1998). The ablation of one of the main PFR structural components (PFR2) in BSF cells causes lethal phenotypes both in *in vitro* cultures and *in vivo*, in mouse infections (Griffiths *et al*., 2007), that manifest in aberrant defects in cytokinesis and cell morphology (Portman and Gull, 2010, Broadhead *et al*., 2006).

Along the length of the cell, the flagellum and the cell body are held by a network of cytoskeletal and membranous connections that together comprise the flagellar attachment zone (Ralston and Hill, 2008, Gull, 1999). Although the FAZ is not part of the flagellum, it is closely associated to the flagellum and its functions. When the flagellum emerges from the flagellar pocket, it bends over the cell body, attaching to the cell body membrane. The flagellar pocket and the cell body membrane remain in tight contact and the FAZ can be recognized from the flagellar pocket area, following the flagellum and ending at the anterior tip of the parasite (Kohl and Bastin, 2005, Kohl and Gull, 1998). Its components are mostly unknown, but the ultrastructure of FAZ is extensively characterized. It contains 2 distinct structures, the FAZ filament on the cytoplasmic side and a unique set of 4 microtubules associated with the membranous compartment. The FAZ filament is connected to both the axoneme and the PFR by a network of filaments promoting the contact of the cell body membrane with the flagellum (Ralston *et al*., 2009, Ralston and Hill, 2008). The flagellum and the FAZ together provide structural and positional support to the parasite, that influence cytokinesis and cell morphogenesis and the disruption of flagellum attachment results in failing to initiate cytokinesis (Ralston and Hill, 2006, Kohl *et al*., 2003).

Although it has critical roles in mobility, morphogenesis and cell division throughout the parasite's life cycle, most studies of flagellum structure and function have been conducted in the procyclic form of *T. brucei* (Ralston and Hill, 2006). The new flagellum emerges from the flagellar pocket and extends along the cell body towards the anterior end of the parasite, following a left-handed helical path. As it elongates, the new flagellum is always located to the left of the old one, when looking at cell from the posterior end. In procyclic trypomastigotes, the distal tip of the new flagellum is connected to the side of the old one by the flagellar connector, a transmembrane complex of unknown composition, important in providing all the vital morphogenetic information for the daughter cell's flagellum to assemble correctly (Field and Carrington, 2009, Davidge *et al*., 2006, Briggs *et al*., 2004).

This physical contact held between the old and the new flagellum ensures that as the new flagellum elongates, it follows the same helical path along the cell as the old one, maintaining its structure, polarity and alignment (Davidge *et al*., 2006, Briggs *et al*., 2004).

During the assembly of the new flagellum, the transport of all flagellar precursors to the distal tip of the flagellum is dependent on intraflagellar transport (IFT), a bidirectional transport system of proteins in the flagella matrix. The IFT is driven by a two motor complexes, the heterotrimeric kinesin II that moves particles towards the flagellum tip and a dynein complex that moves the particles back to the base of the flagellum (Absalon *et al*., 2008b, Briggs *et al*., 2004). Functional studies reveal that IFT is required for the correct flagellar biogenesis in *T. brucei* and the presence of IFT particles in the old and new flagella of the same cell suggests that IFT operates in both and is not only required for the growth of the new flagellum but also for the maintenance of the mature one (Absalon *et al*., 2008b).

The silencing of IFT genes results in cells with shorter flagella and in some cases with no flagella, leading to progressively shorter cells (Absalon *et al*., 2008b). The absence of normal flagellum elongation does not affect the flagellar pocket formation, which remains present in these cells. Nevertheless, abnormally shorter parasites exhibit flagellar pocket with different shapes, suggesting that normal flagellum elongation is essential for the organization, orientation and function of the flagellar pocket (Absalon *et al*., 2008a).

Once it exits the cytoplasm, through the flagellar pocket, the flagellum is surrounded by its own membrane and is attached to the cell body, along most of its length. The cell membrane, the flagellar pocket and the flagellar membrane comprise the three contiguous but morphologically and biochemically distinct domains of the parasite's surface membrane, each one with unique functions (Ralston and Hill, 2008, Landfear and Ignatushchenko, 2001). All 3 domains are covered by the densely packed VSG coat in the bloodstream form parasites or during the metacyclic stage in the tsetse fly salivary gland or by a procyclin coat in the other procyclic forms (Bastin *et al*., 2000).

In the flagellar pocket domain, the density of this protein coat seems to be different from the remaining membrane domains and the subpellicular microtubules are absent, with the exception of a quartet of specialized microtubules that run along one surface of the flagellar pocket, allowing the endo- and exocytosis events to occur at this site (Gull, 2003, Bastin *et al*., 2000). All vesicular traffic passes through the flagellar

pocket defining it as a dynamic portal to host or vector environment. This dynamic interaction provides resistance to the host's innate and acquired immune responses and although the flagellar pocket is a critical organelle for the trypanosome biology with important roles in immune evasion, very little is known about its architecture and how molecules get to and from the flagellar pocket (Lacomble *et al*., 2009, Gull, 2003).

The flagellar pocket has a complex organization and a precise positioning relatively to cytoskeletal elements and other organelles. It can be divided into several subdomains, with the basal body used to define one pole of this structure. The membrane and luminal volume of the flagellar pocket are asymmetric due to the association with the Golgi complex and the probasal body. Associated with the Golgi apparatus is the neck region which is located distal to the flagellum exit point. The neck of the flagellar pocket is a specialized membrane area also associated with the FAZ and where a microtubule quartet integrates into the subpellicular array, defining an axis for the entire flagellum and its associated structures (Field and Carrington, 2009, Lacomble *et al*., 2009). The flagellar pocket has 2 boundary subdomains associated with organized structures connected across the membrane and cytoskeleton, the collar, defining the flagellum exit point, and the collarette, the point where it enters the flagellar pocket (Field and Carrington, 2009).

With the flagellar pocket as the only site of endocytosis and exocytosis, the *T. brucei* cell, and thus the *T. brucei* endomembrane system, is highly polarized. This high degree of polarization of the endomembrane system is reflected in the localization of the secretory and endocytic organelles, with the endoplasmic reticulum (ER) widely distributed throughout the cytoplasm and all the rest compactly organized in the posterior portion of the cell, between the nucleus and the kinetoplast and the single lysosome close to the nucleus (Field and Carrington, 2009, Morgan *et al*., 2002a).

The flagellar pocket has a distinct proteome with most of the protein families required for vesicle trafficking in other eukaryotic organisms represented in it, like the 16 Rab and Rab-related proteins encoded in *T. brucei* genome (Ackers *et al*., 2005, Berriman *et al*., 2005).

Rab proteins are small GTPases involved in endocytic, exocytic and recycling pathways, with TbRAB7 associated with the lysosome and pre-lysosome and TbRAB4,

TbRAB5A, TbRAB5B and TbRAB11 as part of the early endosome and recycling arms of the endocytic pathway (Morgan *et al*., 2002b, Field *et al*., 1998).

Although trypanosomes have conventional endomembrane system, it has some distinct unusual features, such as the clathrin dependence of all endocytosis (Allen *et al*., 2003). These mechanisms seem to have an extreme importance in immune evasion and emphasize the high level of endocytic activity in BSF trypanosomes as a potential reason for the protection against the mammalian immune system (Natesan *et al*., 2010).

Trypanosomes can be efficiently eliminated by mammalian anti-VSG antibodies and complement activation. Nevertheless, the VSG-antibody complex doesn't remain bound to the cell surface and is rapidly internalized, degraded and the VSG is recycled. This antibody uptake by the parasite appears to be mediated by hydrodynamic flow that drives the antibody bound to the highly abundant GPI-anchored VSG to the flagellar pocket where it is internalized (Natesan *et al*., 2011, Engstler *et al*., 2007). This process involves transport steps mediated by RAB5 and RAB11, both proteins regulated according to the developmental stage (Pal *et al*., 2003), suggesting that the endocytic system is activated in the bloodstream stage (Grünfelder *et al*., 2003, Pal *et al*., 2002).

Degradation of immunoglobulins inside the parasite is extremely selective, occurring with low proteolysis of the VSG molecules and the details the enzymes used in this selective process are unknown. There are metacaspases present in endosomal vesicles, co-located with RAB11. However they have no direct involvement in the anti-VSG antibody degradation or VSG recycling since their knockdown and knockout produce no major effect on these processes(Helms *et al*., 2006).

It is not clear if there is any similar defensive role in PCF parasites or if there is an adequate explanation for the relatively low endocytic activity in insect stage parasites, although there are evidences that parasites do not require high endocytic activity in order to survive in the insect vector (Natesan *et al*., 2007).

Apart from the singularity of the flagellum complex organization and functionality, *T. brucei* has some other distinct features. One of these distinguishing features is the presence of the kinetoplast, a sub-cellular structure found near the basal body, at the base of the flagellum. The kinetoplast is a highly complex disk-shaped structure located within the matrix of the single mitochondrion of the *T. brucei* cell and

composed by a structural mass of proteins and catenated circular DNA molecules, the kinetoplastid DNA (kDNA) (Stuart *et al*., 2005). The structure of the kDNA is unique, consisting of a network of thousands of circular DNA molecules, minicircles, topologically interlocked with a few dozen of larger DNA molecules, maxicircles (Chen *et al*., 1995, Shapiro and Englund, 1995).

The kinetoplast and the basal body are connected by an attachment complex that crosses both the mitochondrial and cell membrane and through which the mitochondrial genome segregation and the basal body replication and segregation events are linked (Ogbadoyi *et al*., 2003).

The mitochondrion itself is an elongated structure that in BSF parasites is devoid of cristae, reflecting the absence of oxidative phosphorilation at this stage. Energy generation in BSF parasites is dependent on glycolytic reactions that take place within specialized organelles, the glycosomes (Parsons, 2004). Glycosomes are organelles belonging to the family of peroxisomes, but with an almost exclusively glycolytic role in *T. brucei*, with glycolytic enzymes comprising around 90% of protein content of these organelles in the BSF parasite. Compartmentation of glycolysis is unique and essential for BSF parasite to develop properly, enabling these organisms to overcome short periods of anaerobiosis, although without sustained growth (Michels *et al*., 2006).

When in the mammalian host, parasites encounter a large supply of glucose constantly available in the bloodstream or cerebrospinal fluid. The mitochondrion is largely repressed and all ATP is generated by a high rate of aerobic glycolysis inside the glycosome (Parsons, 2004). These parasites are not adapted to live in the insect vector and quickly die if ingested by the fly, unless they differentiate into short stumpy parasites which, although still glycolysis dependent, have a partially de-repressed mitochondrial system (Michels *et al*., 2006).

In the insect host, amino acids are the primary nutrients for parasites and even though glycosomes remain abundant, their enzymatic content changes.

Most of the glycolytic enzymes decrease to very low levels while other glycosomal enzyme levels increase and the oxidative phosphorylation replaces glycolysis as the primary energy generation mechanism (Parsons, 2004).

This enzymatic content variation between different life-cycle stages of the parasite is extremely important for the rapid and efficient adaptation to the different environments and glycosomes may play a significant role in this metabolic adaptation (Michels *et al*., 2006, Parsons, 2004).

T. brucei also contains another distinct organelle involved in the storage of polyphosphates, calcium and other cations (Docampo *et al*., 2010). Acidocalcisomes are electrondense acidic organelles present in a wide variety of prokaryotic and eukaryotic organisms, but absent in mammalian cells (Moreno and Docampo, 2003). The membrane of acidocalcisomes has numerous pumps, exchangers and at least one channel and the matrix is filled with enzymes involved in polyphosphate metabolism. Acidocalsisomes have an important role not only in the storage of phosphorus and cations but also in calcium signaling, pH homeostasis and osmoregulation in response to environmental stress (Docampo *et al*., 2010).

This interesting and complex cellular organization of *T. brucei* is not constant and different morphological forms of the parasite can be observed depending on its life cycle stage (See section 1.2.1).

These morphological forms are distinguished according to the position of the kinetoplast and flagellar pocket in relation to the nucleus. In trypomastigotes, the kinetoplast and flagellar pocket are located on the posterior end of the cell with a centrally located nucleus and the flagellum emerging from the anterior end of the cell.

In epimastigotes the kinetoplast and flagellar pocket are anterior to the nucleus and the flagellum emerges approximately from the middle of the parasite (Field and Carrington, 2009).

Life cycle progression is closely connected to the cell cycle regulation with proliferative parasites alternating with non-proliferative ones, where the cell cycle is arrested as a form of pre-adaptation for transmission between hosts (McKean, 2003).

Although *T. brucei* cell cycle is broadly similar to the mammalian one, there are some unique aspects to be discussed in the following chapter, such as the coordinated replication and segregation of the parasite's single copy organelles and the independent replication of the two unit genome of the parasite.

1.2.3 *T. brucei* Cell Cycle

The cell cycle of trypanosomes has the same nuclear events characteristic of normal eukaryotic cells, consisting of four periods of nuclear activity – G0/G1, S, G2 and M. However, unlike other eukaryotes, duplication of nuclear and kinetoplastid DNA is coordinated but not simultaneous and trypanosomes exhibit a periodic S phase for the kinetoplast (S_K) in addition to the nuclear S phase (S_N) (Ploubidou *et al*., 1999, Woodward and Gull, 1990). Kinetoplast S phase (S_K) begins immediately before the nuclear S phase (S_N). It is much shorter and kinetoplast segregation occurs before the mitosis initiates (Hammarton, 2007, McKean, 2003).

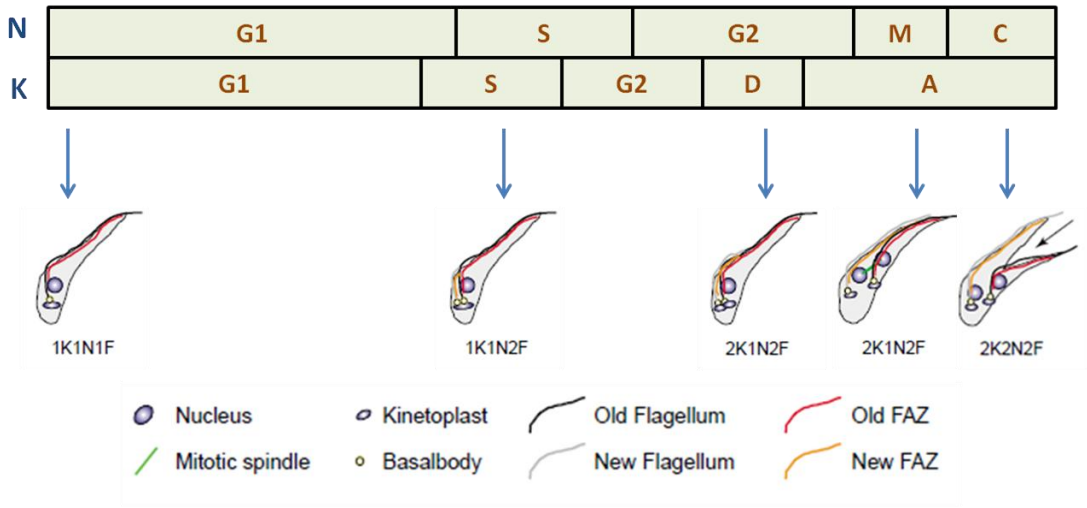

Figure 1.5 – The cell cycle of PCF *T. brucei*.

Diagram showing highly organized replication and organelle position of procyclic *T. brucei*, throughout the stages of the parasite's cell cycle. The number of nuclei (N) and kinetoplasts (K) is indicated for each one of the cell cycle stages (G1/G2: gap phases; S: DNA synthesis; M: mitosis; C: cytokinesis; D: kinetoplast segregation; A: "apportioning phase"). Adapted from (McKean, 2003).

Some of the major events occurring during the cell cycle, such as kinetoplast segregation, basal body duplication, flagellar axoneme growth, mitosis and cytokinesis are microtubule dependent, involving its polymerization/depolimerisation (Ploubidou *et al*., 1999).

The timing and order of such events in *T. brucei* varies according to the life stage and subtle differences can be observed between procyclic and bloodstream trypomastigotes, specifically the relative position of the nucleus and the kinetoplast before cytokinesis occurs (Figure 1.5) (Briggs *et al*., 2004, McKean, 2003).

The first indicator of the cell cycle initiation is the elongation and maturation of the probasal body adjacent to the mature basal body and the single flagellum. Cell cycle progresses through the initiation and elongation of the new flagellum, along with the duplication of the basal body (Sherwin and Gull, 1989). After the basal body duplication, the Golgi apparatus begins to duplicate and stays located close the newly formed basal body and the endoplasmic reticulum exit point (He *et al*., 2004). Replication of kinetoplastid and nuclear DNA commences independently, with the segregation of the kinetoplast taking place before the mitotic division of the nucleus.

In procyclic form parasites, mitosis is then followed by the positioning of the nucleus (N) between the two kinetoplasts (K), in a linear arrangement referred to as KNKN, whereas in bloodstream form both nuclei remain next to each other and anterior to the kinetoplasts, in a KKNN formation (Figure 1.6).

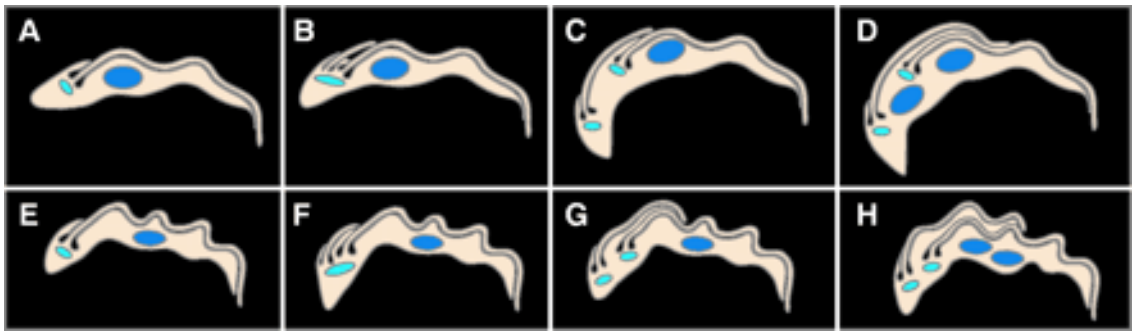

Figure 1.6 – The cell cycle of *T. brucei* trypomastigotes.

Cartoon illustrating the main differences between cell cycle in procyclic (A – D) and bloodstream form (E – H) parasites (Briggs *et al*., 2004).

Finally cytokinesis occurs, marking the end of the cell cycle, through the unidirectional ingression of a cleavage furrow formed along the helical axis of the dividing cell, from the anterior to the posterior end (Hammarton, 2007, McKean, 2003).

Cell cycle regulation is essential for the parasite's survival. Mis-regulation of cell cycle events can have severe consequences, so the cell developed a mechanism of checkpoints in which the integrity of the DNA is monitored ensuring the accuracy of DNA replication, the appropriate cell division and the production of two healthy daughter cells (McKean, 2003).

There are two major families implicated in the regulation of cell cycle progression in eukaryotes: cyclins and cyclin-dependent kinases (CDKs). The concentration of cyclins varies regularly during the cell cycle while CDKs are constantly expressed throughout the cycle but only become active when bound to a specific cyclin. Further regulation of CDKs activity is done by phosphorylation of conserved residues and the interaction with inhibitory proteins (CKIs) (Hammarton, 2007, Ploubidou *et al*., 1999).

There are 10 cyclins (CYC2–11) and 11 CDKs CRK1–4 and CRK6–12) homologous identified in *T. brucei*. Although the parasite's cell cycle presents some typical features from eukaryotes, it shows some major differences in regulatory mechanisms and molecules that can also vary according to the parasite's life cycle stage. This suggests that *T. brucei* has developed new cell cycle control mechanisms and exclusive checkpoints in order to coordinate the independent replication of the parasite's two unit genome (Hammarton, 2007, McKean, 2003).

1.3 Peptidases and their Natural Inhibitors

1.3.1 Peptidases

Peptidases, also termed proteases or proteinases are hydrolytic enzymes that catalyse the cleavage of peptide bonds in macromolecular proteins in a process known as proteolysis (Quesada *et al*., 2009, López-Otín and Bond, 2008, Rosenthal, 1999). Peptidases appeared early in evolutionary terms and show an enormous diversity with sizes ranging from small molecules of 10 kDa to multiple multimeric complexes with several hundreds of kDa.

The diversity of peptidases is also evident in their specificity. Most enzymes are non-specific and therefore can act on multiple substrates, cleaving different peptide bonds. In contrast, some peptidases are highly specific and catalyse the hydrolysis of a single peptide bond of a particular protein (López-Otín and Bond, 2008, Puente *et al*., 2003, Sajid and McKerrow, 2002).

Initially, peptidases were classified in endo and exopeptidases. The action of endopeptidases is directed to the internal peptide bonds, while exopeptidases act on peptide bonds at the amino or carboxyl terminus (López-Otín and Bond, 2008, Rosenthal, 1999). Currently, peptidases are classified according to the catalytic mechanism of proteolysis in: aspartic peptidases, serine peptidases, cysteine peptidases, glutamic peptidases, metallo-peptidases, threonine peptidases, asparagine peptidases and peptidases of unknown catalytic mechanism. Peptidases with significant similarity in amino acid sequence can be grouped into families and families with similar 3D structures can be assembled in clans (Rawlings *et al*., 2010).

This diverse group of enzymes has been identified in all biological systems, from viruses to vertebrates and is involved in several biological processes, playing essential roles in cell cycle progression, differentiation, morphogenesis, homeostasis, inflammation, immunity, angiogenesis, necrosis and apoptosis, amongst others (Quesada *et al*., 2009, López-Otín and Bond, 2008). Abnormal peptidase activity is also associated with numerous pathological conditions such as cancer, neurodegenerative disorders and cardiovascular diseases (Quesada *et al*., 2009, López-Otín and Bond, 2008, Puente *et al*., 2003).

Likewise, proteolytic enzymes seem to be central pieces in the life cycle of many parasitic protozoans causing diseases, such as malaria, leishmaniasis, amebiasis, cryptosporidiosis, toxoplasmosis and trypanosomiasis. Peptidases from all major classes have key roles in various functions, including host cell's invasion and host's immune system evasion (Rosenthal, 1999).

Additionally, some protozoan peptidases are considered to be of great interest as potential targets for chemotherapy. The importance of peptidases in the life cycle of many protozoan parasites suggests that their inhibition may be a powerful antiparasitic therapy tool. In *T. cruzi*, the cysteine peptidase cruzipain is a validated target of

effective inhibitors such as the vinyl sulfone inhibitor K777, in late preclinical trials for Chagas disease treatment (Doyle *et al*., 2007).

In *Plasmodium*, the antimalarial effects of several peptidase inhibitors have been extensively studied. For example, the cysteine peptidase inhibitor E-64 and the aspartic peptidase inhibitor pepstatin have been shown to block the development of *P. falciparum* (Glushakova *et al*., 2009) and several peptide inhibitors of falcipain have been shown to inhibit *P. falciparum* growth and maturation (Korde *et al.*, 2008).

Several studies have been focused on peptidases and their potential as targets for therapy and hundreds of peptidase inhibitors have been generated to be used for the treatment of several diseases, from cancer to auto-immune diseases, from infectious diseases caused by viruses to bacterial and parasitic infections (Coombs and Mottram, 1997).

1.3.1.1 Cysteine Peptidases in Trypanosomatids

In cysteine peptidases, the thiol group of the cysteine residue in the active site acts as the nucleophile in catalysis. The catalytic activity depends upon a catalytic dyad and is enhanced by the proximity of a histidine residue that acts as a proton donor.

The catalytic dyad is formed by the –SH group of the cysteine residue and the imidazole of the histidine and is often stabilized by the existence of a highly conserved asparagine residue. One other aminoacid can be found in the active site. Glutamine preceding the catalytic cysteine helps to form the oxyanion hole.

During hydrolysis, the enzyme is transiently bound to the substrate, forming an unstable tetrahedral intermediate (Rosenthal, 1999).

Cysteine peptidases are normally synthesized as precursors containing a pro-domain, a catalytic domain and, in some cases, an acid carboxyl-terminal domain. The pro-domain has several roles. It acts as a reversible inhibitor, regulating the proteolytic activity; it ensures the correct folding of the protein during translation and is also involved in the trafficking of the peptidase precursor to the appropriate compartment,

maintaining the enzyme in its inactive form until it reaches its destination, normally the lysosome (Rosenthal, 1999, Huete-Pérez *et al*., 1999).

Cysteine peptidases from trypanosmes are very different from their mammalian counterparts and exhibit several functions, some related to the host's cells and tissues invasion and to the immune system evasion. Once they are highly immunogenic and exhibit significant structural and biochemical differences, cysteine peptidases have been exploited as potential targets for diagnostic therapy of parasitic diseases. In mammals, cysteine peptidases exhibit optimal activity at slightly acid or neutral pH, while in parasites they remain active through a wider range of pH, including alkali pH, are generally larger and more numerous than the mammalian ones and exhibit essential differences in substrate specificity, domain extensions and cellular localization (Sajid and McKerrow, 2002, North *et al*., 1990).

A great number of peptidases have been identified and characterized in parasitic protozoa. Although this vast group of peptidases includes members of all main classes, the majority of peptidases identified in parasitic organisms belongs to the cysteine class and are homologous to the cathepsin L in mammals (Rosenthal, 1999, Coombs and Mottram, 1997). Cathepsin L and cathepsin B–like peptidases belong to family C1, clan CA (papain-like peptidases), the largest cysteine peptidase clan, comprising 84% of all peptidases identified in parasitic protozoa (Atkinson *et al*., 2009, Sajid and McKerrow, 2002).

Apart from clan CA, cysteine peptidases can be classified in 8 additional clans (CD, CE, CF, CH, CL, CM, CN, CO) plus one unclassified clan. The classification of peptidases is done according to similarities in the amino acid sequence, presence of peptide loops and substrate specificity (Atkinson *et al*., 2009, Sajid and McKerrow, 2002).

In kinetoplastid parasites, the best characterized cysteine peptidases also belong to the family C1 of the clan CA. In this family, amino acids histidine and cysteine form the catalytic diad in the active site. Cysteine peptidases belonging to family C2 (calpains) of clan CA and to the families C13 (GPI:protein transaminase), C14 (metacaspase) and C50 (separase) of clan CD were also described in kinetoplastids (Caffrey *et al*., 2000).

As in other papain–like peptidases, cathepsin L and cathepsin B–like peptidases from kinetoplastids include a signal peptide, a pro-peptide essential for the activation of the catalytic domain and a PepC1 catalytic domain. Additionally, kinetoplastid cathepsin L–like peptidases have a C–terminal extension, which function is yet to be determined with accuracy. Although this C–terminal extension has no catalytic role, it is highly immunogenic and can be used for diagnostic purposes (Caffrey and Steverding, 2009, Caffrey *et al*., 2000).

The active site of these enzymes has a conserved cysteine, histidine and asparagines residue and is surrounded by highly conserved peptide motifs. Like in other cathepsin B–like peptidases, kinetoplastid ones also have an insertion of 20 aminoacids in the catalytic domain, the occluding loop, that contributes to the dipeptidyl carboxiyl peptidase activity of cathepsin B (Caffrey and Steverding, 2009).

The genome of kinetoplastids has several copies of cathepsin L–like peptidases genes. In *T. brucei*, there are more than 20 copies of the gene arranged in tandem array and in *T. cruzi* there are more than 130 polymorphic genes arranged in clusters located in different chromosomes. The expression of cathepsin B–like peptidases is much simpler and is normally restricted to one or two copies of the gene (Caffrey and Steverding, 2009, Mottram *et al*., 1998).

There is a total of 65 cysteine peptidases encoded in the genome of *Leishmania major*. Like in other parasitic protozoa, most studies are focused on family C1 peptidases, CPA and CPB, both cathepsin L–like peptidases and CPC, a cathepsin B–like peptidase. *Leishmania's* cathepsin L peptidases are stage regulated and mainly expressed in amastigotes, where they are restricted to large lysosomes, also termed megasomes (Caffrey and Steverding, 2009).

CPB exists as multiple isoenzymes encoded by a tandem array of CPB genes (19 in *L. mexicana* and 8 in *L. major*) in a single locus (Mottram *et al*., 2004, Mottram *et al*., 1998). These isoenzymes are slightly different, presenting distinct catalytic properties and substrate preferences and probably, different functions in the host-parasite interaction (Mottram *et al*., 1998). The generation of null mutants of CPA, CPB and CPC in *Leishmania* showed that these enzymes have a significant role in the host-parasite interaction, acting as modulators of the mammalian's immune system and

enabling the parasite's survival and proliferation inside the macrophages (Mottram *et al*., 2004, Mottram *et al*., 1998).

Cruzipain, the main cysteine peptidase of *T. cruzi*, can be found in all life cycle stages, although its expression is higher in the replicating forms of the parasite, particularly, in epimastigotes. Cruzipain localization is different in epimastigotes, where it is found in the endosomal/lysosomal system, and amastigotes, where it is localized on the cell surface (Caffrey and Steverding, 2009, Mottram *et al*., 2004). The enzyme seems to be involved not only in the host's immune system evasion but also in metacyclogenesis (McKerrow *et al*., 2009). Additionally, cruzipain has significant roles in amastigote replication, intracellular development and cellular invasion (Caffrey and Steverding, 2009).

T. brucei has cysteine peptidases belonging to both cathepsin L and cathepsin B–like peptidases. Brucipain, a cathepsin L–like peptidase, is the major CP of the parasite. It has been identified in all life cycle stages and its levels of expression is approximately 5 to 10 times higher in short stumpy forms than in long slender BSF or procyclic forms, where it has comparatively little activity. Its cellular localization is dependent on cell cycle stage. In BSF the enzyme is confined to the lysosomes while in PCF the localization of brucipain is yet to be determined (Caffrey and Steverding, 2009, Caffrey *et al*., 2000). Cathepsin B–like peptidases of *T. brucei* (TbCatB) are expressed essentially in the bloodstream forms of the parasite, while in *T. cruzi* and *Leishmania* these enzymes are expressed throughout the life cycle (Caffrey and Steverding, 2009).

Both cathepsin L and cathepsin B–like peptidases are essential for the parasite successful survival within the mammal host. RNAi of TbCatB resulted in engorged lysosome, growth arrest and death of parasites *in vitro*. Similar studies involving brucipain RNAi *in vitro* showed no perceptible phenotype. In *in vivo* studies, the knockdown of TbCatB cured the infection whereas the RNAi against brucipain led to an extended life time of infected mice (Caffrey and Steverding, 2009, Abdulla *et al*., 2008).

Further studies show that brucipain assists the parasite migration through the blood brain barrier into the brain, suggesting that although the enzyme is not essential for parasite viability, it has an important role in the nervous system invasion and the

development of the second stage of the sleeping sickness disease (Abdulla *et al*., 2008, Nikolskaia *et al*., 2006).

Great progress has been made in the establishment of cysteine peptidases as drug targets in *T. brucei*. Inhibitory studies using synthetic inhibitors such as benzyloxycarbonyl-phenylalanine-alanine diazomethane (Z-Phe-Ala-CHN_2) have been conducted with some success, resulting in parasite death both *in vitro* and *in vivo* in a murine model (Caffrey and Steverding, 2009, Mackey *et al*., 2004).

Although TbCatB has already been validated as drug target (Mallari *et al*., 2009), brucipain is still a main focus in the effort of finding an effective trypanocidal inhibitor. The enzyme is yet to be validated as chemotherapeutic target since the complete silencing has not been achieved and the importance of brucipain to the infection and disease progression is still undetermined (Caffrey and Steverding, 2009).

1.3.1.2 Serine Peptidases in Trypanosomatids

Serine peptidases belong to the most abundant and diverse group of proteolytic enzymes, accounting for more than one third of all peptidases. Grouped in 40 families distributed over 13 Clans, serine peptidases are widely disseminated in nature and can be found in the most diverse organisms from animals and plants to virus and bacteria (Di Cera, 2009, Page and Di Cera, 2008). These enzymes are normally endopeptidases and use a catalytic triad of serine, aspartate and histidine, exhibiting similar special arrangement but different order in the amino acid sequence (Polgár, 2005). Other serine peptidases can use either simple dyad mechanisms of serine and lysine or histidine in the active site or different catalytic triads (Page and Di Cera, 2008).

The –OH group of the serine residue acts as a nucleophile on the carbonyl carbon of the scissile peptide bond of the substrate while the pair of electrons on the histidine accepts the hydrogen from the serine –OH group, coordinating the attack of the peptide bond. The carboxyl group of the aspartate makes the pair of electrons much more electronegative (Di Cera, 2009). The combination of the three aminoacid residues that comprise the catalytic triad is known in four different 3D protein folds (trypsin,

subtilisin, prolyl oligopeptidase and ClpP peptidase), suggesting different evolutionary origins (Page and Di Cera, 2008).

Clan PA is the largest and best studied clan of serine peptidases with members involved in many critical physiological processes. It includes family S1A and S1B, two phylogenetically different groups of enzymes that that have in common the two β-barrel architecture and the order His/Asp/Ser of catalytic residues on the polypeptide chain (Page and Di Cera, 2008). S1A or chymotrypsin like peptidases, are divided into 6 different groups in humans, according to their function, in: digestive enzymes (trypsin and chymotrypsin), coagulation and immunity enzymes, tryptases (components of secretory granules in mast cells), matriptases (membrane bound enzymes with substrate selectivity similar to trypsin), kallikrein (peptidases involved in blood pressure regulation) and granzymes (apoptosis mediators and defense against viral infections). This group of enzymes has limited distribution in plant, prokaryotes and *archaea*. In contrast, S1B peptidases are established throughout all organisms and are involved in protein turnover (Di Cera, 2009).

The abundance of S1 peptidases reflects the selective advantage of chymotrypsin-like fold of this family. However, the dissemination of clan PA peptidases only took place in eukaryotic organisms, while in prokaryotes, plant and fungi, the predominant serine peptidases belong to can SB and SC (Page and Di Cera, 2008).

Clan SB includes subtilisin and is more abundant in plants and bacteria with little expression in the animal kingdom (Page and Di Cera, 2008). Clan SB and clan PA peptidases exhibit similar architecture but different 3D structures, suggesting an independent but yet convergent evolution (Polgár, 2005). With parallel β-sheet arrangement and Asp/His/Ser order of catalytic residues, subtilisin family (family S8) is a very successful group of enzymes with representatives with simple proteolytic activity in fungi and bacteria and more intricate ones in eukaryotes (Barrett and Rawlings, 1995). Nevertheless, their biological role tends to be related with nutrition and protein processing (Page and Di Cera, 2008).

Clan SC peptidases are the second largest group of serine peptidases in humans. The α/β hydrolase-fold, characteristic of SC peptidases, provides a versatile catalytic

platform and these enzymes can present additional catalytic activity, acting as esterases, lipases, dehalogenases, haloperozidases, lyases or epoxide hydrolases (Page and Di Cera, 2008). Enzymes belonging to Clan SC present both, endo- or exoproteolytic activity, a characteristic contrasting with other families of serine peptidases that are usually constituted either by endopeptidases or exopeptidases (Page and Di Cera, 2008). The S9 family is the most representative family of Clan SC peptidases, with 41 homologous identified in the human genome. Prolyl oligopeptidase (POP) exhibits the order Ser/Asp/His in the polypeptide chain, characteristic of clan SC peptidases. POP is one of the best characterized enzymes from family S9, and it has been suggested that it plays a putative role in neuropeptide metabolism (Page and Di Cera, 2008).

Clan SK peptidases are mostly represented in bacteria and have the important purpose of maintaining intracellular protein levels. The catalytic unit of clan SK enzymes is varied, but in ClpP peptidase, an important enzyme for protein turnover in *E. coli*, the conventional catalytic triad is used in a novel arrangement of residues in the polypeptide chain (Ser/His/Asp) (Page and Di Cera, 2008).

Despite the extensive studies carried out on serine peptidases, in trypanosomatids there are just a few members identified and well characterized and only two have been used as chemotherapeutic targets, oligopeptidase B, a member of POP family found in the cytosol of *T. cruzi*, *T. brucei*, *T. congolense* and *L. amazonensis*, and POP Tc80, identified in *T. cruzi* (Coetzer *et al*., 2008, Beatriz Vermelho *et al*., 2007).

POP Tc80 activity is detectable in all developmental stages of *T. cruzi*. The enzyme is secreted by trypomastigotes and is also associated with the parasite's flagellar pocket. This enzyme's activity is specifically directed to major components of the extracellular matrix such as type I and IV collagen and also fibronectin. This suggests that POP Tc80 may be involved in the host cell invasion by cleavage of collagen and interaction with the integrin receptors, or it may assist in the parasite's migration through the extracellular matrix, providing its access to any cell of the host organism (Beatriz Vermelho *et al*., 2007).

Oligopeptidase B, or OPB is a serine peptidase member or family S9 from clan SC. Although it exhibits trypsin-like substrate specificity, this enzyme has some

properties that place it in the serine peptidases group, namely the sensitivity to inhibitory molecules of serine peptidase activity and the insensitivity to inhibitors of cysteine peptidase activity (Beatriz Vermelho *et al*., 2007). To date, its biological role has not been established with accuracy, although it has been identified as an important virulence factor in trypanosomatids (Coetzer *et al*., 2008).

In *T. cruzi*, oligopeptidase B is a cytosolic peptidase associated with the parasite's ability to invade mammalian cells and the establishment of infection (Beatriz Vermelho *et al*., 2007). For the invasion to occur, the parasite must recruit the host's lysosome, a process dependent on the intracellular concentration of free calcium ($[Ca^{2+}]i$). Infective trypomastigotes trigger the increase of intracellular calcium in mammalian cells, essential for the parasite's invasion and associated with the activity of the parasite's OPB. Inhibition of *T. cruzi* OPB activity using protease inhibitors or specific antibodies results in inhibition of the Ca^{2+} signaling activity. The same effect is observed in OPB null mutant trypomastigotes, resulting in defective cell invasion and establishment of infection in mice (Coetzer *et al*., 2008, Caler *et al*., 1998, Burleigh *et al*., 1997).

In *Leishmania* is possible that OPB mediates the activation of cytosolic proteins that can damage the membrane of macrophages through the formation of transmembrane pores (Leishporins) (Coetzer *et al*., 2008). Generation of OPB null mutants in *L. major* led to a decrease of the metacyclic promastigotes population and to a reduction of the ability to infect macrophages *in vitro*.

However, when used to infect mice, OPB null mutants showed no significant effect, suggesting that the enzyme itself is not an important virulence factor in *L. major*, contrasting with the observed in trypanosomes (Munday *et al*., 2011).

T. brucei oligopeptidase B is released by the parasites into the mammalian bloodstream and there it stays acting on the host's peptide hormones and promoting the pathogenesis. Despite the presence of numerous peptidase inhibitors in the mammalian bloodstream, the enzyme retains full catalytic activity since it's not inhibited by the plasma serpins. Once in the bloodstream, the enzyme acts on cleaving regulatory peptides present in the host's serum, suggesting a possible role of *T. brucei* OPB in the

disruption of the host's hormone metabolism during infection (Coetzer *et al*., 2008, Beatriz Vermelho *et al*., 2007, Morty *et al*., 1999).

There are no oligopeptidase B homologous identified in mammals, but the trypanosomal enzyme has similar specificity to several mammalian plasma serine peptidases, making it difficult to design highly specific inhibitors (Beatriz Vermelho *et al*., 2007, Troeberg *et al*., 1996).

1.3.2 Natural Inhibitors of Peptidases

Peptidases catalyze mainly irreversible hydrolytic reactions and can be potentially hazardous to the environment. As a result, their activity has to be strictly regulated (Bode and Huber, 2000).

This can be done in the living organism by several mechanisms, such as, regulation of gene expression; activation of inactive zymogens; targeting to specific cellular compartments; post-translational modifications; and inhibition by endogenous inhibitors (López-Otín and Bond, 2008, Rawlings *et al*., 2004).

The number of endogenous inhibitors identified to date is extremely low when compared to the number of peptidases and they all seem to be proteins, although some microorganisms can produce small non-protein molecules capable of inhibiting proteolytic activity of host peptidases (López-Otín and Bond, 2008, Bode and Huber, 2000). The disparity of peptidases and peptidase inhibitors numbers results from the low specificity of inhibitors and from the fact that some peptidases have their proteolytic activity regulated through another mechanism and are not inhibited by any endogenous inhibitor (López-Otín and Bond, 2008).

Peptidases inhibitors can be classified into families according to the catalytic class of the target peptidase. There are 67 families of peptidase inhibitors identified in MEROPs database. From these, 49 families are grouped into 38 different clans according to their tertiary structure. No clan was assigned to the remaining 18 families, once their tertiary structure is yet to be solved (Rawlings, 2010).

The classification of peptidase inhibitors can also be based on the mechanism of inhibition in four different groups. Canonical inhibitors include serine peptidase inhibitors (Serpins) and act on the target peptidase by binding to the active site of the enzyme in a way that resembles the substrate. Exosite-inhibitors group includes cysteine peptidase inhibitors (Cystatins) and some thrombin inhibitors. These inhibitors bind to a region adjacent to the active site of the target peptidase, preventing the access of substrate to the active site, without blocking the catalytic residues. (López-Otín and Bond, 2008) A third group of endogenous inhibitors use an inhibition mechanism that combines both the canonical and the exosite-binding mechanism. This group includes the TIMPs (Tissue Inhibitors of Metalloproteinases), which are natural inhibitors of matrix metalloproteinases found in most tissues and body fluids. Finally a fourth group of inhibitors binds to a region distantly located from the active site, inhibiting the peptidase by preventing its dimerization and blocking its activity. (López-Otín and Bond, 2008)

Inhibition mechanisms must be coordinated to ensure that the right substrates are processed at the right time and place and thus preventing the deregulation of proteolytic activity that can be potentially harmful for the cell. (López-Otín and Bond, 2008) Understanding how inhibitors and peptidases interact with each other may be helpful to discover new approaches for the design of synthetic inhibitors to use as therapeutic drugs. (Rawlings *et al*., 2004)

1.3.2.1 Inhibitors of Cysteine Peptidases

In plants and mammals, the activity of cysteine peptidases is controlled by endogenous inhibitors of the cystatin and thyrotropin classes. (López-Otín and Bond, 2008)

Members of the cystatin superfamily are low molecular, single chain proteins that bind reversibly to the cysteine peptidases, forming tight-binding complexes (Beatriz Vermelho *et al*., 2007). In lower eukaryotes, such as protozoan parasites, there is no evidence of the existence of cystatin-like inhibitors, despite the presence of large amounts of cysteine peptidases. Studies focused on identifying endogenous inhibitors of

cysteine peptidases in parasitic protozoa led to the discovery of inhibitory activity against papain in leishmania cell lysates. Nevertheless the responsible molecule was not recognized and in 2001, using *T. cruzi* as a model, a protein capable of inhibiting papain-like cysteine peptidases was finally identified in all life stages of the parasite. (Monteiro *et al*., 2001)

The endogenous inhibitor identified as chagasin is a low molecular weight, thermo-resistant protein that acts as a tight-binding reversible inhibitor with strong affinity to cruzipain and other papain-like cysteine peptidases. Its biochemical properties are similar to those of cystatins but its primary structure differs significantly from the members of the cystatin superfamily or from any other known protein (Monteiro *et al*., 2001, Rigden *et al*., 2001). In fact, chagasin adopts an unusual immunoglobulin-type fold (Rigden *et al*., 2001), exhibiting high sequence similarity with variable light chains, and may be the result of horizontal gene transfer from a host animal (Lima and Mottram, 2010, Rigden *et al*., 2001).

Homologous of chagasin were found in several eukaryotes, bacteria and archaea, being the first peptidase inhibitors to be identified in prokaryotes. The sequence is highly conserved and all chagasin-like inhibitors are typically 110-130 aminoacids long with no additional domains with a conserved core structure consisting of seven β-strands plus one or two more potential β-strands. (Rigden *et al*., 2002) By NMR spectroscopy it was determined that members of the chagasin family have several conserved residues located at one end of the molecule distributed along three exposed loops, L2, L4 and L6.

These loops contain the NPTTG motif responsible for inhibiting papain and are most likely involved in binding to target peptidases, with the conserved residues T31 and T32 in loop L2 involved in the formation of key hydrogen bonds with the peptidase near the catalytic triad (Lima and Mottram, 2010, dos Reis *et al*., 2008, Salmon *et al*., 2006).

The mode of interaction with cysteine peptidases is also conserved and exhibits similarities to the mode of interaction between members of the cystatin superfamily and their cysteine peptidases. (Rigden *et al*., 2002) These findings resulted in the classification of the chagasin-like peptidase inhibitors as clan IX, family I42 in the

MEROPS database a new family of inhibitors of cysteine peptidases, commonly designated ICP (*I*nhibitors of *C*ysteine *P*eptidases). Representatives of the ICP family were also identified and characterized in *T. brucei*, *L. mexicana* and *L. major*, all effective inhibitors of clan CA, family C1 cysteine peptidases from mammals and protozoa. (Santos *et al*., 2005, Sanderson *et al*., 2003)

T. cruzi parasites depend on their major lysosomal cysteine peptidase, cruzipain, to invade and proliferate within mammalian host cells. Studies with synthetic inhibitors have suggested that cruzipain activity is crucial for the parasite's growth and differentiation, by blocking the maturation of the pro-enzyme, resulting in the accumulation of unprocessed pro-cruzipain in the late Golgi vesicles in epimastigotes (Monteiro *et al*., 2001).

The co-localization of cruzipain and chagasin in the Golgi complex and in reservosomes (a late endocytic compartment of *T. cruzi* and main deposit of active cruzipain) suggests that the inhibitor must combine with the mature peptidase inside these compartments, once the maturation of cruzipain is thought to occur inside the Golgi. The overexpression of chagasin in *T. cruzi* epimastigotes results in decreased cruzipain activity, reduced differentiation to metacyclic trypomastigotes and increased resistance of the parasite to synthetic cysteine peptidase inhibitors.

Trypomastigotes overexpressing chagasin have also revealed to be less infective in culture, suggesting that chagasin modulates *T. cruzi* differentiation and invasion of mammalian cells through the regulation of endogenous cruzipain activity (Lima and Mottram, 2010, Santos *et al*., 2005).

In *Leishmania mexicana* the deletion of ICP produced no significant phenotype *in vitro* with null mutant growing normally and infecting macrophages as wild type parasites. Additionally, the processing, trafficking and activity of cysteine peptidases from null mutants was similar to the wild type and only a small proportion of ICP co-localized with the parasite's CPA and CPB, the only peptidases to which ICP binds to.

However, null mutants were less virulent to mice which suggested that ICP plays a role in protecting the parasite from the host's hostile environment rather than modulating the activity of the parasites cysteine peptidases (Lima and Mottram, 2010, Besteiro *et al*., 2004).

In *T. brucei*, the importance of cysteine peptidases as targets for antitrypanosomal chemotherapy was established by studies in which small molecule inhibitors were used to control the activity of cysteine peptidases *in vitro* and *in vivo*.

The peptidyl inhibitor Z-Phe-Ala-diazomethyl ketone (Z-Phe-Ala-CHN_2) killed BSF *T. b. brucei* in culture. Furthermore, the treatment of mice infected with *T. brucei* resulted in decreased parasitemia and extended survival than control mice (Scory *et al*., 1999).

Another study using several irreversible cysteine peptidase inhibitors revealed that these molecules have an effect in the activity of brucipain, acting as a trypanocidal agent for cultured bloodstream forms of *T. brucei* and emphasizing the biological significance of brucipain for the parasite's biology (Troeberg *et al*., 1999).

After being identified and characterized, ICP was further investigated in order to determine its function in *T. brucei*. Although it is expressed at low levels and its localization remains unknown, it was determined that ICP regulates the endogenous cysteine peptidases.

The deletion of ICP in *T. brucei* led to increased cysteine peptidase activity with no change in the expression levels of brucipain and cathepsin B. ICP null mutants also exhibit slower growth in culture than wild type without any perceptible morphological change or defect in the cell cycle progression.

In contrast, mice infected with ICP null mutants showed higher parasitemia and lower survival rates than mice infected with wild type parasites, meaning that the absence of ICP results in increased virulence of the parasites *in vivo* (Santos *et al*., 2007).

Differentiation of *T. brucei* bloodstream form to procyclic form *in vitro* was also affected by the deletion of ICP. Parasites lacking this inhibitor have an accelerated rate of differentiation in the presence of cis-aconitate, and return to normal differentiation rates in the presence of synthetic CP inhibitors, suggesting that the differentiation of *T. brucei* BSF to procyclic form, and the coat exchange associated with it, is mediated by cysteine peptidase activity (Santos *et al*., 2007).

These data suggest that ICP regulates the endogenous CP activity and may play an important role in the parasite-host interaction.

1.3.2.2 Inhibitors of serine peptidases

Serpins are a large group of proteins that can be found mainly in plants, animals and viruses. Most of these proteins are serine peptidase inhibitors that target chymotrypsin-like serine peptidases, such as thrombin, trypsin and human neutrophil elastase, comprising the largest and most diverse family of peptidase inhibitors. Because they regulate several physiological processes activated by proteolytic cascades, including coagulation or inflammation and complement pathways, serpins have been extensively studied in mammals (Otlewski *et al.*, 1999).

As with cystatins, there are no predicted serpins in the genome of trypanosomatids. The identification of chagasin in *T. cruzi* triggered the search of other natural inhibitors of peptidases, leading to the discovery of a group of inhibitors of serine peptidases homologous to ecotin (Lima and Mottram, 2010).

Ecotin is a heat stable 18 kDa protein, first identified in the periplasm of *E. coli*, capable of inhibiting a wide range of serine peptidases from family S1A such as trypsin, chymotrypsin, elastase, kallikrein and blood clotting factor Xa (Gillmor *et al*., 1995, McGrath *et al*., 1995, Ulmer *et al*., 1995, Chung *et al*., 1983). It consists of two identical subunits, each one containing an enzyme's binding site, therefore establishing stable tetrameric complexes with the target peptidases. (Chung *et al*., 1983)

Usually, an inhibitor binds to its target peptidase through a reactive site loop that interacts directly with the peptidase's active site, in a substrate-like conformation, forming a one-to-one complex. This binding site represents the only interaction between inhibitor and peptidase and is normally the principal responsible for the inhibitor's specificity towards a particular peptidase (Yang *et al*., 1998, McGrath *et al*., 1995).

Ecotin is different from other serine peptidase inhibitors once it exhibits a secondary binding site. With a shape resembling that of an antibody binding site, this smaller site is the result of the dimer arrangement of ecotin. Two ecotin monomers form a dimer through their C-termini that binds to two peptidase molecules at opposite ends. While each monomer binds to the peptidase active site through the "primary binding site" consisting of the reactive loop (80s loop and 50s loop), the other monomer contacts with the C-terminal region of the peptidase through the "secondary binding

site" that includes surface loops 60s and 110s, establishing a unique inhibitor-peptidase interaction in which each ecotin monomer contacts another monomer and two peptidases. (Figure 1.7)

The combination of both binding sites may be the responsible for the affinity of ecotin towards different peptidases, allowing it to bind a wider range of targets (Eggers *et al*., 2001, Yang *et al*., 1998, Gillmor *et al*., 1995, McGrath *et al*., 1995).

Given the lack of peptidases sensitive to ecotin action in *E. coli*, and its specificity towards pancreatic digestive peptidases, it was suggested that the inhibitor may protect the cell against the exogenous peptidase activity in the mammalian gut (Chung *et al*., 1983). Further studies determined that Ecotin may play an important role in defending the bacteria against the effects of neutrophil elastase, a bactericidal agent secreted by neutrophils (Eggers *et al*., 2004) and modulates the biological activity of thrombin (Castro *et al*., 2006).

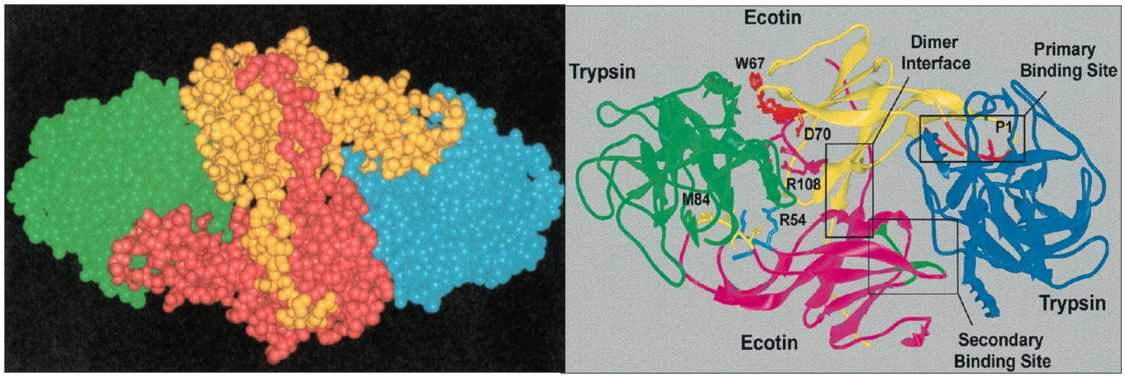

Figure 1.7 – Representation of the ecotin-trypsin tetrameric complex

A. Spatial organization of the complex showing one ecotin monomer contacting another monomer (represented in yellow and pink) and interacting with two molecules of trypsin, represented in green and blue (McGrath *et al*., 1995) **B.** Network of interactions between both ecotin monomers and between the ecotin monomers and the trypsin molecule showing the primary binding site and the secondary binding sites (Yang *et al.*, 1998)

To the Ecotin-like inhibitors of peptidases identified in trypanosomatids was given the generic name of ISPs (Inhibitors of Serine Peptidases). There are three ISP genes identified in *L. major* named ISP1, ISP2 and ISP3. Only ISP2 is common to the three species of trypanosomatids, while ISP1 can also be found in *T. brucei* and ISP3 seems to be restricted to *Leishmania* species.

These genes show significant similarity and high degree of conservation of the primary and secondary binding sites (Lima and Mottram, 2010). Like in *E. coli*, there are no peptidases belonging to S1A family encoded in the genome of Trypanosomatids, suggesting that the inhibitors must be targeting the host's serine peptidases (Lima and Mottram, 2010, Eschenlauer *et al.*, 2009, Ivens *et al.*, 2005).

Research focused on the biological role of ISPs in Trypanosomatids is scarce and very little is known about these inhibitors and their function. In *L. major*, ISP1 and ISP2 genes encode a 16.5 kDa and a 17.5 kDa, respectively, and ISP3 encodes a larger protein of about 41.8 kDa. While ISP2 is expressed throughout the parasite's life cycle, with higher levels in metacyclic promastigotes and amastigotes, ISP1 is only expressed in procyclic and metacyclic promastigotes and ISP3 could not be detected in any life stage. This expression pattern suggests that while ISP1 may have a role in the sandfly vector, ISP2 may play its part in the infection of the mammalian host. (Eschenlauer *et al*., 2009)

Generation of ISP2/3 null mutants (Δ*Isp*2/3) led to normal growth and differentiation *in vitro*, but mutant parasites were internalized more efficiently by macrophages, due to the upregulation of phagocytosis by a serine peptidase dependent mechanism. Once inside the macrophages, Δ*Isp*2/3 promastigotes differentiate into amastigotes but have decreased ability to multiply.

Infection of BALB/c mice with Δ*Isp*2/3 parasites results initially in higher parasitemia that becomes equivalent to the wild type parasites as infection progressed. These results suggest that ISPs of *L. major* have an effect in the early infection of the mammalian host and, since the expression of ISP3 could not be detected in any life stage of the parasite, this effect is most probably due to the activity of ISP2 (Eschenlauer *et al*., 2009).

The effect of ISPs in the interaction between macrophages and *Leishmania* was also observed in C57/B6 mice, where Δ*Isp*2/3 parasites were phagocytosed more efficiently than wild type parasites, via the combined action of complement type-3 receptor (CR3), toll-like receptor 4 (TLR4) and neutrophil elastase (NE), the primary target for ISP2 in macrophages.

NE is not only required to promote the parasite's initial uptake and death by macrophages, but is also associated with reduced parasitemia in later stages of the infection, suggesting that ISP2 exists in *Leishmania* to regulate the activity of NE allowing the infection to successfully establish and progress (Faria *et al*., 2011).

Very little is known about ISPs in *T. brucei.* The identification of *L. major* ISP2 targets and the determination of its role in macrophage infection and parasite survival is extremely valuable information that can be used as a starting point for the assessment of ISPs biological role in *T. brucei*, one of the main issues addressed in present research project.

Chapter 2

Materials and Methods

2.1 Bacterial Cultures

2.1.1 Strains used

For general recombinant DNA techniques, the cells used were competent *E. coli* XL1–Blue (Sratagene), genotype *rec*A1 *end*A1 *gyr*A96 *thi*-1 *hsd*R17 *sup*E44 *rel*A1 lac, tetracycline resistant. As these cells are endonuclease and recombination deficient, the DNA quality and plasmid their stability is greatly improved. For the expression of recombinant proteins the strain used was *E. coli* BL21 (D3) (Novagen), an *E. coli* strain containing an IPTG inducible T7 RNA polymerase and specifically designed for high level of expression of recombinant proteins in pET vectors.

2.1.2 Bacterial culture and storage

E. coli cells were spread onto agar plates containing the appropriate antibiotics (100 µg/ml of ampicillin; 50 µg/ml of kanamycin or 40 µg/ml of chloramphenicol) and incubated overnight at 37°C. Single colonies were used to inoculate liquid Luria-Bertani broth medium (LB medium) with the appropriate antibiotics and grown overnight at 37°C, shaking. For long term storage, 500 µl of an overnight culture were mixed with equal volume of 2% (W/V) peptone, 40% (V/V) glycerol and stored at -80°C.

2.1.3 Preparation of *E. coli* competent cells

Competent cells were prepared using rubidium chloride. A single colony of the desired strain was inoculated into 5 ml of liquid LB medium and grown overnight at 37°C, shaking. This overnight culture was diluted 1:1000 into 50 ml of fresh LB medium and grown at 37°C, shaking, until it reached an optical density of 0.6 at 600 nm. The culture was then incubated on ice for 10 minutes and centrifuged at 2000 g for

15 minutes, at 4°C. The bacterial pellet was gently resuspended in 16 ml of cold RF1 solution (100 mM RbCl, 50 mM $MnCl_2$.4H2O, 30 mM potassium acetate pH 7.5, 10 mM $CaCl_2$ (dihydrate), 15 % glycerol, adjusted to pH 5.8 using acetic acid, filter sterilized), incubated on ice for 15 minutes and centrifuged as before. The pellet was then resuspended in 4 ml of RF2 solution (10 mM MOPS pH 6.8, 10 mM RbCl, 75 mM $CaCl_2$ (dihydrate), 15 % (w/v) glycerol, pH adjusted to 6.8 with NaOH, filter-sterilized) and incubated on ice for 1 hour. The cells were aliquoted for single use and snap frozen in ethanol on dry ice. Aliquotes were stored at -80 °C.

2.2 Molecular Biology Techniques

2.2.1 Polymerase Chain Reaction (PCR) and oligonucleotides used

PCRs for bacterial colony screening, experiment optimization or other experiments that did not require proof reading activity were performed with *Taq* DNA polymerase (New England Biolabs). For cloning or sequencing, PCRs were performed using high fidelity proof reading enzymes such as *Pfu*Turbo (Stratagene) and Phusion (Finnzymes).

The standard PCR reaction was typically performed using 2.5 µl of 10× PCR Mix (1.13 mg/ml BSA, 450 mM Tris pH 8.8, 110 mM ammonium sulphate, 45 mM $MgCl_2$, 68.3 mM β-mercaptoethanol, 44 mM EDTA pH 8.0, 10 mM dATP, 10 mM dCTP, 10 mM dGTP, 10 mM dTTP). To each PCR reaction were added 10 pmol of each oligonucleotide primer, 100 ng of DNA template and 1 unit of *Taq* DNA polymerase, in a final volume of 25 µl. For the PCR reactions using high fidelity enzymes, volumes and concentrations of each component were adjusted according to the manufacturer's instructions.

PCRs were performed in a Hybaid PCR Express thermocycler and the PCR conditions were optimized for each reaction, adjusting the annealing temperature according to the melting temperature (Tm) of the primers and the extension time

according to the sequence length. The typical PCR program used was composed by an initial denaturation step of 5 minutes at 95°C followed by 25-30 cycles of 30 seconds of denaturation at 95°C, 30 seconds of annealing (Tm of primers - 2°C) and extension at 72°C (1 minute for each kb of DNA sequence to amplify).

All oligonucleotide primers used in this study were designed using Vector NTI software (Invitrogen) and produced by Eurofins MWG Operon (Ebersberg, Germany). Detailed oligonucleotide primers used in this study are listed on Table 2.1.

2.2.2 Agarose gel electrophoresis

DNA analysis by agarose gel electrophoresis was carried out using 1% gel (w/v) of UltraPure agarose (Invitrogen) in 0.5× TBE buffer (20 mM Tris, 20 mM boric acid, 0.5 mM EDTA, pH 7.2).

Gels were prepared by boiling the agarose solution in a microwave. After cooling down, Sybr safe™ DNA stain (Invitrogen) was added to allow DNA visualization.

The gel was then cast and left to solidify. Samples were prepared with 6× DNA loading dye (0.25% (w/v) bromophenol blue, 0.25% (w/v) xylene cyanol FF, 30% (v/v) glycerol, in H_2O) and run at 100 V in Life Technologies Horizon gel tanks.

A 1 kb molecular weight marker (Invitrogen) was used at a concentration of 0.5 µg per lane as a reference to determine DNA size and concentration of the DNA fragments analyzed.

To visualize the DNA, gels were exposed to UV light using a BioRad Gel-Doc imager with Quantity One software.

Whenever the DNA was to be excised from a gel, a DarkReader blue light transiluminator was used. DNA extractions from agarose gels were performed using a Gel Extraction kit (Qiagen) according to the manufacturer's instructions.

Oligo Number	Target sequence	Direction	Sequence	Restriction Sites
ISP1 knockout constructs				
OL2417	Tb927.5.1730	Forward	G**GCGGCCGC**TGCAGTGACAGACGGCAGGAG	*Not*I
OL2418	5' ISP1 flanking region	Reverse	G**TCTAGA**TGTCAGTATTGTGCGAACGGG	*Xba*I
OL2419	Tb927.5.1730	Forward	T**GGGCCCC**ACCGAAAGTTGATCCCGTAC	*Apa*I
OL 3257	3' ISP1 flanking region	Reverse	C**GGGCCCCTCGAG**TGAGAAGGGTTCTCCTACCACT	*Apa*I; *Xho*I
ISP2 knockout constructs				
OL2421	Tb927.5.1880	Forward	T**GCGGCCGC**GAGCATGAATTAGGCAGAATG	*Not*I
OL2422	5' ISP2 flanking region	Reverse	G**TCTAGA**TCGCTTCCTTTCGCGGGTAAC	*Xba*I
OL2423	Tb927.5.1880	Forward	T**GGGCCC**TCGTTACAACAGCCAACTACC	*Apa*I
OL3258	3' ISP2 flanking region	Reverse	CC**GGGCCCCTCGAG**ACGCACACTGACGGCCACAC	*Apa*I; *Xho*I
ISP1 and ISP2 knockout analysis				
OL2508	Tb927.5.1730	Forward	GCAGTGAATCGCCAAGAATC	
OL2509	ISP1 locus	Reverse	GATTGAAGGAACCAATACAC	
OL2510	Tb927.5.1880	Forward	GAAGGTGAAGGTGAGGCAAC	
OL2511	ISP2 locus	Reverse	TGCGGAAGGCAACAAAAGAC	
OL13	Hygromycin resistance	Reverse	GGTGAGTTCAGGCTTTTTCA	
OL14	cassette	Forward	CGTCCGAGGGCAAAGGAATA	
OL1360	Neomycin resistance c	Forward	GTGCTTTACGGTATCGCCGC	
OL1361	assette	Reverse	CCGGACAGGTCGGTCTTGAC	
OL536	Blasticidin resistance	Reverse	TTGAGACAAAGGCTTGGCCAT	
OL537	cassette	Forward	GGTTATGTGTGGGAGGGCTAA	
OL15	Puromycin resistance	Reverse	CCGTGGGCTTGTACTCGGTCA	
OL16	cassette	Forward	ACCCGCAAGCCCGGTGCCTGA	
ISP1 re-expression constructs				
OL3635	Tb927.5.1730	Forward	GC**GATATC**ATGTTTGGTTCCCGGAAGGC	*Eco*RV
OL3636	Tb ISP1	Reverse	GC**GATATC**TTATTCTTCGGCTTTCTTGG	*Eco*RV
ISP2 re-expression constructs				
OL3637	Tb927.5.1880	Forward	GC**GATATC**ATGACAGACCGACCTCCGAC	*Eco*RV
OL3638	Tb ISP2	Reverse	GC**GATATC**CTAACCCGCCCTCTCCTCGA	*Eco*RV
In situ N-terminal YFP tagging constructs				
OL2773	Tb927.5.1730	Forward	CC**AAGCTT**CCGCCACCATGTTTGGTTCCCGG	*Hind*III
OL2774	Tb ISP1	Reverse	GC**GGATCC**AGAACCTTATTCTTCGGCTTTCTTG	*Bam*HI
OL2771	Tb927.5.1880	Forward	CC**AAGCTT**CCGCCACCATGACAGACCGACCT	*Hind*III
OL2772	Tb ISP2	Reverse	CG**GGATCC**AGAACCCTAACCCGCCCTCTCCTC	*Bam*HI
ICP site directed mutagenesis construct				
OL2765	Tb927.8.6450	Forward	CGAAGCCACGTGTAGCCTGGGTTGCTCTCAAG	
OL2766	Tb ICP	Reverse	CTTGAGAGCAACCCAGGCTACACGTGGCTT	

Table 2.1 – Oligonucleotides used in this study

2.2.3 Cloning of PCR products

The PCR products were sub-cloned into commercial vectors such as pGEM-T-Easy (Promega) and pPCR-Script (Stratagene) to establish stable DNA propagation. When using the pGEM-T-Easy Vector System, after a PCR performed with a high fidelity proof reading enzyme, the PCR product was incubated at 72°C for 15 minutes

with 0.5 units of *Taq* DNA polymerase (A-tailing step needed to allow the ligation of the A-tail from the PCR product to the T-overhangs at the end of the vector).

The pPCR-Script vector has blunt ends and can be used for subcloning directly after the PCR with a high fidelity proof reading polymerase. For either subcloning systems, 2 µl of PCR product was ligated with the vector according to the manufacturer's instructions and transformed into competent *E. coli* XL1-Blue cells. Transformants were then selected as described on section 2.2.7.

2.2.4 Restriction endonuclease digestion

DNA was digested using restriction enzymes from New England Biolabs and their specific buffers. Digestion reactions were supplemented with BSA and carried out at room temperature or 37 °C, for 1-4 hours according to the manufacturer's instructions. Digested DNA was visualized by agarose gel electrophoresis as described in section 2.2.2, and purified from the gel using a Gel Extraction kit (Qiagen) when required.

2.2.5 Ligation of DNA fragments

Ligations were performed using T4 DNA ligase and T4 DNA ligase buffer (New England Biolabs) according to the manufacturer's instructions.

Typically, both digested plasmid and insert were purified from agarose gels using a Gel Extraction kit (Qiagen) and added to a 10 µl reaction in several insert:vector ratios.

Reactions were incubated overnight at 16 °C or 1 hour at room temperature. For blunt ended ligations, digested plasmids were treated with CIP (calf intestinal alkaline phosphatase, New England Biolab) to dephosphorylate the DNA ends and prevent self ligation.

2.2.6 Transformation of DNA fragments in *E. coli*

Transformation of plasmid DNA into competent *E. coli* cells was performed by heat shock. 50 µl of competent cells were mixed with 1 µl of isolated plasmid or 5 µl of ligation reaction and kept on ice for 20 minutes. The transformation reaction was heat shocked in a water bath at 42 °C for 40 seconds and placed immediately on ice for 5 minutes before plating the cells on agar plates.

2.2.7 Selection of transformants

Selection of successful transformants was done by antibiotic selection and the insertion of a PCR product in the vector was assessed by blue/white colony screening. Agar plates were prepared with the appropriate antibiotic (100 µg/ml of ampicillin, 50 µg/ml of kanamycin or 40 µg/ml of chloramphenicol) and supplemented with 80 µg/ml X-Gal and 0.5 mM of IPTG. Plates were incubated overnight at 37 °C and white colonies were selected for further analysis by colony PCR or plasmid purification and restriction digestion.

2.2.8 Colony screening by PCR

To confirm the PCR product integration, single white colonies were picked from the agar plate with a sterile pipette tip and resuspended in 20 µl of PCR reaction mix, after being patched onto a fresh agar plate for reference. PCR was performed as described previously (section 2.2.1), using T3/T7 or M13F/M13R oligonucleotides when screening for an insert in the pPCR-Script or pGEM-T-Easy vector or specific oligonucleotides when using different plasmids, to determine the presence of an appropriate size insert. PCR products were analyzed on agarose gel and the relevant colonies used to inoculate 5 ml of LB medium. After an overnight incubation at 37 °C, the bacterial culture was stored at - 80 °C or used to purify the plasmid DNA.

2.2.9 Plasmid DNA purification

To purify the plasmid DNA, 3 ml of bacterial culture of the positive clones previously screened by colony PCR were processed with a MiniPrep kit (Qiagen), according to the manufacturer's instructions. DNA was eluted in water, quantified using an Eppendorf BioPhotometer and stored at - 20 °C. When larger amounts of DNA were needed, as for DNA transfections for example, 50 ml of bacterial culture was grown overnight at 37 °C and the DNA was extracted using a MidiPrep kit (Qiagen).

2.2.10 DNA sequencing

DNA sequencing was performed by the Sequencing Service of the University of Dundee (www.dnaseq.co.uk) and results were analyzed using vector NTI application, ContigExpress (Invitrogen).

2.2.11 DNA preparation for transfection

Plasmid DNA used to transfect *T. brucei* was linearised by digestion with the appropriate restriction enzymes and precipitated with 0.1 volumes of 3 M sodium acetate pH 5.2 and 0.7 volumes of isopropanol overnight at - 20 °C. The precipitated DNA was centrifuged at 13000 × g for 20 minutes at 4 °C and the pellet was washed with cold 70 % ethanol for 15 minutes at 13000 × g. The DNA pellet was then dried and resuspended in sterile H_2O.

2.2.12 Site directed mutagenesis

To delete specific aminoacids of previously expressed proteins, targeted mutations were introduced in the DNA sequence by site directed mutagenesis, using the

Quick Change Mutagenesis Kit (Stratagene), according to the manufacturer's instructions. All DNA sequences generated were confirmed by sequencing before protein expression.

2.2.13 Plasmid generation

Plasmid	Plasmid	Description
pGL1830	pGL1493	*T. brucei* ICP (Tb927.8.6450) protein expression mutated binding site; Kan^R
pGL1688	pGL1224	*T. brucei* ISP1 (Tb927.5.1730) knock out; Amp^R/Hyg^R
pGL1689	pGL1217	*T. brucei* ISP1 (Tb927.5.1730) knock out; Amp^R/Neo^R
pGL1947	pGL1689	*T. brucei* ISP1 (Tb927.5.1730) knock out; Amp^R/Bsd^R
pGL1948	pGL1689	*T. brucei* ISP1 (Tb927.5.1730) knock out; Amp^R/Pur^R
pGL1959	pGL1688	*T. brucei* ISP2 (Tb927.5.1880) knock out; Amp^R/Hyg^R
pGL1960	pGL1689	*T. brucei* ISP2 (Tb927.5.1880) knock out; Amp^R/Neo^R
pGL2049	pGL884	*T. brucei* ISP1 (Tb927.5.1730) re-expression; $Amp^R/Phleo^R$
pGL2050	pGL884	*T. brucei* ISP2 (Tb927.5.1880) re-expression; $Amp^R/Phleo^R$

Table 2.2 – Plasmids generated and used in this study

2.2.13.1 Mutant ICP construct

The deletion of 2 amino acids in the binding site, leading to an inactive ICP, was performed by site directed mutagenesis of ICP expression plasmid, pGL1493, as described in section 2.2.12. Primers used were OL2765 and OL2766, both containing the mutation to introduce in the ICP sequence.

The mutant ICP sequence was confirmed by sequencing and the plasmid generated was named pGL1830 (Table 2.2).

2.2.13.2 ISP knock out constructs

The 5’ and 3’ ISP1 and ISP2 flanking regions were amplified from *T. brucei rhodesiense* genomic DNA by PCR using *Taq* DNA polymerase with primers OL2417/OL2418 for 5’ISP1, OL2419/OL3257 for 3’ISP1; OL2421/OL2422 for 5’ISP2 and OL2423/OL3258 for 3’ISP2 (Table 2.2). The resulting PCR products were individually sub-cloned into pGEM-T-Easy vector and sequences were confirmed by sequencing. 5´ and 3’ISP1 flanking regions were digested from the sub-cloning vectors with the enzymes *Not*I/*Xba*I and *Apa*I/*Xho*I, respectively, and sequentially ligated into pGL1224 and pGL1217 previously digested with the same enzymes. Plasmids generated were named pGL1688 and pGL1689 (Table 2.2). These plasmids were then used as backbones for the generation of ISP2 knock out constructs and for switching the resistance marker in the ISP1 knock out constructs.

The 5’and 3’ISP2 flanking regions were digested from pGEM-T-Easy vector with *Not*I/*Xba*I and *Apa*I/*Xho*I, respectively, and ligated into pGL1688 and pGL1689, generating pGL1959 and pGL1960 (Table 2.2).

For switching the resistance markers, pGL1689 was digested with *Eco*RI to remove neomycin resistance gene. In parallel, pGL1124 and pGL808 were also digested with *Eco*RI to excise blasticidin resistance gene and puromycin resistance gene, respectively. These two fragments were then ligated into the pGL1689 backbone to generate pGL1947 and pGL1948 (Table 2.2).

2.2.13.3 ISP1 and ISP2 re-expression constructs

To generate ISP1 and ISP2 re-expression constructs, both ISP genes were amplified from *T. brucei rhodesiense* genomic DNA using *Pfu* Turbo polymerase and cloned into pPCR Script vector. After confirming the DNA sequence, the ISP1 and ISP2 were excised from the sub-cloning vector using *Eco*RV and ligated into pGL884 previously treated with the same enzyme, generating plasmids pGL2049 and pGL2050, respectively (Table 2.2).

2.2.14 Southern Blotting

Southern Blotting was used to confirm the ISP1 and ISP2 gene deletion in the *T. brucei rhodesiense* genome. For each cell line generated, approximately 5µg of genomic DNA was digested overnight with the appropriate enzymes. The enzymes were chosen according to the size of fragments originated, in order to allow the visualization of the difference between wild type and knock out alleles in the heterozygous and homozygous cell lines. Digested DNA from the different cell lines analyzed was electrophoresed at a low voltage in a large, thick 0.8% agarose gel stained with SYBR-Safe (Invitrogen). The gel was photographed alongside a fluorescent ruler to allow the correlation of DNA sizes in the ladder with the migration distance. The gel was washed for 10 minutes in 0.25 M HCl to remove purines and rinsed in distilled water. After depurinated, the gel was washed with denaturation buffer (1.5 M NaCl, 0.5 M NaOH) for 15 to 30 minutes before rinsed again with distilled water. Finally, the gel was washed with neutralization buffer (3M NaCl, 0.5 M Tris-HCl, pH 7.0) for 30 minutes and rinsed with distilled water. All washings were performed with gentle shaking.

DNA was then transferred overnight to a nylon membrane by capillary force. The gel was placed on a blotting paper wick, the ends of which were immersed in 20× SSC buffer (3 M NaCl, 0.3 M sodium citrate pH7.0). The membrane (Hybond-N nylon membrane, GE Healthcare) was pre-soaked in distilled water and then in 20× SSC buffer and then placed on top of the gel, followed by two layers of blotting paper, a thick stack of paper towels and a weight on top of a plastic plate. After the transfer, the membrane was washed for 10 minutes in 2× SSC buffer and the DNA was crosslinked to the membrane in a UV Stratalinker 2400 crosslinker (Stratagene) at 1200 mJoules.

For the probing, the Gene Images Alk-Phos Direct Labelling and Detection System (GE Healthcare Amersham) was used, according to the manual, to generate a fluorescent-labelled DNA probe, allowing this to bind the cross linked DNA on the membrane and therefore visualize it on film after incubation with a chemiluminescent substrate. The probe used was the 5' flanking region of both ISP1 and ISP2, digested out of the respective plasmids and purified from agarose gel. Signal was detected using CDP-Star detection reagent (GE Healthcare Amersham).

2.3 Protein Biochemistry

2.3.1 Expression and purification of recombinant proteins

Recombinant protein expression plasmids were transformed into *E. coli* BL21 cells (Stratagene) and one single colony was used to inoculate 5 ml of liquid LB medium and grown overnight at 37 °C with shacking. This overnight starter culture was used to inoculate 500 ml of liquid LB medium and grown for 3 to 4 hours until it reached an optical density of 0.6 at 600 nm. Once the optical density was reached, protein expression was induced with 0.1 mM of IPTG for 5 hours at 37 °C with shacking. The cells were then harvested by centrifugation at 4500 g for 20 minutes and the pellet frozen at -20 °C until required for purification.

For His-tagged recombinant proteins purification, cell pellets were thawed on ice and lysed using Bacterial Protein Extraction Reagent (B-PER) (Pierce) with 10 µg/ml of DNAse I (Sigma) and incubated at 4 °C for 30 minutes. The solution was then fractionated by centrifugation at 16000 g for 20 minutes and the soluble fraction was filtered through a 0.2 µM filter (Ministart) and kept on ice.

Recombinant proteins were then purified from the soluble fraction by immobilized metal ion affinity chromatography (IMAC) in column packed with Metal Chelate-20 matriz (Poros) on a BioLogic Duo-Flow purification system (BioRad). The column was equilibrated with equilibration buffer (50 mM NaH_2PO_4, 300 mM NaCl, 0.5 mM Imidazole, pH 8.0) and the soluble fraction was then applied to the column. Contaminants were washed with washing buffer (50 mM NaH_2PO_4, 300 mM NaCl, 50 mM Imidazole, pH 8.0) and the recombinant proteins bound to the column were eluted with elution buffer (50 mM NaH_2PO_4 300 mM NaCl, 500 mM Imidazole, pH 8.0).

Peak fractions were pooled, desalted and subsequently applied to an ion exchange column previously equilibrated with equilibration buffer (50 mM Tris, 5 mM EDTA pH 7.0). Flow through was collected and peek fractions were pooled and its purity assessed by SDS-PAGE.

2.3.2 Determination of protein concentration

Protein concentration was determined using Bradford reagent (Sigma) according to the manufacturer's instructions. Assays were performed in 96 well plates and standard BSA curves were prepared with concentrations ranging from 0 to 2 mg/ml. Protein concentration was also determined using BCA Protein Assay (Pierce) according to manufacturer's instructions. For both methods, all samples were done in triplicates and results were read in microplate reader (Molecular Devices) at a wavelength of 592 nm and analyzed with SoftMaxPro software.

2.3.3 Polyacrylamide gel electrophoresis (SDS-PAGE)

Whole cells extracts or purified recombinant proteins were separated a visualized by SDS-PAGE (Sodium dodecyl phosphate polyacrylamide gel electrophoresis), typically using a 15% (w/v) polyacrylamide gel.

Gels were made with 30% acrylamide-bis solution (BioRad) in plastic casting cassettes (Invitrogen) with a 5% (w/v) stacking gel layer above the 15% (w/v) resolving gel, to help load and focus the protein samples before separation.

Protein samples were prepared in 6× SDS-PAGE loading buffer (2× SDS-PAGE loading buffer: 20% (v/v) glycerol, 2.5% (w/v) SDS, 0.05% (w/v) bromophenol blue, 0.2 M Tris-HCl pH 6.8, 10% DTT in H_2O) and boiled for 5 minutes at 100°C.

Electrophoresis was performed in XCell SureLock Mini Cell chambers (Invitrogen) with 1× SDS-PAGE running buffer (25 mM Tris, 192 mM glycine, 0.1% (w/v) SDS).

Voltage was set initially at 100 V and then increased to 180 V once the samples reached the resolving gel, until the protein dye front reached the bottom of the gel. In each gel, 2µg of protein marker (Pre-stained Protein Marker Broad Range, New England Biolabs) was run alongside with the protein samples to estimate their molecular weight.

A gradient gel (NuPAGE®Novex 4-12% was also used to separate and visualize differences between small proteins. Protein samples were prepared in 4× NuPAGE® LDS Sample Buffer and boiled for 5 minutes at 100 °C. Electrophoresis was performed in XCell SureLock Mini Cell chambers (Invitrogen) with 1× NuPAGE® MES SDS Running Buffer at 200 V for 35 minutes.

2.3.4 Coomassie staining of SDS-PAGE

After electrophoresis, protein gels were stained with Coomassie stain solution (2.5% (w/v) Coomassie Brilliant Blue R-250, 45% (v/v) methanol, 10% (v/v) glacial acetic acid in H_2O) for one hour at room temperature, shacking. Gels were then immersed in several changes of destaining solution (10% methanol (v/v), 10% (v/v) glacial acetic acid in H_2O) until a good resolution was observed. After destaining, gels were washed in distilled water and photographed.

2.3.5 Western Blotting

For Western Blotting analysis, proteins were transferred from a SDS-PAGE gel to a nitrocellulose membrane (Hybond-C, GE Healthcare) using either Mini Trans-Blot® Electrophoretic Transfer Cell (BioRad) or Trans-Blot® SD Semi-Dry Electrophoretic Transfer Cell (BioRad) with transfer buffer (20% (v/v) methanol, 25 mM Tris, 192 mM glycine in H_2O) for 1 hour at 360 mA or 30 minutes at 20 V, respectively.

After the transfer, the membrane was stained in Ponceau S Staining Solution (Sigma) to ensure that the transfer was successful. After washing in water, membranes were blocked with 5% powdered milk (Marvel) in TTBS buffer (25 mM Tris, 150 mM NaCl, 2 mM KCl, 0.1% Tween-20) for 1 or 2 hours at room temperature or overnight at 4ºC, shaking. Primary antibody was diluted to the appropriate concentration in fresh blocking solution and membranes were incubated with the primary antibody for 1 or 2 hours at room temperature or overnight at 4ºC shacking.

After incubation with the primary antibody, membranes were washed three times for 5-10 minutes and incubated with secondary antibody diluted to the appropriate concentration in fresh blocking solution.

Secondary antibody used was either Anti-Mouse IgG HRP Conjugate (Promega) or Anti-Mouse IgG (Whole Molecule) Alkaline Phosphatase Conjugate (Sigma) and labeled proteins were revealed by applying an ECL (enhanced chemiluminescent substrate) (SuperSignal west Pico Chemiluminescent Substrate, Pierce ThermoScientific) or by color development using Alkaline Phosphatase Conjugate Substrate Kit (BioRad), depending on the secondary antibody used. Chemiluminescence was visualized by exposing the membrane on photographic film processed in a Kodak film processor. Color development on the alkaline phosphatase substrate treated membranes was stopped when completed by immersion in distilled water for at least 10 minutes.

2.4 *T. brucei* cell culture

2.4.1 Bloodstream form *T. brucei* culturing

T. brucei brucei (strain 427) and *T. brucei rhodesiense* (strain IL1852) were cultured as bloodstream form (BSF) at 37 °C in a 5% CO_2 incubator. *T. brucei* (strain 427) was grown in HMI-9 medium supplemented with 10 % heat-inactivated fetal calf serum (FCS), 10 % serum plus and 0.5 µg/ml penicillin-streptomycin solution (Sigma).

T. brucei rhodesiense was grown in HMI-9 medium supplemented with 20 % serum plus (JRH Biosciences). All culture work was done under sterile conditions in a laminar flow hood.

For parasite growth analysis, culture cell density was determined by counting cells in an Improved Neubauer haemocytometer counting chamber (Weber Scientific). BSF parasites were seeded at 1×10^4 cells/ml and grown to a maximum cell density of 1×10^4 cells/ml.

When monitoring parasite growth, cultures were seeded at 1×10^5 cells/ml every 24 hours and cell density was determined at regular time intervals during that time.

For cryopreservation, mid-log phase cultures were harvested and resuspended in HMI-9 with 10% (v/v) glycerol, aliquoted in cryovials and stored at -80 °C for 24 hours before being transferred to liquid nitrogen tanks for long term storage.

2.4.2 BSF transfections

BSF (*T. brucei rhodesiense*) parasites were grown as described above until they reached mid-log phase. 1×10^7 cells were harvested by centrifugation at 1500 g for 10 minutes and the pellet was resuspended in 100 µl of Human T Cell Nucleofector Solution (Lonza) before transferred to an electroporation cuvette and mixed with 20 µg of linearized DNA, previously precipitated and resuspended in 20 µl of sterile dH_2O.

The mixture was then pulsed on program X-001 using the Human T Cell Nucleofector machine (Amaxa).

A control was prepared by using the same method without any DNA. The parasites were immediately transferred to 30 ml of prewarmed HMI9 and incubated at 37 °C, 5% CO_2.

48 hours after the transfection, selective antibiotics were added to the media and three different dilutions (1:10; 1:100 and 1:500) were plated onto 24 well plates. After 6 to 8 days clones were detected and expanded to 25 cm^2 tissue culture flasks for further analysis.

Antibiotic concentrations used in *T. brucei rhodesiense* selection were 5 µg/ml hygromycin B (Calbiochem), 1 µg/ml G418 (Calbiochem), 10 µg/ml blasticidin (Calbiochem), 1.5 µg/ml puromycin (Calbiochem) and 1.5 µg/ml phleomycin (InvivoGen).

2.4.3 Targeted gene replacement

T. brucei rhodesiense ISP1 and ISP2 genes were deleted by replacing both alleles with antibiotic resistance markers, by homologous recombination. The constructs generated for the ISP1 and ISP2 knock out were linearised, precipitated and transfected into *T. brucei rhodesiense* wild type cells for integration into the genome.

To generate the ISP1 knock out cell line (determined Δ*isp1*) pGL1688 and pGL1689 were transfected, sequentially replacing both wild type alleles with hygromycin and neomycin resistance markers.

Another ISP1 knock out cell line was generated by transfecting pGL1947 and pGL1948, replacing the wild type alleles with blasticidin and puromycin resistance markers.

An ISP2 knock out cell line (Δ*isp2*) was generated by transfecting pGL1959 and pGL1960 into *T. brucei rhodesiense* cells, replacing both wild type alleles with hygromycin and neomycin resistance markers.

Transfectants were cloned by diluting the parasites in HMI-9 with the appropriate antibiotics. Parasites were diluted 10×, 100×, 500× and 1000×, plated on 24 well plates and selected preferably from the most diluted plates where the population is most likely to be clonal, using either hygromycin and neomycin or blasticidin and puromycin.

For the double ISP1/ISP2 knock out (Δ*isp1/2*), ISP2 knock out constructs (pGL1959 and pGL1960) were transfected into the ISP1 knock out cell line generated from the transfection of pGL1947 and pGL1948 into wild type cells. The resulting cell line was cloned and selected by the addition of hygromycin, neomycin, blasticidin and puromycin.

For every potential knock out clone generated, whole genomic DNA was isolated and analyzed for positive gene deletion by PCR and Southern Blot. Whole protein extracts were also used to confirm the absence of ISP1 and ISP2 expression by Western Blot.

2.4.4 Isolation of *T. brucei* genomic DNA

Genomic DNA was isolated from *T. brucei* cultures using DNeasy Blood and Tissue kit (Qiagen) according to the Cultured Animal Cell protocol outlined in the manufacturer's instructions.

2.4.5 Preparation of whole cell extracts

2×10^6 of mid-log phase parasites were centrifuged at 1500 g for 10 minutes. The supernatant was carefully removed and the cell pellet was washed 2× in PBS (137 mM NaCl, 2.7 mM KCl, 4.3 mM Na_2HPO_4, 1.47 mM KH_2PO_4, pH 7.4) by centrifugation at 1500 g for 5 minutes and resuspended in 1× SDS-PAGE loading buffer.

Samples were boiled at 100 °C for 5 minutes to run in SDS-PAGE gels.

2.4.6 *T. brucei* animal infection and parasitemia determination

For infection with *T. brucei rhodesiense* (IL1852), mice were previously treated with cyclophosphamide before inoculated with 1×10^5 cultured parasites by intra peritoneal injection.

Parasitemia was determined daily by haemocytometer cell counting of blood taken from the tail, diluted in 0.83% ammonium chloride.

Parasites taken from a donor mouse were then used to infect 4 ICR mice in each infection experiment. To infect mice with *T. brucei*, the same procedure was applied, without the cyclophosphamide treatment.

2.5 Monoclonal Antibodies

2.5.1 Generation of hybridomas

Female BALB/c mice were immunized intraperitoneally with 10 µg of recombinant protein emulsified with Freund's adjuvant (Sigma-Aldrich), every 2-3 weeks until a satisfactory antibody titer was reached. After 3 to 5 immunizations, blood samples were obtained from mice for serum titer determination by enzyme-linked immunosorbent assay (ELISA). If the titer was still too low, mice were boosted until an adequate response was achieved. Once the titer was high enough cell fusion was performed.

3 days before the cell fusion, mice were boosted with the antigen and then euthanized for spleen removal. Sp2/0 myeloma cells were cultured in 8-azaguanine (Sigma-Aldrich) medium to ensure their sensitivity to hypoxanthine-aminopterin-thymidine (HAT) selection medium used after the cell fusion has occurred. A week before the cell fusion, the 8-azaguanine was removed from the medium and myeloma cells were cultured in GIBCO® DMEM (Dulbecco's Modified EagleMedium) with 10% GIBCO® FBS (fetal bovine serum). Single spleen cells from immunized mice were then fused with the myeloma cells by co-centrifugation in the presence of polyethylene glycol (PEG).

After being removed from the mouse, the spleen was immersed in DMEM, in a petri dish, and the cells were removed by injecting medium inside the spleen, repeatedly until all the cellular content was all in suspension. The spleen cell suspension was then centrifuged for 10 minutes at 1200 rpm and cells resuspended in 10 ml of DMEM. 10 µl of resuspended cells were used to determine cell density and viability with Trypan blue (Sigma-Aldrich) in an Improved Neubauer haemocytometer counting chamber. In parallel, the cellular density of the Sp2/0 cells was also determined and both cellular suspensions were mixed in a 1:10 proportion of Sp2/0:spleen cells. The Sp2/0 and spleen cells suspension was then centrifuged at 1200 rpm for 10 minutes and the supernatant discarded.

0.8 ml of PEG-DMSO (Sigma-Aldrich) was slowly added and gently mixed with the cell pellet, leaving it to rest for 1 minute. The PEG-DMSO was then diluted first by slowly adding and gently mixing 1 ml of DMEM and then by an additional volume of 20 ml of DMEM over 5 minutes time.

The suspension was centrifuged at 1200 rpm for 10 minutes and the cell pellet was resuspended in 25 ml of complete DMEM medium supplemented with 10% FBS and HAT 1× (Sigma – Aldrich) and plated on four 96-well plates. 24 hours after the cell fusion, 100 µl of complete DMEM medium was added to each well and plates were left to grow at 37 °C in a 5% CO_2 incubator.

2.5.2 Screening for antibody producing Hybridomas

The principle for creating an antibody secreting hybridoma is based on the cellular fusion between antibody producing spleen cells, with limited life spam, with cells derived from an immortal tumor of lymphocytes that do not synthesize immunoglobulin, myeloma cells. The resulting hybridoma not only is capable of producing and secreting antibodies but also of unlimited growth.

As the myeloma cell line is defective in the enzyme hypoxanthineguanidinephosphoribosyltransferase (HGPRT), they die when cultured in DMEM supplemented with HAT (aminopterin blocks the main DNA synthesis pathway and the alternative pathway that requires the use of exogenous hypoxanthine depends on the enzyme HGPRT). Only hybrids between myeloma and spleen cells is capable of surviving in HAT supplemented medium. The first selection tool is then the culture medium.

After 4 to 6 days, small groups of cells started to emerge from the cellular debris in bottom of the plate and could be visualized under the microscope. At day 10, supernatants of the wells containing hybridomas (previously screened under the microscope) were tested by ELISA using the recombinant protein as antigen. 0.1 µg of antigen was used to coat ELISA microtiter plates (Costar® 96-Well EIA/RIA plates) and plates were incubated at 4 °C overnight.

After being washed once with TBS buffer (25 mM Tris, 150 mM NaCl, 2 mM KCl), plates were blocked with 2% gelatin in TBS buffer for 1 hour at room temperature. Plates were then washed 3× with TTBS (25 mM Tris, 150 mM NaCl, 2mM KCl, 0.1% Tween-20) and incubated with hybridoma supernatants for 1 hour at 37 °C.

Plates were again washed 3× with TTBS and incubated with Anti-Mouse IgG (whole molecule) Alkaline Phosphatase Conjugate (Sigma) for 1 hour at 37 °C. After washing 5× with TTBS, plates were incubated with 1 mg/ml of p-nitrophenil phosphate in substrate buffer (100 mM glycine, 1 mM $MgCl_2$, 1 mM $ZnCl_2$, pH 10.4) at room temperature in the dark, until the color yellow is developed.

Plates were then read in a microplate reader (BioRad) at a wavelength of 405 nm and analyzed with Microplate manager 4.0 software (BioRad). A no antigen control was added to the plate and supernatants considered positive with absorbance values 5× the control value.

The selected hibridomas by ELISA were then expanded to 24-well plates and subsequently to 25 cm^2 tissue culture flasks and supernatants tested again by ELISA and also by Western Blotting as described in section 2.3.5.

2.5.3 Hybridomas culture and storage

Hybridomas were cultured initially in complete DMEM medium (10% FBS and HAT 1×) at 37 °C in a 5% CO_2 incubator. When expanded from 24-well plates to 25 cm^2 tissue culture flasks, hibridomas were cultured either in DMEM with 5% FBS and HAT 1× or DMEM with 5% FBS with HT (hypoxanthine-thymidine). All culture work was done under sterile conditions in a laminar flow hood.

For cryopreservation, hybridoma cultures were centrifuged at 1200 rpm for 10 minutes Cell pellet was resuspended in 1ml of FBS with 4% DMSO (dimethyl sulfoxide), aliquoted in cryovials and stored immediately at -80 °C for 24 hours before being transferred to liquid nitrogen tanks for long term storage.

2.5.4 Determination of antibody isotype

Antibody isotyping was done with Mouse MonoAB ID kit (HRP) (Invitrogen) according to the Antigen Dependent Protocol for Isotyping Mouse Monoclonal Antibodies. The antigen used in isotyping assays was the recombinant protein against which the antibodies were generated.

2.5.5 Antibody purification

After determined the isotype, monoclonal antibodies were affinity purified using a HiTrap™ Protein G HP column (GE Healthcare), a pre-packed column with 1 ml of Protein G Sepharose™ High Performance, designed for purification of IgG from ascites, serum and cell culture supernatants.

50 ml of cell culture supernatants were centrifuged at 1200 rpm for 10 minutes and filtered through a 0.45 µm filter to remove particulate material. Samples were then dialyzed in a dialysis membrane immersed in binding buffer (20 mM sodium phosphate, pH 7.0) at 4 °C overnight.

The column was equilibrated with 10 volumes of binding buffer and the sample was then applied to the column. Non binding material was washed with 5 volumes of binding buffer. Elution was performed with 5 volumes of elution buffer (0.1 M glycine-HCl, pH 2.7) and purified antibody was collected in 0.5 ml fractions. After the elution, the column was washed with 10 volumes of binding buffer.

Purified fractions were pooled, concentrated with 4 M ammonium sulphate and dialyzed against PBS buffer at 4 °C overnight.

Purified antibodies were filter sterilized, stored at 4 °C and used in Western Blotting analysis, immunofluorescence assays and also in growth inhibition (*in vitro*) and treatment studies (*in vivo*).

2.6 Indirect Immnunofluorescence Analysis (IFA)

For indirect immunofluorescence analysis, mid-log phase parasites were harvested by centrifugation at 1500 g for 10 minutes and washed in ice cold Voorhei's modified PBS (vPBS) (137 mM NaCl, 3 mM KCl, 16 mM Na_2HPO_4, 3 mM KH_2PO_4, 46 mM sucrose, 10 mM glucose, pH 7.6). The cells were then fixed on ice in 3% paraphormaldehyde for 10 minutes. After fixation, an excess of vPBS was added to dilute the fix solution and the cells were washed twice in vPBS, for paraphormaldehyde removal.

Fixed cells were then applied to microscope glass slides pre-coated with 0.01% poly-l-lysine and allowed to settle for 20 minutes. To stain the internal structures of the parasite, cells were permeabilized in PBS with 0.1% Triton X-100 for 10 minutes and washed three times with excess PBS before blocking for 1 hour with 20% (v/v) FCS in PBS.

After washing the slides again with excess PBS, primary antibody diluted in blocking solution, was applied and the slides incubated for 2 hours at room temperature.

The slides were then washed three times with PBS and the appropriate secondary antibody, Alexa Fluor 594 (red)-conjugated anti-mouse (Molecular Probes), diluted in blocking solution was applied and slides incubated for 1 hour at room temperature. After washing three times with PBS, excess liquid was drained and cells were stained with 1 µg/ml DAPI in mounting solution (PBS, 50% (v/v) glycerol, 2.5% (w/v) DABCO) before being sealed with a coverslip. Slides were kept in a moist dark box until microscopic analysis to prevent drying and fluorescence fading.

2.7 Scanning Electron Microscopy

For Scanning Electron Microscopy (SEM) parasites were allowed to settle out from culture medium onto poly-L-lysine coated glass coverslips, rinsed briefly with PBS to remove unattached cells and subsequently fixed with 2.5% glutaraldehyde in

0.1M cacodylate buffer. The attached parasites were then osmicated, acetone dehydrated and critical point dried from liquid CO_2, sputter-coated with Au/Pd and imaged at 6 kV in a JSEM 6400.

2.8 *In vitro* growth inhibition assays

For the growth inhibition assay, BSF parasites were cultured as described previously on section 2.4.1 and diluted to a concentration of 1×10^5 cells/ml. For a preliminary study, 100 µl of supernatant from selected cultures of hybridomas were added to a *T. brucei* (strain 427) culture and grown in HMI-9 supplemented with 10% FCS and 10% Serum Plus at 37 °C in a 5% CO_2 incubator. Culture cell density was determined by counting the cells every 24 hours until they reached stationary phase. One *T. brucei* culture without antibodies and one *T. brucei* culture with 100 µl of complete DMEM (hybridoma culture medium) were used as control.

For the final *in vitro* growth inhibition assay, 4 different amounts of purified antibody (0 µg, 25 µg, 50 µg and 100 µg) were added to 1×10^4 cells/ml of mid log phase parasites and grown as described previously. Culture cell density was determined by counting the cells every 24 hours until they reached stationary phase. The same amounts of affinity purified pre-immune IgG were used as a control.

2.9 *In vivo* growth inhibition assays

2.9.1 Protection of *T. brucei* infected mice by ISP Immunization

For this assay, 4 groups of 5 specific pathogen free (SPF) BALB/c mice were used. Group 1 was used as a control and was injected with PBS and Freund's adjuvant. Group 2 was immunized with recombinant ISP1, group 3 was immunized with recombinant ISP2 and group 4 was immunized with a mixture of ISP1 and ISP2.

Animals were immunized 3× with 10 µg of each recombinant protein at days 0, 15 and 30. 2 days before the final boost, blood samples were obtained for serum titer determination by ELISA and 2 days after the final boost, mice were infected with 1×10^3 cultured BSF *T. brucei* (strain 427) by intraperitoneal injection. Parasitemia was then determined daily by haemocytometer cell counting as described in section 2.4.6.

2.9.2 Neutralization of *T. brucei* in infected mice by ISP MAb's

For the neutralization of *T. brucei* infection in mice by monoclonal antibodies, 4 groups of 5 SPF BALB/c mice were infected with 1×10^3 parasites on day 1. On days 0, 1, 3 and 5 group A was inoculated with 25 µg of control IgG (purified from pre-immune serum) and used as control group. Group B was inoculated with 25 µg of anti ISP1 purified monoclonal antibody; group C was inoculated with 25 µg of anti ISP2 purified monoclonal antibody and group D with 25 µg of each antibody. All inoculations were done by intraperitoneal injection. Parasitemia was determined daily by haemocytometer cell counting as described previously (section 2.4.6).

2.10 Statistical analysis

T. brucei growth curves were analysed by two-way ANOVA with Bonferroni's post test. All analysis were done using GraphPad Prism version 5.00 for Windows, GraphPad Software, San Diego California USA, www.graphpad.com.

Chapter 3

Results

3.1 Generation of Monoclonal Antibodies

3.1.1 Generation of MAb's against ICP

For the generation of monoclonal antibodies against *T. brucei* ICP, two female BALB/c mice were immunized with 10 µg of recombinant ICP (provided by Prof. Jeremy Mottram, University of Glasgow) every 2 weeks. During the immunization process, blood samples were collected and the serum titre was determined for each mouse by ELISA, using the recombinant ICP (rICP) as antigen. After a total of 6 immunizations, the immune response against rICP was very low, with OD 405nm values for the immune sera similar to the pre-immune serum (Figure 3.1).

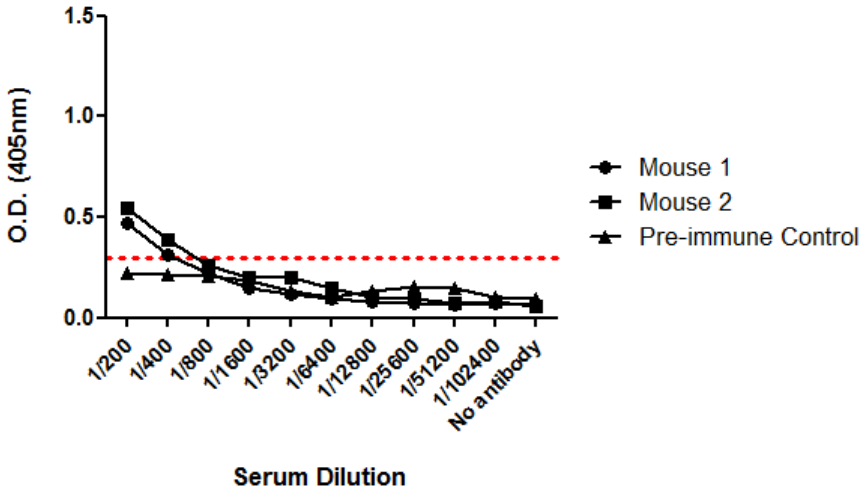

Figure 3.1 – ICP serum titre determination by ELISA.

Serum titre was determined for each mouse after 6 immunizations with rICP. Threshold level represents the triple of the negative control OD value

Despite the low serum titre (1:400), both mice were sacrificed and their spleens were used to perform two separate cell fusions. After 10 days all 96 well plates were observed under the microscope for the presence of hybridomas. One of the cell fusions was not successful and after 20 days all plates were discarded without showing any cellular growth.

From the other fusion, a total of 13 hybridomas were identified among a total of 240 wells seeded, revealing an extremely low fusion efficiency (5.4%). The 13 hybridomas were screened by ELISA and even though all supernatants had OD 405nm values close to the negative control, they were used as a primary antibody in Western Blotting, where they all failed to recognise the rICP (results not shown).

The results obtained indicate that ICP is a poor immunogenic agent, as it failed to trigger an immune response in mice. There are several aspects that can influence a protein's immunogenicity, such as molecular size, epitope density, chemical composition, protein structure or degradability. Combined with its low immunogenicity, rICP had a deleterious effect on mice, causing hair loss, blindness and premature aging and therefore, it was not suitable to use as antigen in the generation of monoclonal antibodies against ICP.

rICP is functionally active not only against *T. brucei* cysteine peptidases, but also against mammalian ones (Sanderson *et al.*, 2003). Abnormal or deficient activity of mammalian CPs are responsible by several pathological conditions that can cause the clinical symptoms similar to the ones observed in mice when immunized with rICP, suggesting that they are inhibiting the mice's CPs (Quesada *et al*., 2009, López-Otín and Bond, 2008, Puente *et al*., 2003).

The deletion of conserved residues T31 and T32 in chagasin's loop L2 modifies its length and has an effect on the inhibitory function of ICP, no matter against which enzyme (Lima and Mottram, 2010, dos Reis *et al*., 2008, Salmon *et al.*, 2006).

In an attempt to reduce the harmful effect of rICP in mice, site directed mutagenesis was used to remove residues T31 and T32. After sequence confirmation, ΔT31-T32 ICP expression was induced at different temperatures (15ºC, 25ºC and 37ºC) using 0.1 mM IPTG. The protein could be detected in the soluble fraction when expressed at 25ºC, and it was purified as described previously in Chapter 2.

ΔT31-T32 ICP was then used to immunize two female BALB/c mice following the immunization scheme previously established. In parallel, two other female BALB/c mice were immunized with the non-mutated rICP and after 6 immunizations serum titre was determined by ELISA for each mouse.

Both mice immunized with ΔT31-T32 ICP revealed higher OD 405nm values than mice immunized with rICP, with serum titres of 1:128000 and 1:800 respectively (Figure 3.2).

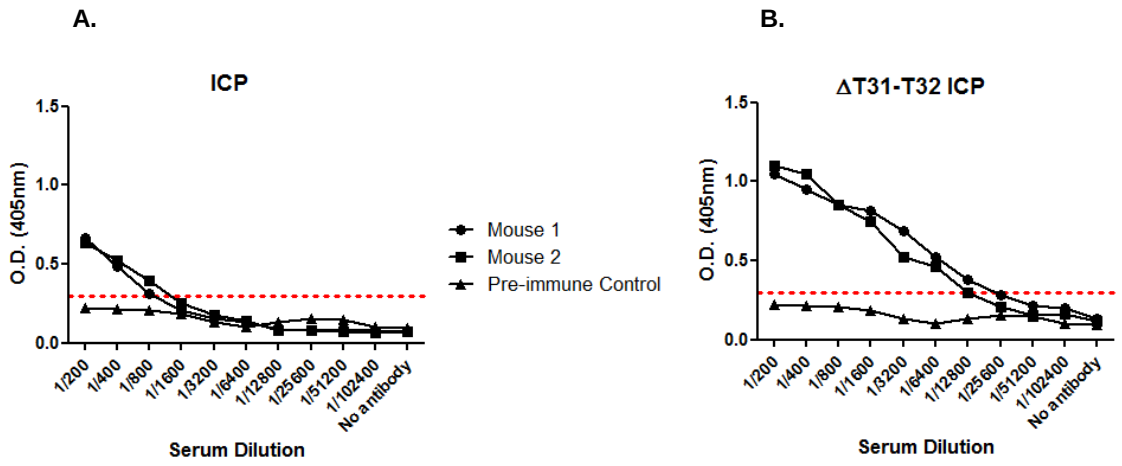

Figure 3.2 – rICP and ΔT31-T32 ICP Serum titre determination by ELISA.

Serum titre was determined for each mouse after 6 immunizations with **(A)** rICP and **(B)** ΔT31-T32 ICP. Threshold level represents the triple of the negative control OD value

After a final boost with 10 µg of ΔT31-T32 ICP, both mice were sacrificed and their spleen removed to perform the fusion with the Sp2/0 myeloma cells. After 6 days small groups of cells started to appear in the bottom of the plates and 10 - 12 days post-fusion hybridomas were screened microscopically.

Supernatants from apparent single clones occupying more than half the well were tested by ELISA. From the 480 wells seeded in the 96 well plates, 384 (80%) revealed significant growth and the supernatants were tested by ELISA. From these, only 30% were positive and expanded to 24 well plates and left to grow for 7 days before submitted to a new screening by ELISA.

From the 117 supernatants tested, 74 remained positive and were expanded to 25 cm^2 culture flasks. After a final screening only 26 supernatants were considered positive, with OD 405nm values above the triple of the negative control. These 26 supernatants were then tested by Western Blotting against recombinant ΔT31-T32 ICP where they recognised a band with approximately 13.4 kDa (Figure 3.3).

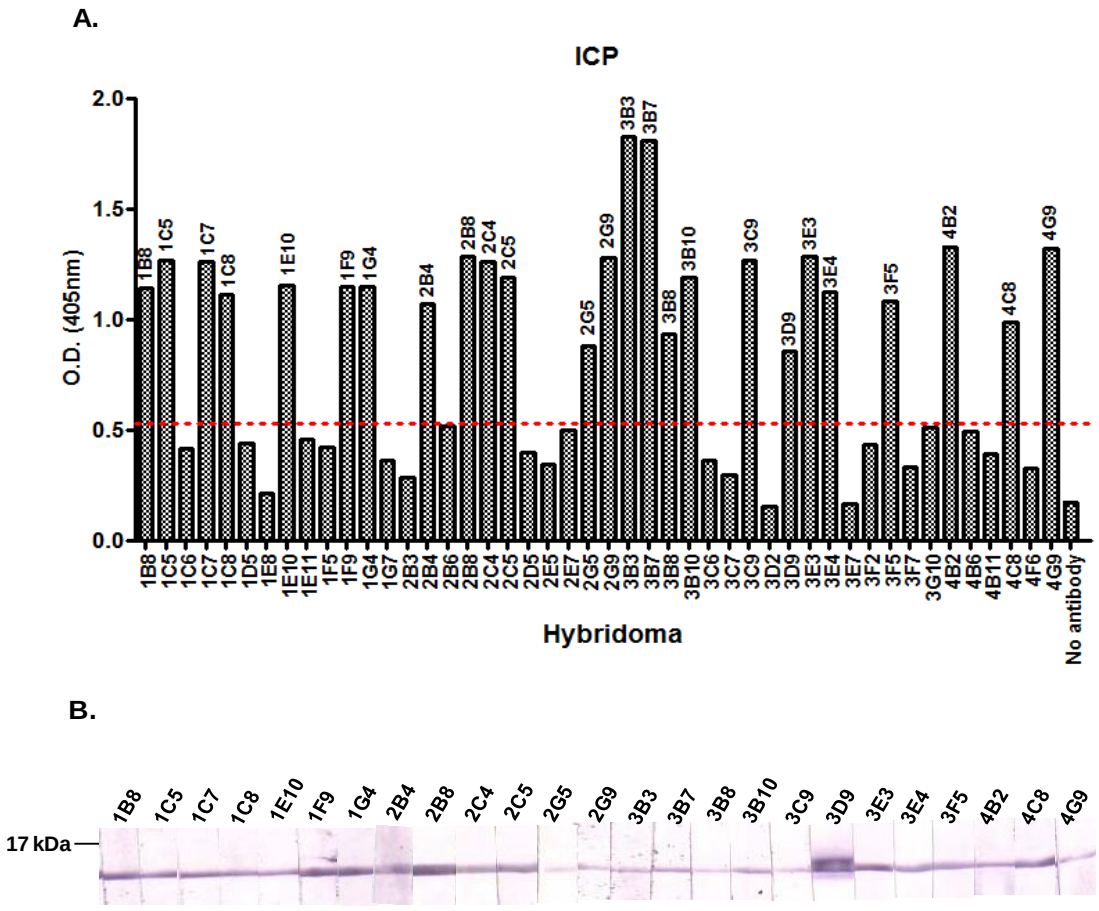

Figure 3.3 – Screening for anti-ICP antibody producing hybridomas by ELISA and Western Blotting.

(A) Supernatants were tested by ELISA using recombinant ΔT31-T32 ICP as antigen. Supernatants with OD values above 0.350 (triple of the negative control) were considered positive and selected for further screening by **(B)** Western Blotting against recombinant ΔT31-T32 ICP

To determine the specificity of the antibodies present in the supernatants tested, 8 hybridomas were selected based on the best combination of ELISA/Western Blotting results and used as primary antibodies in Western Blotting against recombinant ΔT31-T32 ICP and against another recombinant protein from *T. brucei* (rISP2).

Surprisingly, all supernatants recognized the rISP2 as well as the protein against which the antibodies were generated (Figure 3.4).

The remaining supernatants were also tested by Western Blotting against ΔT31-T32 ICP and rISP2 and all of them recognized both proteins (results not shown).

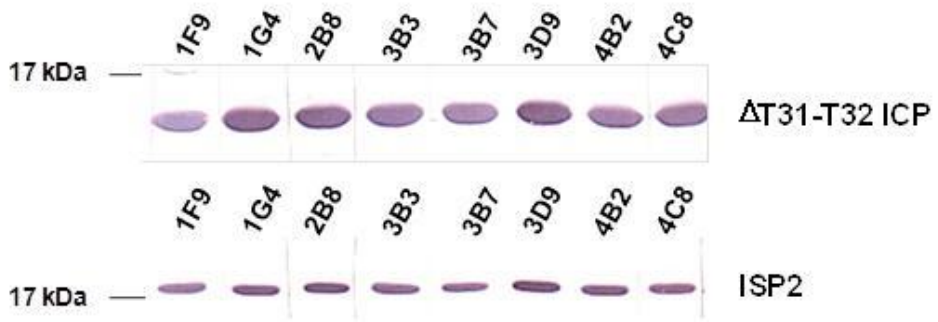

Figure 3.4 – Western Blotting with anti-ICP MAb's.

The 8 supernatants with the best results in the initial screening by ELISA and Western Blotting against ΔT31-T32 ICP tested positive by Western Blotting against rISP2

The recognition of rISP2 by the supernatants indicates that all hybridomas selected were producing non-specific antibodies. These antibodies are probably targeting the 6x His-tag, the common feature to both proteins. Poly-histidine tags are low molecular weight tags (1 kDa) that are normally poorly immunogenic when compared to larger fusion tags such as GST (26 kDa) or MBP (40 kDa) and should have minimal impact on the protein's overall size, fold and immunogenicity (Hochuli, 1988, Porath *et al.*, 1975).

Thus, it would not be expected that the 6x His-tagged ΔT31-T32 ICP stimulated significantly the immune response in mice giving rise to antibodies against the His-tag instead of antibodies against the target protein.

To prevent the possibility of producing non-specific antibodies against the histidine, the tag could be removed from the protein prior to immunization. However, the constructs used to express the rICP or the ΔT31-T32 ICP don't possess the cleavage site to remove the tag and new constructs would have to be done.

With time as a major limitation, it was not possible to do new constructs and test whether the cleavage of the tag would successfully improve the generation of monoclonal antibodies against ICP within the project's life span and this line of work was discontinued.

3.1.2 Generation of MAb's against ISP 1 and ISP2

Monoclonal antibodies against *T.brucei* ISP1 and ISP2 were generated using similar procedures to the ones used for the generation of monoclonal antibodies against *T. brucei* ICP. After 4 immunizations with 10 µg of recombinant protein (provided by Prof. Jeremy Mottram, University of Glasgow), the serum titre was evaluated by ELISA for each mouse. Mice immunized with rISP1 presented a titre of 1:3200 and 1:6400 while mice immunized with rISP2 showed higher OD 405nm values with titres of 12800 and 25600 (Figure 3.5).

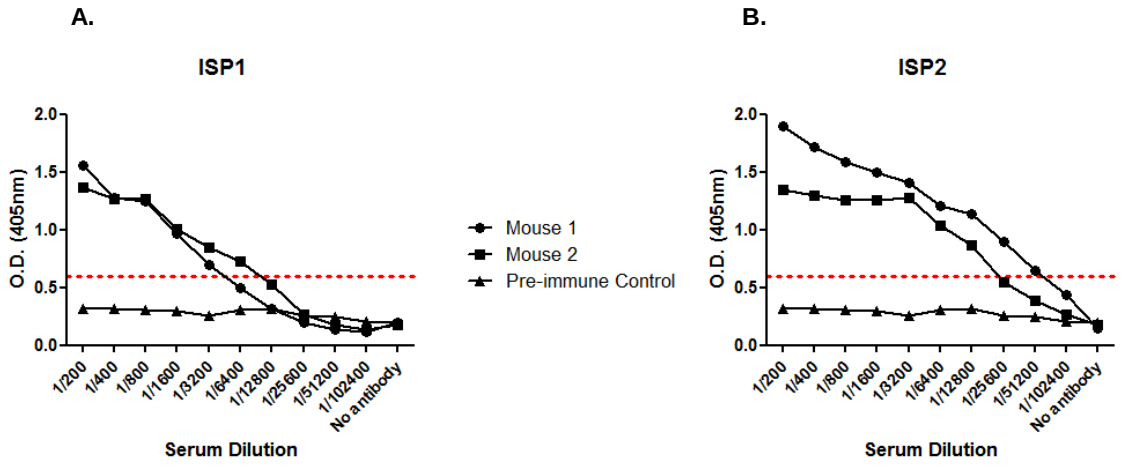

Figure 3.5 – IS1 and ISP2 serum titre determination by ELISA.

Serum titre was determined for each mouse after 6 immunizations with **(A)** rISP1 and **(B) r**ISP2**.** Threshold level represents the triple of the negative control OD value

After a final boost with 10 µg of recombinant protein all mice were sacrificed and four separate cell fusions were performed. Both cell fusions of ISP1 splenocytes were successful, resulting in 82 hybridomas growing in the 240 wells seeded in one

fusion (34.2%) and 109 wells with hybridomas growing among the 240 seeded in the other fusion (45.4%). The ISP2 cell fusions were less successful, with one showing no cellular growth 20 days post-fusion and the other one with 175 hybridomas growing in the 240 wells seeded (62.9%).

Supernatants from the emerging hybridomas were tested by ELISA and the positive ones were collected and expanded initially to 24 well plates and subsequently to 25 cm^2 culture flasks, after new screening by ELISA (Table 3.1).

	Hybridomas					
	96 well plates		24 well plates		25 cm^2 flasks	
	Tested	Positive	Tested	Positive	Tested	Positive
ISP1 fusion	191	89 (46.6%)	89	40 (44.9%)	40	24 (60%)
ISP2 fusion	175	74 (42.3%)	74	57 (77%)	57	18 (31.6%)

Table 3.1 – Hybridomas screened by ELISA.

Supernatants from hybridoma cultures were considered positive when showing OD values above the triple of the negative control value

Once in flasks, hybridomas were left to grow for approximately 7 days and supernatants were tested simultaneously by ELISA and Western Blotting against the respective recombinant and also against *T. brucei* ICP, to assess their specificity (Figure 3.6 and Figure 3.7).

Based on the results obtained both by ELISA and Western Blotting, two antibodies against each ISP were selected for further characterization and purification.

Despite the high values of OD 405nm displayed by most antibodies generated against ISP1, only four recognized the recombinant protein by Western Blotting and from those, only two were specific since the others also recognized a band with approximately 13.4 kDa, corresponding to ICP (Figure 3.6B).

From the twelve antibodies that recognized rISP2 by Western Blotting, four also recognized rICP and from the remaining ones, the two antibodies selected had a substantially stronger signal in the Western Blotting against rISP2 (Figure 3.7B).

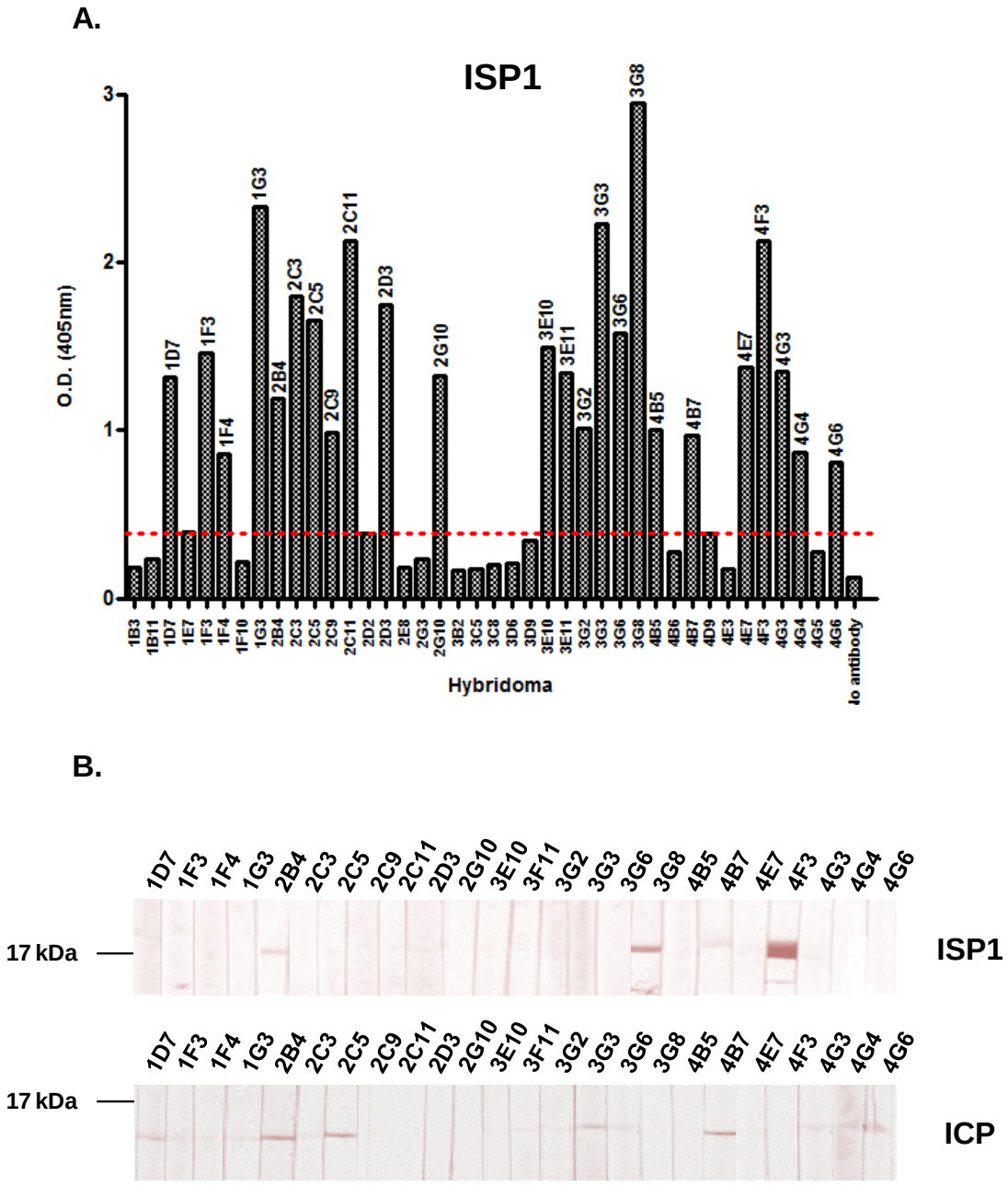

Figure 3.6 – Screening for anti-ISP1 antibody producing hybridomas by ELISA and Western Blotting.

(A) Supernatants were tested by ELISA using rISP1 as antigen. (**B)** Western Blotting. rISP1 or rICP was used to run a 15% SDS-PAGE gel, transferred to a nitrocellulose membrane and incubated with the supernatants previously selected by ELISA.

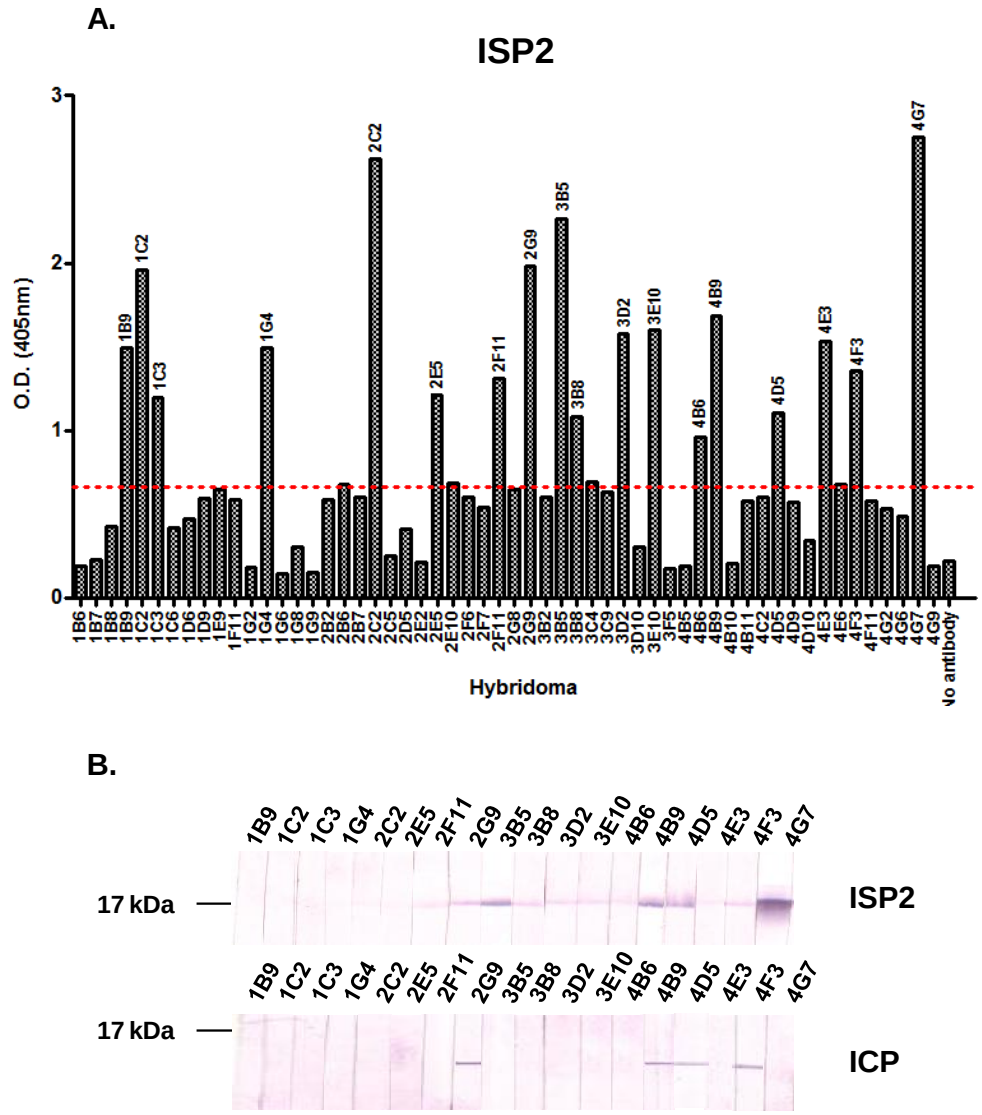

FIGURE 3.7 – Screening for anti-ISP2 antibody producing hybridomas by ELISA and Western Blotting.

(A) Supernatants were tested by ELISA using rISP2 as antigen. **(B)** Western Blotting. rISP2 or rICP was used to run a 15% SDS-PAGE gel, transferred to a nitrocellulose membrane and incubated with the supernatants previously selected by ELISA.

The isotype of anti-ISP1 antibodies designated as 3G8 and 4F3 and anti-ISP2 antibodies 3B5 and 4G7 was determined using the Antigen Dependent Protocol for Isotyping Mouse Monoclonal Antibodies from Mouse MonoAB ID kit (HRP) (Invitrogen).

rISP1 and rISP2 were used to coat a microtiter plate and a three-step ELISA procedure was performed using the selected supernatants as primary antibodies, subclass specific rabbit anti-mouse antibodies as secondary antibody and a goat anti-rabbit IgG HRP Conjugate as tertiary antibody.

Normal rabbit serum was used as negative control and one mouse IgG1 monoclonal antibody was used as positive control. Subclass specific antibodies were added to each column and primary antibodies were added to each row as represented in Table 3.2.

	1	2	3	4	5	6	7	8	9	10
	PBS	Normal Serum	IgG1	IgG2a	IgG2b	IgG3	IgA	IgM	k light chain	λ light chain
A	Mouse IgG1 mAb									
B	α-ISP1 3G8 mAb									
C	α-ISP1 4F3 mAb									
D	α-ISP2 3B5 mAb									
E	α-ISP2 4G7 mAb									

TABLE 3.2 – Isotype determination scheme.

Schematic representation of the microtiter plate layout used for the determination of class and subclass of the selected antibodies against ISP1 and ISP2.

All antibodies selected were composed of an IgG1 heavy chain paired with a k light chain, as observed in Table 3.3.

Hybridomas were left to grow in 175 cm^2 culture flasks for 21 to 28 days to allow maximum production of antibodies.

Cultures were centrifuged and after discarding cellular debris, supernatants were filtered through a 45 µm filter. Antibodies were affinity purified on a protein G column, precipitated and dialyzed before being filter sterilized and stored for further use.

	PBS	Normal Serum	IgG1	IgG2a	IgG2b	IgG3	IgA	IgM	k light chain	λ light chain
Mouse IgG1	0.088	0.086	**0.215**	0.091	0.091	0.093	0.095	0.093	**0.188**	0.092
α-ISP1 3G8	0.113	0.113	**0.208**	0.118	0.110	0.124	0.111	0.106	**0.242**	0.105
α-ISP1 4F3	0.124	0.121	**0.283**	0.129	0.130	0.131	0.130	0.126	**0.296**	0.126
α-ISP2 3B5	0.106	0.100	**0.204**	0.099	0.101	0.115	0.104	0.103	**0.218**	0.105
α-ISP2 4G7	0.123	0.119	**0.258**	0.123	0.123	0.121	0.121	0.121	**0.262**	0.122

TABLE 3.3 – Isotype determination results.

OD 405 nm values obtained for the determination of class and subclass of antibodies generated against ISP1 and ISP2.

To confirm the specificity and assess their sensitivity, purified antibodies were used to perform a Western Blotting analysis against both rISP1 and rISP2 and also against *T. brucei* whole cell lysates (Figure 3.8).

Antibodies 4F3 and 3G8 against ISP1 recognized the respective recombinant but not the rISP2. In the whole cell lysate, both antibodies recognized a strong band between 17 and 25 kDa and some faint bands above 25 kDa (Figure 3.8 A.).

As the level of expression of ISP1 and ISP2 in *T. brucei* is extremely low and antibodies could not detect anything but background when using the standard 1×10^6 parasites per lane, an increased amount of parasites was used to test the antibodies. Approximately 5×10^6 parasites per lane were used. This larger amount of protein has implications in the outcome of the Western Blotting and can lead to an increase in background labelling.

Despite the presence of some background, the signal correspondent to the ISP1 band is strong enough to consider that both antibodies are specific to *T. brucei* ISP1.

The same was found with ISP2 antibodies 4G7 and 3B5. Both antibodies recognize rISP2 but not rISP1. In the whole cell lysate, both antibodies recognize a protein with the predicted size of 17.8 kDa and some accessory proteins with higher molecular weight, especially antibody 3B5 (Figure 3.8 B).

Again, this background could be due to an excess of protein loaded on the gel, but could also be consistent with excess of primary antibody.

Different dilutions of antibody 3B5 were used and for the purpose (identify a band corresponding to ISP2 in *T. brucei* whole cell lysates) the dilution used was the one giving the best results.

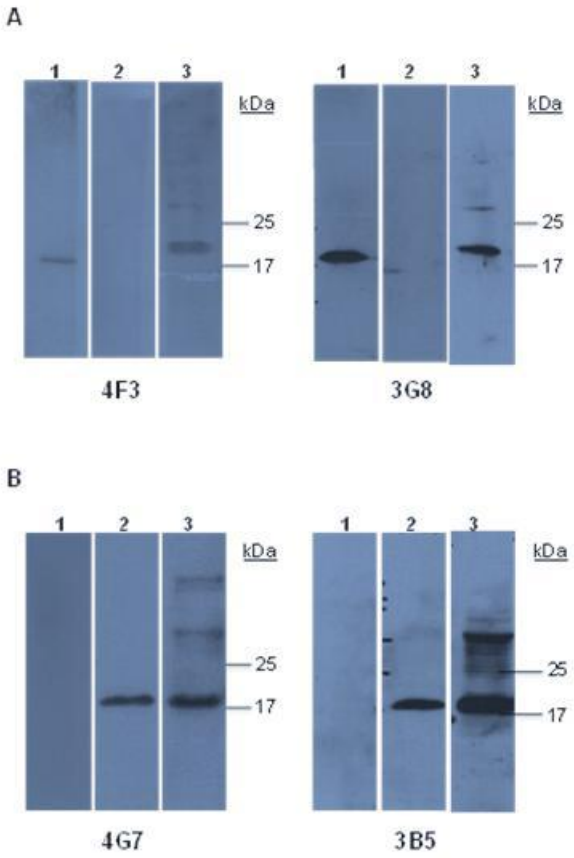

Figure 3.8 – Western Blotting analysis of purified antibodies.

(A) Antibodies 4F3 and 3G8 against ISP1 and **(B)** antibodies 4G7 and 3B5 against ISP2 tested against rISP1 (lane 1), rISP2 (lane 2) and *T. brucei* whole cell lysate (lane 3)

3.2 Localisation of ISP 1 and ISP2 in *T. brucei* cells

Affinity purified monoclonal antibodies anti-ISP1 and anti-ISP2 were used in fluorescence microscopy to determine the localization of ISP1 and ISP2 on bloodstream form (BSF) *T. brucei*. Mid-log phase cells were fixed in paraphormaldehyde and permeabilized with Triton X-100. Fixed cells were then incubated with anti-ISP1 and anti-ISP2 (diluted 1/25) overnight at 4ºC and anti-mouse Alexa fluor 594 conjugate (diluted 1/4000).

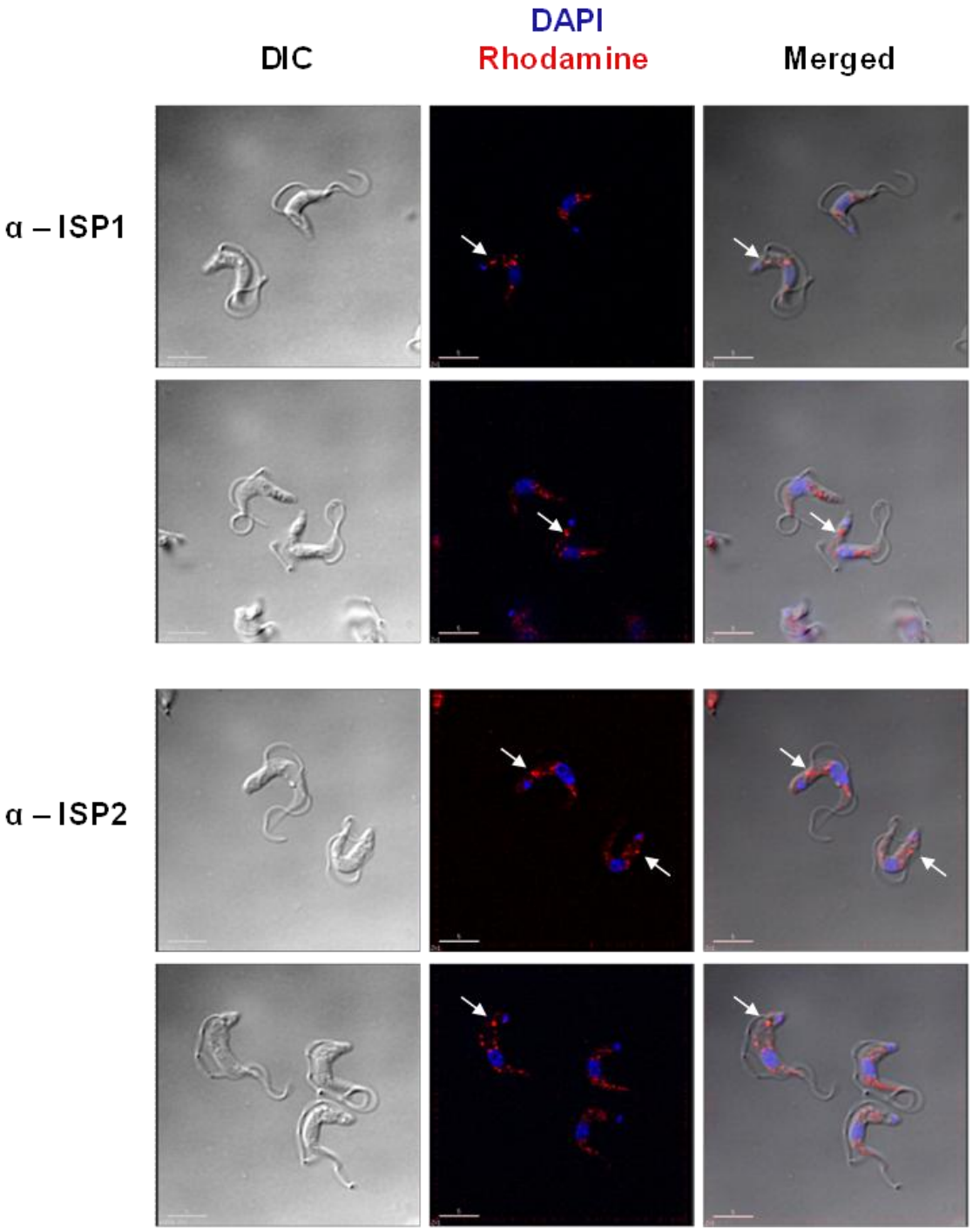

Figure 3.9 – Immunofluorescence analysis of ISPs in BSF *T brucei*.

BSF *T. brucei* parasites were harvested and washed in vPBS before fixed in 3% paraformaldehyde in an eppendorf tube. Cells were then were applied to poly-L-lysine treated slides and permeabilized. Slides were blocked and subsequently incubated with anti-ISP1 3G8 antibody or anti-ISP2 4G7 antibody. Anti-mouse Alexa fluor 594 conjugated was used as secondary antibody and slides were visualized using Rhodamine filter set (red). Nuclear and kinetoplast DNA was stained with DAPI. Scale bar 5 µm. Experiment performed in collaboration with Dr William Proto (University of Glasgow)

Both ISP1 and ISP2 were found mainly in the cytosol with some punctate structures located near the flagellar pocket and the kinetoplast (Figure 3.9).

Antibody specificity was confirmed by incubating wild type parasites only with secondary antibody. No fluorescence was observed in these slides, showing that the signal detected could be attributed to ISP1 and ISP2 specific labelling.

3.3 Deletion of *T. brucei* ISP1 and ISP2 by targeted gene replacement

3.3.1 Generation of ISP null mutant cell lines of *T. brucei*

To investigate the function of ISPs, *T. brucei* cell lines deficient in ISP1 (Δ*isp1*), ISP2 (Δ*isp2*) and both ISP1 and 2 (Δ*isp1/2*) were generated by sequential replacement of both alleles of the wild type gene *loci*. The 5' and 3' flanking regions of the *ISP1* and *ISP2* ORFs were cloned into separate knock out constructs containing a drug resistance marker. For each gene, two resistance markers were used, resulting in 4 different constructs that allowed the generation of the Δ*isp1/2* cell line.

Initially, the plasmids designed for the *ISP1* knock out contained hygromycin (*HYG*) and neomycin (*NEO*) as resistance markers (pGL1688 and pGL1689) and the plasmids designed for the *ISP2* knock out contained blasticidin (*BSD*) and puromycin (*PAC*) as resistance markers (pGL1690 and pGL1691). However, due to some initial difficulties with cloning the appropriate flanking regions in the corresponding plasmids the strategy had to be re-adjusted and 4 new constructs were designed: pGL1947 and pGL1948 for the ISP1 knock out containing BSD and PAC as resistance markers and for the ISP2 knock out, pGL1959 and pGL1960 containing HYG and NEO as resistance markers (Figures 3.10 and 3.11).

pGL1688 and pGL1689 were created by cloning 5'*ISP1* and 3'*ISP1* flanking regions into the backbone of plasmids pGL1224 and pGL1217 (provided by Prof. Jeremy Mottram, University of Glasgow).

Fragments were amplified from genomic DNA isolated from *T. brucei rhodesiense* IL1852 and sub-cloned into pGEM-T-Easy vector. Once confirmed the right sequence by DNA sequencing, the 5'*ISP1* flanking region fragment was digested from the sub-cloning vector using *NotI* and *XbaI* and ligated with pGL1124 and pGL1217 previously treated with the same enzymes. After confirming the insertion of the 5'*ISP1* fragment, the 3'*ISP1* flanking region was digested from the sub-cloning vector with *ApaI* and ligated to the pGL1224 and pGL1217 containing the 5'*ISP1* flanking region, also digested with *ApaI*, creating pGL1688 and pGL1689.

pGL1947 and pGL1948 were created by replacing the resistance marker in pGL1688 by BSD and PAC respectively. *BSD* and *PAC* fragments were digested from plasmids pGL1124 and pGL808 (provided by Prof. Jeremy Mottram) using *Eco*RI and ligated with pGL1688 previously digested with the same enzyme.

pGL1688 and pGL1689 were also used as backbone for the construction of pGL1959 and pGL1960. 5'*ISP2* flanking region was amplified with oligonucleotides OL2421 and OL2422 and subcloned into pGEM-T-Easy vector. The fragment was digested from the sub-cloning vector using *NotI* and *XbaI* and cloned into both pGL1688 and pGL1689 previously digested with the same enzymes. Similar approach was done for the cloning of 3'*ISP2* flanking region. The fragment was amplified with oligonucleotides OL2424 and OL3258 and sub-cloned. After confirmation of the right sequence, the fragment was digested with *ApaI* and cloned into pGL1688 and pGL1689 containing the 5'*ISP2* fragment, treated with the same enzyme. All sequences were then confirmed by DNA sequencing.

Each resistance marker cassette with the cloned 5' and 3' flanking regions was digested out of the plasmid backbone with the restriction enzymes *Not*I and *Xho*I and after precipitated, DNA was separately transfected into wild type BSF *T. brucei rhodesiense* strain IL1852 cells, integrating into the parasite's genome through homologous recombination.

After the first round of transfections, heterozygous parasites resistant to one antibiotic were isolated and subsequently transfected with a second resistance cassette, producing double resistant cell lines.

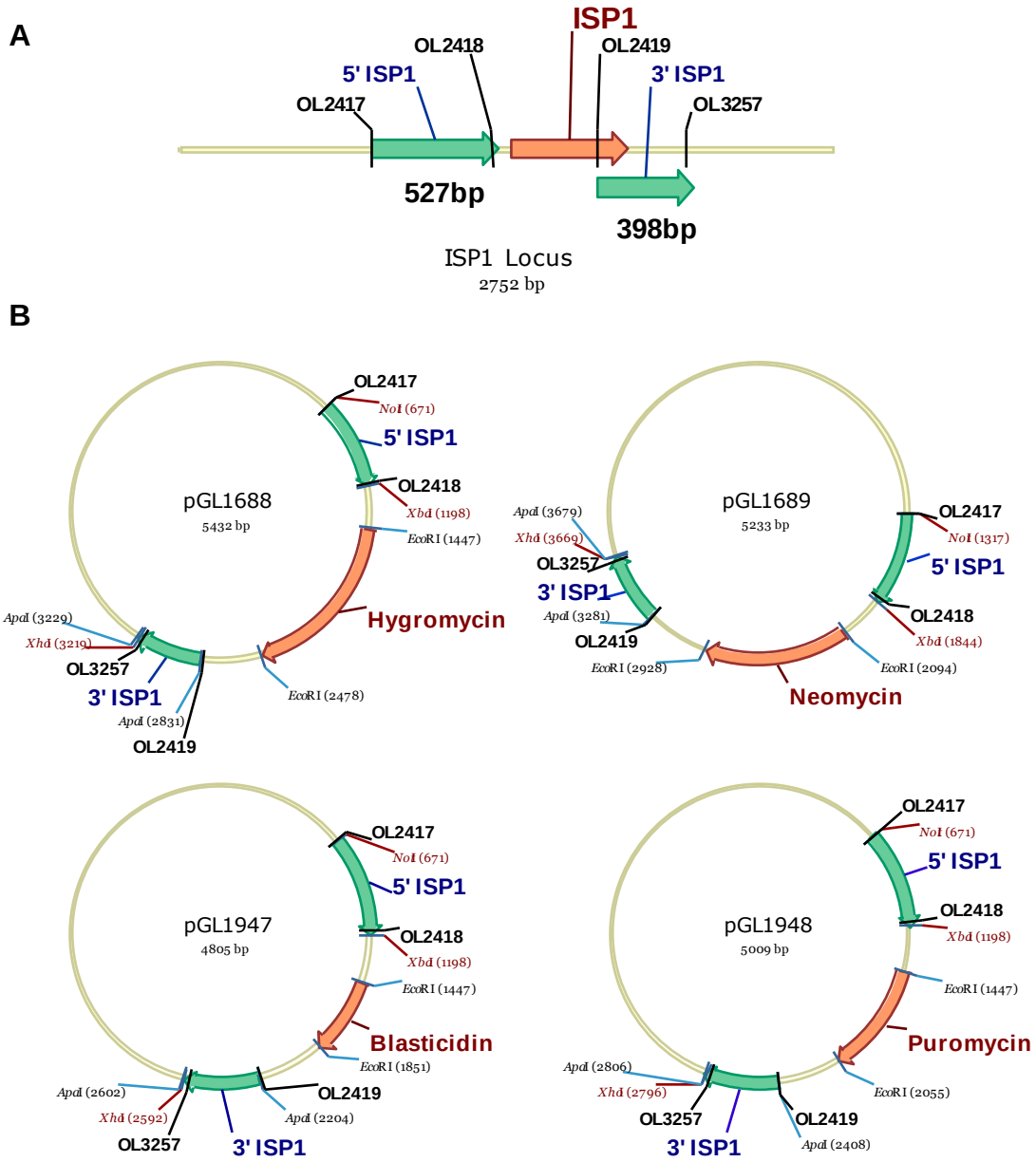

Figure 3.10 – Generation of ISP1 null mutants

(A) Schematic representation of *T. brucei ISP1 locus* and flanking regions used**. (B)** Constructs used for the generation of two different Δ*isp1* cell lines. Constructs pGL1688 and pGL1689 were used to generate Δ*isp1* clones resistant to HYG and NEO and Δ*isp1* clones resistant to BSD and PAC were created using constructs pGL1947 and pGL1948.

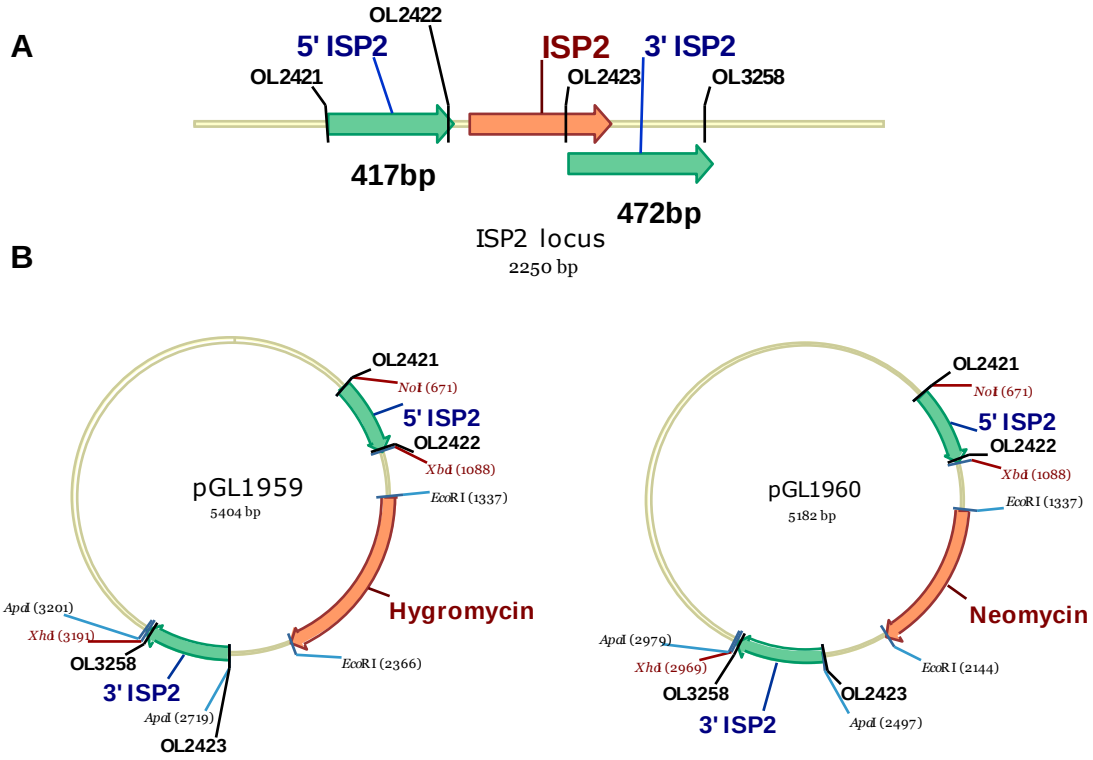

Figure 3.11 – Generation of ISP2 null mutants

(A) Schematic representation of *T. brucei ISP2 locus* and flanking regions used**. (B)** Constructs used for the generation of Δ*isp2* cell line

The main purpose of generating a null mutant cell line is to analyse if there's a modification of any kind in the organism's phenotype. In order to determine if that modification can be directly linked to the absence of the deleted gene, its expression has to be re-established and the phenotype of resulting parasites compared to the wild type.

For the re-expression of the deleted genes, *ISP1* and *ISP2* ORFs were cloned into plasmids pGL2049 and pGL2050 and targeted into the tubulin locus of Δ*isp1* and Δ*isp2* mutants, generating the cell lines designated respectively as Δ*isp1:ISP1* and Δ*isp2:ISP2* (Figure 3.12).

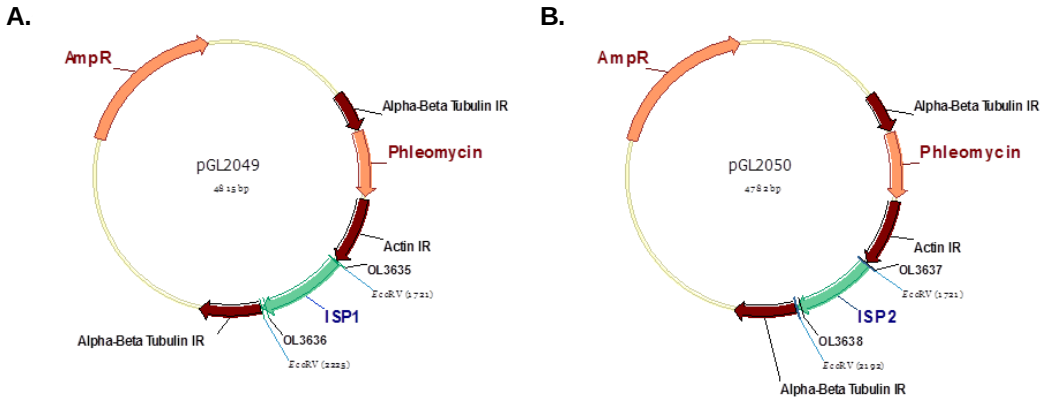

Figure 3.12 – Generation of ISP re-expression cell lines.

Constructs used for the re-expression of ISP1 (A) and ISP2 (B) in *T. brucei rhodesiense* Δ*isp1* and Δ*isp2* mutants, generating Δ*isp1:ISP1* and Δ*isp2:ISP2* cell lines

Altogether, between null mutants and re-expression cell lines, 7 final cell lines were created (Table 3.4)

	1st round of transfections		2nd round of transfections		
Cell line generated	**Cell line used**	**Plasmid**	**Cell line used**	**Plasmid**	**Antibiotic Resistance**
Δ*isp1* HYG/NEO	WT	pGL1688	isp1 (+/-) HYG	pGL1689	HYG/NEO
Δ*isp1* BSD/PAC	WT	pGL1947	isp1 (+/-) BSD	pGL1948	BSD/PAC
Δ*isp2*	WT	pGL1959	isp2 (+/-) HYG	pGL1960	HYG/NEO
Δ*isp1/2*	Δ*isp1* BSD/PAC	pGL1959	Δ*isp1*/isp2 (+/-) HYG	pGL1960	BSD/PAC/HYG/NEO
Δ*isp1:ISP1* HYG/NEO	Δ*isp1* HYG/NEO	pGL2049	---	---	HYG/NEO/PHLEO
Δ*isp1:ISP1* BSD/PAC	Δ*isp1* BSD/PAC	pGL2049	---	---	BSD/PAC/PHLEO
Δ*isp2:ISP2*	Δ*isp2*	pGL2050	---	---	HYG/NEO/PHLEO

Table 3.4 – Cell lines generated.

Brief description of the plasmids used to generate the null mutants and re-expression cell lines and antibiotic resistance displayed by each cell line

The first round of transfections resulted in 6 different heterozygous cell lines, resistant to the respective antibiotic. Although all heterozygous cell lines were viable, the ones selected for the second allele transfection were descendent from clones growing in the most diluted plates. Therefore, to create Δ*isp1* HYG/NEO cell lines, the HYG heterozygous was transfected with pGL1689 and to create Δ*isp1* BSD/PAC the BSD heterozygous was transfected with pGL1948. Like in ISP1, to generate the Δ*isp2* cell line pGL1959 was used to yield the HYG heterozygous cell line that was subsequently transfected with pGL1960.

To generate the Δ*isp1/2* cell line, ISP2 knock out constructs (pGL1959 and pGL1960) were used to transfect the Δ*isp1* BSD/PAC cell line. One heterozygous cell line resistant to HYG was created and subsequent integration of NEO cassette gave rise to a cell line resistant to all 4 antibiotics.

One clone of each null mutant cell line was used to transfect both pGL2049 (Δ*isp1* cell lines) and pGL2050 (Δ*isp2* cell lines). Transfectants were cloned and selected under antibiotic pressure with phleomycin (PHLEO) together with HYG and NEO or BSD and PAC, depending on the cell line transfected.

3.3.2 Confirmation of null mutant and re-expression cell lines

Double resistant parasites were analysed by PCR, Southern Blotting and Western Blotting to confirm correct integration of the antibiotic resistance cassettes and consequent gene deletion and also to check for the absence of protein expression.

3.3.2.1 PCR

Genomic DNA was isolated from double resistant clones selected from the most diluted plates, when possible, and used to confirm gene deletion by PCR with different oligonucleotide combinations.

To confirm the deletion of *ISP1* in Δ*isp1* HYG/NEO cell lines the oligonucleotide combinations used included the amplification of *ISP1* ORF (OL3635/OL3636), the amplification of 5' *ISP1* with the 5' terminal sequence of the antibiotic resistance gene (OL2508/OL13 for *HYG* and OL2508/OL1361 for *NEO*), the amplification of 3' *ISP1* with the 3' terminal sequence of the antibiotic resistance gene (OL14/OL2509 for *HYG* and OL1360/OL2509 for *NEO*) and finally the amplification of the entire integration cassettes with oligonucleotides designed outside the limits of the integration cassette (OL2508/OL2509) (Figure 3.13).

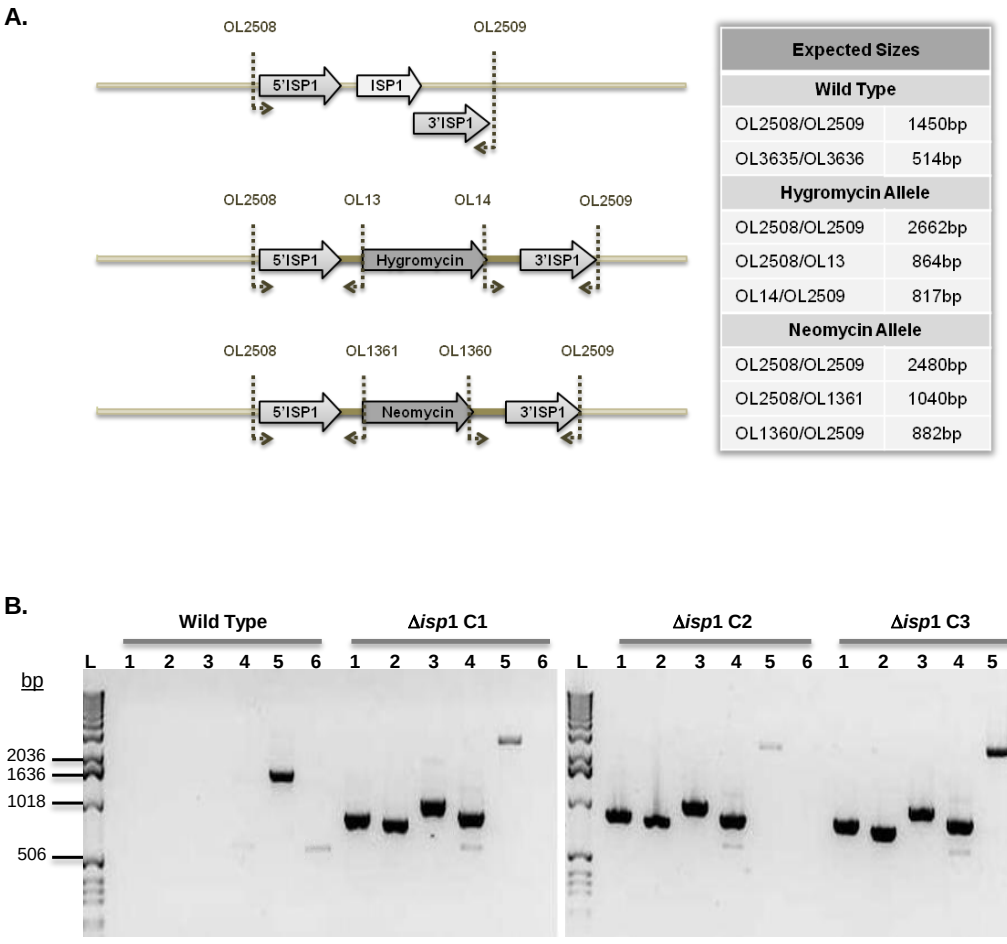

Figure 3.13 – Confirmation of Δ*isp1* HYG/NEO by PCR.

(A) Schematic representation of *ISP1 locus* in *T. brucei* before and after integration of *HYG* and *NEO* resistance cassettes. Oligos used are highlighted in the diagram and the predicted size for each oligo combination is displayed on the table nex to the diagram. **(B)** PCR analysis of Δ*isp1* HYG/NEO cell line. DNA from potential Δ*isp1* clones 1 – 3 (Δ*isp1* C1, Δ*isp1* C2 and Δ*isp1* C3) was used to confirm the integration of the *HYG* allele (Lanes 1, 2 and 5 corresponding to oligo combinations OL2508/OL13; OL14/OL2509 and OL2508/OL2509) and the *NEO* allele (Lanes 3, 4 and 5 corresponding to oligo combinations OL2508/OL1361; OL1360/OL2509 and OL2508/OL2509). Wild Type DNA was used as control with oligo combination OL3635/OL3636 used to amplify *ISP1* ORF (Lane 6)

Wild Type DNA was used as a control with the amplification of *ISP1* ORF resulting in a PCR product of 514 bp contrasting with the absence of PCR product observed in the Δ*isp1* HYG/NEO clones.

All the other oligo combinations were also used to amplify wild type DNA resulting in no product except for the amplification with OL2508 and OL2509 that

ensued in a PCR product of 1450 bp in contrast with the 2662 bp and 2480 bp product revealed for the *HYG* and *NEO* allele respectively (Figure 3.13B).

All Δ*isp1* HYG/NEO clones tested were positive for the presence of the *HYG* and *NEO* integration cassettes and for the absence of *ISP1* and the DNA isolated was used for further confirmation by Southern Blotting.

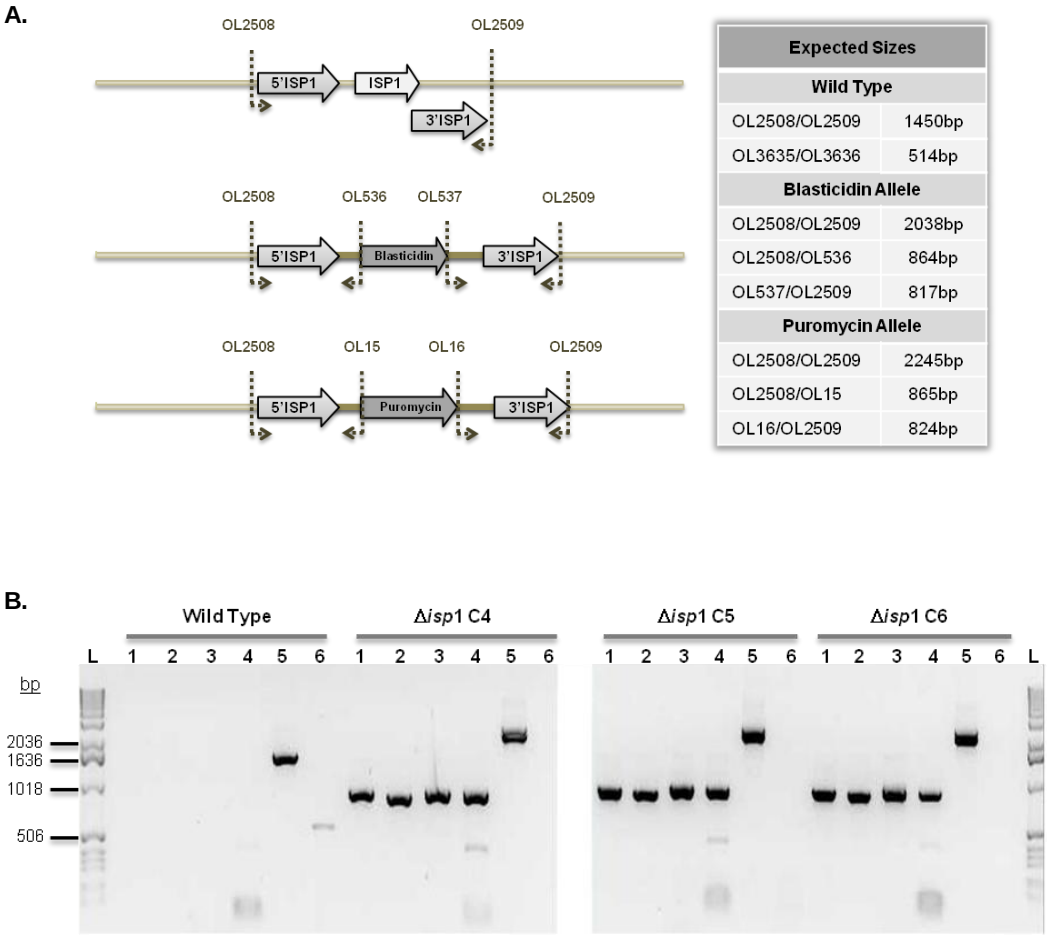

Expected Sizes	
Wild Type	
OL2508/OL2509	1450bp
OL3635/OL3636	514bp
Blasticidin Allele	
OL2508/OL2509	2038bp
OL2508/OL536	864bp
OL537/OL2509	817bp
Puromycin Allele	
OL2508/OL2509	2245bp
OL2508/OL15	865bp
OL16/OL2509	824bp

Figure 3.14 – Confirmation of Δ*isp1* BSD/PAC by PCR.

(A) Schematic representation of *ISP1 locus* in *T. brucei* before and after integration of *BSD* and *PAC* resistance cassettes. Oligos used are highlighted in the diagram and the predicted size for each oligo combination is displayed on the table next to the diagram. **(B)** PCR analysis of Δ*isp1* BSD/PAC cell line. DNA from potential Δ*isp1* clones 4 – 6 (Δ*isp1* C4, Δ*isp1* C5 and Δ*isp1* C6) was used to confirm the integration of the *BSD* allele (Lanes 1, 2 and 5 corresponding to oligo combinations OL2508/OL536; OL537/OL2509 and OL2508/OL2509) and the *PAC* allele (Lanes 3, 4 and 5 corresponding to oligo combinations OL2508/OL15; OL16/OL2509 and OL2508/OL2509). Wild Type DNA was used as a control with oligo combination OL3635/OL3636 used to amplify *ISP1* ORF (Lane 6)

The same strategy was used to confirm the deletion of *ISP1* in Δ*isp1* BSD/PAC cell lines with the same oligo combinations used to amplify *ISP1* ORF and the integration cassettes.

The amplification of 5' *ISP1* with the 5' terminal sequence of the antibiotic resistance gene was performed with oligo combinations OL2508/OL536 for *BSD* and OL2508/OL15 for *PAC* and the amplification of 3' ISP1 with the 3' terminal sequence of the antibiotic resistance gene with OL537/OL2509 for BSD and OL16/OL2509 for PAC (Figure 3.14 A).

The PCR products obtained correspond to the predicted sizes suggesting that the deletion of *ISP1* was successful in the 3 Δ*isp1* BSD/PAC clones analysed (Figure 3.14B).

To confirm the deletion of *ISP2* in Δ*isp2* cell lines the oligos used to amplify the 5' and 3' terminal sequences of the antibiotic resistance genes were the same as those used in the Δ*isp1* HYG/NEO cell line. These were used in combination with OL2510 for the amplification of 5' *ISP2* and OL2511 for the amplification of 3' *ISP2* (Figure 3.15A*)*.

Oligos OL3637 and OL3638 were used to amplify *ISP2* ORF resulting in a PCR product of 418 bp in wild type and no PCR product in Δ*isp2 clones.* The remaining oligos were also used to amplify wild type DNA.

As expected no PCR product was visible expect for the amplification with OL2510 and OL2511 that resulted in a PCR product of 1740 bp contrasting with the 2750 bp and 2528 bp product observed in the *HYG* and *NEO* alleles (Figure 3.15B).

The results obtained were compatible with the positive integration of *HYG* and *NEO* resistance cassettes and consequently with the successful deletion of *ISP2* gene.

To confirm the deletion of both ISP genes in the potential Δ*isp1/2* clones, PCR was performed with the same oligos used for the confirmation of individual gene deletion in Δ*isp1* and Δ*isp2* cell lines resulting in no PCR product in the amplification of *ISP1* and *ISP2* ORFs and PCR products with the expected sizes in the amplification with the remaining oligo combinations (Figure 3.16).

Again, both Δ*isp1/2* clones analysed by PCR showed positive integration of 4 resistance markers cassettes compatible with the deletion of *ISP1* and *ISP2* from the parasite's genome.

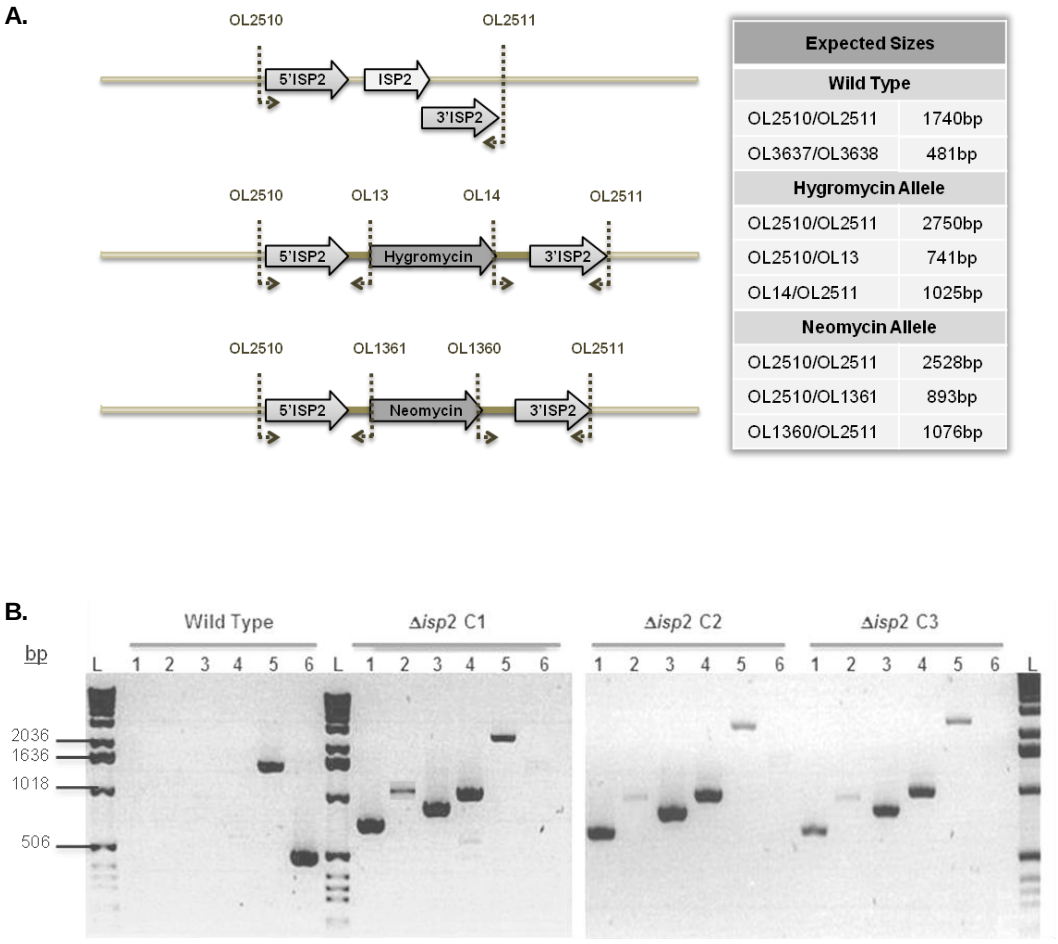

Figure 3.15 – Confirmation of Δ*isp2* by PCR.

(A) Schematic representation of *ISP2 locus* in *T. brucei* before and after integration of *HYG* and *NEO* resistance cassettes. Oligos used are highlighted in the diagram and the predicted size for each oligo combination is displayed on the table nex to the diagram. **(B)** PCR analysis of Δ*isp2* cell line. DNA from potential Δ*isp2* clones 1 – 3 (Δ*isp2* C1, Δ*isp2* C2 and Δ*isp2* C3) was used to confirm the integration of the *HYG* allele (Lanes 1, 2 and 5 corresponding to oligo combinations OL2510/OL13; OL14/OL2511 and OL2510/OL2511) and the *NEO* allele (Lanes 3, 4 and 5 corresponding to oligo combinations OL2510/OL1361; OL1360/OL2511 and OL2510/OL2511). Wild Type DNA was used as control with oligo combination OL3637/OL3638 used to amplify *ISP2* ORF (Lane 6)

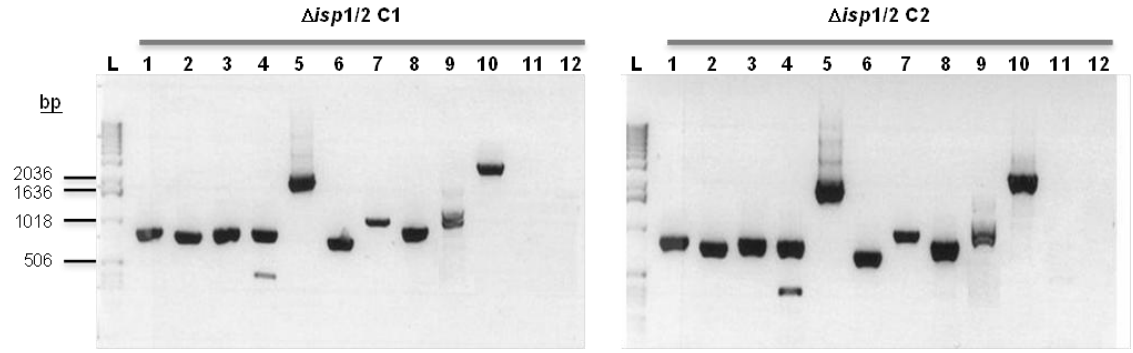

FIGURE 3.16 – Confirmation of Δ*isp1/2* by PCR.

DNA from potential Δ*isp1/2* clones C1 and C2 was used to confirm the integration of the 4 antibiotic resistance cassettes. For the integration of the *BSD* allele the oligo combinations used were OL2508/OL536, OL537/OL2509 and OL2508/OL2509 (Lanes 3, 4 and 5); For the integration of the *PAC* allele the oligo combinations used were OL2508/OL15, OL16/OL2509 and OL2508/OL2509 (Lanes 3, 4 and 5); For the integration of *HYG* allele the oligo combinations used were OL2510/OL13, OL14/OL2511 and OL2510/OL2511 (Lanes 6, 7 and 10); For the integration of the *NEO* allele the oligo combinations used were OL2510/OL1361, OL1360/OL2511 and OL2510/OL2511 (Lanes 8, 9 and 10); Oligo combinations OL3635/OL3636 and OL3637/OL3638 were used to amplify *ISP1* and *ISP2* ORF (Lanes 11 and 12)

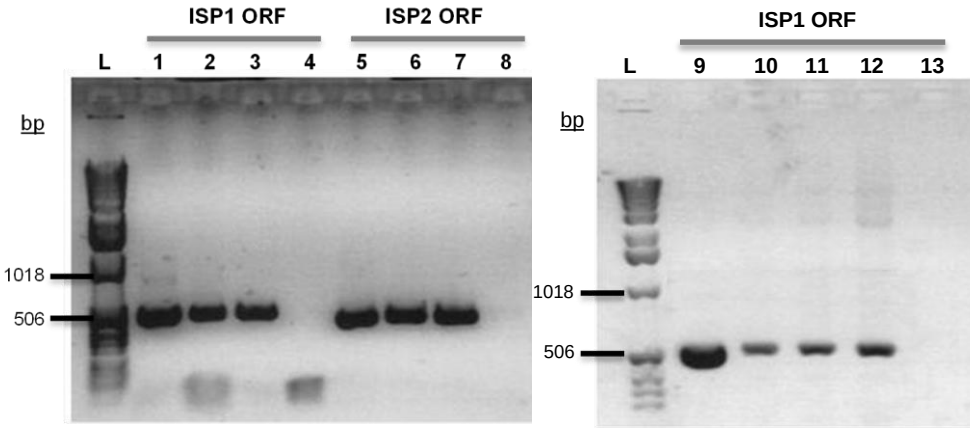

Figure 3.17 – Confirmation of ISP1 and ISP2 re-expression cell lines by PCR.

Oligo combination OL3635/OL3636 was used to amplify *ISP1* ORF in Wild Type (Lanes 1 and 9) in potential Δ*isp1:ISP1* HYG/NEO clones (Lanes 2 and 3) and in Δ*isp1:ISP1* BSD/PAC clones (Lanes 10, 11 and 12). Oligo combination OL3637/OL3638 was used to amplify *ISP2* ORF in Wild Type (Lanes 5) and in potential Δ*isp2:ISP2* clones (Lane 6 and 7). H_2O was used as negative control (lanes 4, 8 and 13)

The PCR analysis of ISP1 and ISP2 re-expression in Δ*isp1* and Δ*isp2* cell lines was performed with the amplification of the respective ORFs with oligos OL3635/OL3636 (ISP1 ORF) and OL3637/OL3638 (ISP2 ORF) resulting in PCR products of 514 bp and 481 bp respectively (Figure 3.17). All clones analysed revealed the presence of the inserted ORF.

3.3.2.2 Southern Blotting

The use of PCR is a fast way to confirm gene deletion and discard clones that although resistant to selection antibiotics still harbour the target gene.

To investigate if the antibiotic resistance of cells is in fact due to integration of the resistance cassette in the gene locus and not in another part of the genome, re-confirmation was done by Southern Blotting with the 5' flanking region used in the knock out constructs as a probe.

For the confirmation of Δ*isp1* HYG/NEO null mutants, genomic DNA was digested with *AvaI* and *BamHI* and probed with the 5' *ISP1* (Figure 3.18 A). One fragment of 3.1 kb was detected in wild type and both heterozygotes.

Fragments corresponding to the *HYG* and *NEO* allele with predicted sizes of 4.4 kb and 2.5 kb could only be detected in the respective heterozygotes and in the 3 clones analysed, showing correct integration of both *HYG* and *NEO* cassettes and loss of wild type allele (Figure 3.18 B).

Similar strategy was used to confirm *ISP1* deletion in *Δisp1* BSD/PAC resistant clones. *AvaI* was used to digest genomic DNA and 5' *ISP1* was used as probe (Figure 3.19 A). The 3.1 kb fragment could be detected in the wild type and both heterozygotes as expected.

The digestion of BSD and PAC resistant heterozygotes with *AvaI* produces fragments with very similar sizes (3.7 kb and 3.9 kb respectively) but difference can be distinguished in the Southern Blotting image (Figure 3.19 B).

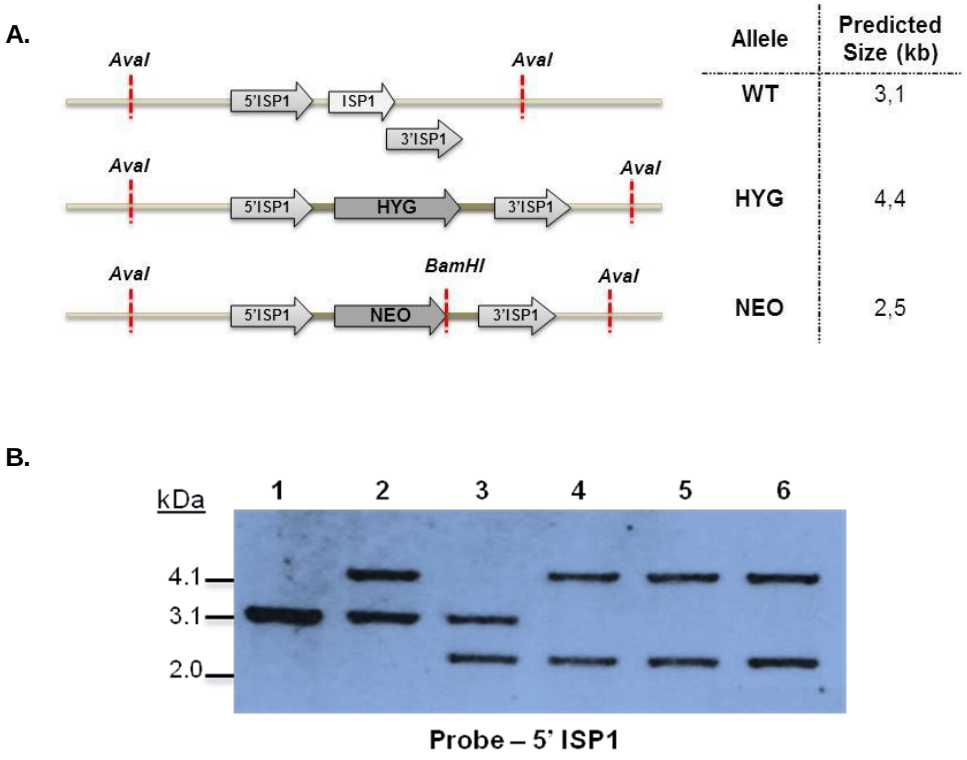

Figure 3.18 – Southern Blotting analysis of Δ*isp1* HYG/NEO null mutants.

(A) Graphic representation of *ISP1* locus before and after integration of *HYG* and *NEO* resistance cassettes. Restriction sites are represented in red and predicted sizes following enzimatic digestion and probing with 5' ISP1 are displayed on the table next to the diagram. **(B)** Genomic DNA was separated on a 0.8% agarose gel and transferred to a nylon membrane before hybridization with 5' *ISP1*. Detection revealed 3 different fragment sizes. A 3.1 kb fragment corresponding to the wild type allele, a 4.4 kb fragment corresponding to the *HYG* allele and a 2.5 kb fragment corresponding to the *NEO* allele. Lane 1, Wild Type *T. brucei rhodesiense* IL1852; Lane 2, HYG resistant heterozygote; Lane 3, NEO resistant heterozygote; Lane 4, Δ*isp1* clone1; Lane 5, Δ*isp1* clone2; Lane 6, Δ*isp1* clone3

The fragment corresponding to the BSD resistant allele could be detected in the respective heterozygote and in clones Δ*isp1* clone 4, Δ*isp1* clone 5 and Δ*isp1* clone 6 and although clone Δ*isp1* clone 4 displayed a 3.9 kb fragment corresponding to the PAC resistant heterozygote, it also showed the presence of a 3.1 kb fragment corresponding to the wild type allele and was not confirmed as an *ISP1* null mutant. Clones Δ*isp1* clone 5 and Δ*isp1* clone 6 showed correct integration of PAC resistance cassette by displaying the corresponding 3.9 kb fragment, and so they were both confirmed to be *ISP1* null mutant (Figure 3.19 B).

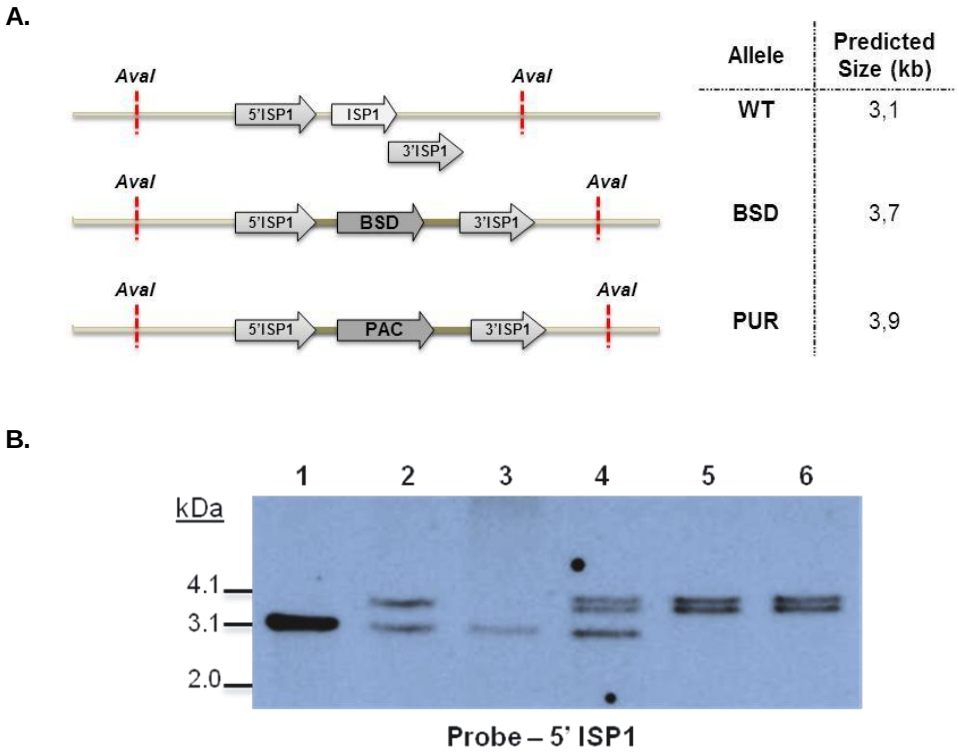

Figure 3.19 – Southern Blotting analysis of Δ*isp1* BSD/PAC null mutants.

(A) Graphic representation of *ISP1* locus before and after integration of *BSD* and *PAC* resistance cassettes. Restriction sites are represented in red and predicted sizes following enzimatic digestion and probing with 5' *ISP1* are displayed on the table next to the diagram. **(B)** Genomic DNA was separated on a 0.8% agarose gel and transferred to a nylon membrane before hybridization with 5' *ISP1*. Detection revealed 3 different fragment sizes. A 3.1 kb fragment corresponding to the wild type allele, a 3.7 kb fragment corresponding to the *BSD* allele and a 3.9 kb fragment corresponding to the *PAC* allele. Lane 1, Wild Type *T. brucei rhodesiense* IL1852; Lane 2, BSD resistant heterozygote; Lane 3, PAC resistant heterozygote; Lane 4, Δ*isp1* clone 4; Lane 5, Δ*isp1* clone 5; Lane 6, Δ*isp1* clone 6

In the PAC resistant heterozygote only the 3.1 kb *ISP1*-containing fragment could be detected and although parasites showed resistance to media containing the antibiotic, the *ISP1* gene was not disrupted and the PAC resistance cassette must have been integrated in some other part of the parasite's genome.

The Southern Blotting analysis of *ISP2* null mutants was done in a similar way and revealed that the 3 double resistant clones selected displayed correct integration of both *HYG* and *NEO* resistance cassettes and loss of wild type allele (Figure 3.20 B).

The 1.35 kb fragment corresponding to the wild type allele was detected in the wild type cell line and both heterozygote cell lines, where 2.6 kb and a 2.4 kb fragments corresponding to the HYG and NEO resistant heterozygotes respectively could be detected.

In the double resistant clones, only the 2.4 and the 2.6 kb fragments were detected, confirming the absence of the wild type alleles (Figure 3.20 B)

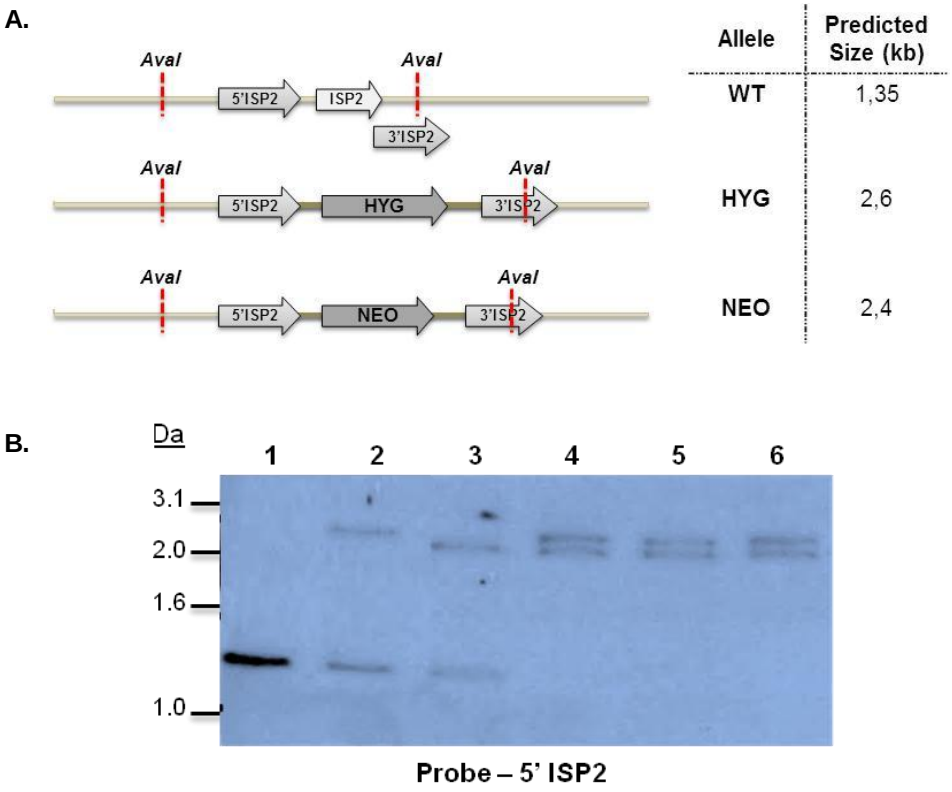

Figure 3.20 – Southern Blotting analysis of Δ*isp2* null mutants.

(A) Graphic representation of *ISP2* locus before and after integration of *HYG* and *NEO* resistance cassettes. Restriction sites are represented in red and predicted sizes following enzimatic digestion and probing with 5' ISP2 are displayed on the table next to the diagram. **(B)** Genomic DNA was separated on a 0.8% agarose gel and transferred to a nylon membrane before hybridization with 5' *ISP2*. Detection revealed 3 different fragment sizes, a 1.35 kb fragment corresponding to the wild type allele, a 2.6 kb fragment corresponding to the *HYG* allele and a 2.4 kb fragment corresponding to the *NEO* allele. Lane 1, Wild Type *T. brucei rhodesiense* IL1852; Lane 2, HYG resistant heterozygote; Lane 3, NEO resistant heterozygote; Lane 4, Δ*isp2* clone 1; Lane 5, Δ*isp2* clone 2; Lane 6, Δ*isp2* clone 3

As previously described, Δ*isp1/2* cell line was generated by transfecting the *ISP2* knock out constructs into Δ*isp1* BSD/PAC the cell line. As the absence of *ISP1* was already confirmed in the transfected Δ*isp1* cell line (Figure 3.19), the deletion of *ISP2* was confirmed by Southern Blotting analysis using 5' *ISP2* as probe.

Although with a weak signal, the 1.35 kb fragment corresponding to the wild type allele could be detected in the Wild Type cell line, in Δ*isp1* BSD/PAC cell line and also in the HYG resistant heterozygote (Figure 3.21, Lanes 1,2 and 4). In Lane 4, another faint band with 2.6 kb could also be seen, corresponding to the *HYG* resistance allele. The difference in the sample's signal strength was expected as the quantity of DNA used was not uniform. While 5 µg of DNA from the remaining samples was used, the available amount of DNA from the Wild Type, Δ*isp1* BSD/PAC and HYG resistant heterozygote samples to digest and load on the agarose gel was significantly lower (± 2 µg) resulting in such discrepancy.

The absence of the 1.35 kb fragment in association with the appearance of 2 fragments with 2.4 and 2.6 kb in lanes 5 and 6 indicates that both resistance cassettes were correctly integrated in the *ISP2* locus (Figure 3.21).

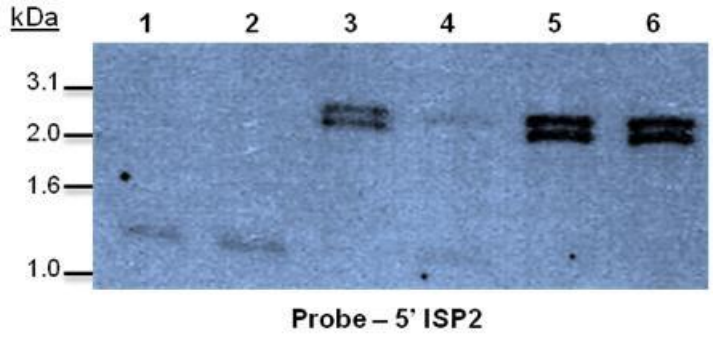

Figure 3.21 – Southern Blotting analysis of Δ*isp1/2* null mutants.

Genomic DNA was digested with *AvaI* and separated in a 0.8% agarose gel and transferred to a nylon membrane before hybridization with 5' *ISP2*. Detection revealed 3 different fragment sizes, a 1.35 kb fragment corresponding to the wild type allele, a 2.6 kb fragment corresponding to the *HYG* allele and a 2.4 kb fragment corresponding to the *NEO* allele. Lane 1, Wild Type *T. brucei rhodesiense* IL1852; Lane 2, Δ*isp1* clone 6; Lane 3, Δ*isp2* clone 3; Lane 4, HYG resistant heterozygote; Lane 5, Δ*isp1/2* clone 1; Lane Δ*isp1/2* clone 2

As *ISP1* deletion had already been confirmed in the cell line used to transfect the *ISP2* constructs (Δ*isp1* clone 6 cell line), Δ*isp1/2* clone 1 and Δ*isp1/2* clone 2 can be positively confirmed as double *ISP1* and *ISP2* null mutants.

3.3.2.3 Western Blotting

Antibodies generated in section 3.1.2 were used to corroborate the successful deletion of *ISP1* and *ISP2* genes in the Δ*isp1*, Δ*isp2* and Δ*isp1/2* cell lines by Western Blotting. Antibody anti-ISP1 3G8 recognized a band corresponding to ISP1 in the wild type and in Δ*isp1*:ISP1 cell lines. As expected, no protein expression could be detected by the anti-ISP1 antibody in Δ*isp1* cell lines or in the Δ*isp1/2* cell lines (Figure 3.22).

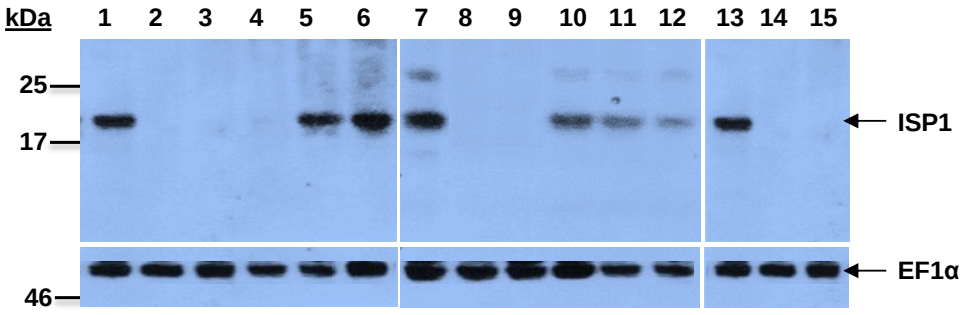

Figure 3.22 – Western Blotting analysis of *Δisp1* cell lines.

Whole cell lysates were obtained from 5×10^6 parasites and analysed by Western Blotting with anti-ISP1 antibody to assess protein expression in different cell lines. Anti EF1-α antibody was used as loading control. Lanes 1, 7 and 13 – Wild Type *T. brucei rhodesiense* IL1852; Lanes 2, 3 and 4 – Δ*isp1* clones 1,2 and 3; Lane 5 and 6 - Δ*isp1*:ISP1 clone 1 and 2; Lane 8 and 9 – Δ*isp1* clones 5 and 6; Lanes 10, 11 and 13 – Δ*isp1*:ISP1 clone 3, 4 and 5; Lanes 14 and 15 – Δ*isp1*/2 clone 1 and 2.

The absence of ISP2 protein expression in Δ*isp2* and Δ*isp1*/2 cell lines was also confirmed by Western Blotting using antibody anti-ISP2 4G7. The band corresponding to ISP2 was only detected in the wild type and Δ*isp1/2* cell lines, confirming once again the successful generation of null mutant and re-expressor cell lines (Figure 3.23).

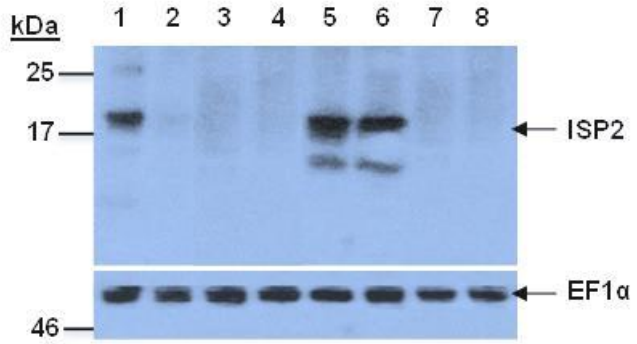

Figure 3.23 – Western Blotting analysis of *Δisp2* cell lines.

Whole cell lysates were obtained from 5×10^6 parasites and analysed by Western Blotting with anti ISP2 antibody to assess protein expression in different cell lines. Anti EF1-α antibody was used as loading control. Lane 1 – Wild Type *T. brucei rhodesiense* IL1852; Lanes 2, 3 and 4 – Δ*isp2* clones 1,2 and 3; Lane 5 and 6 - Δ*isp2*:ISP2 clone 1 and 2; Lane 7 and – Δ*isp1*/2 clone 1 and 2.

3.3.3 *In vitro* analysis of null mutant cell lines

The analysis of all clones confirmed to be ISP1, ISP2 and ISP1 and 2 deficient revealed no gross morphological defects. In order to assess if the absence of ISPs has any impact on the cell's growth rate, culture cell density was determined daily for 4 days. Cells were seeded at 1×10^5 cells/ml every 24 hours and density was determined by haemocytometer counting at regular time intervals for 48 hours.

Results show that all clones were viable in culture and no significant difference in the growth rates of Δ*isp1*, Δ*isp2* and Δ*isp1/2* cell lines when compared to the wild type (Figure 3.24).

Despite the absence of morphological defects observed in all cell lines, Δ*isp1/2* cell clones showed an interesting phenotype in culture. Microscopic observation of these parasites and comparison with the remaining cell lines revealed a motility defect.

Specifically, Δ*isp1/2* parasites are unable of directional cell motility and a great percentage of cells showed uncoordinated beating of the flagellum with parasites moving erratically in a "chasing the tail" manner.

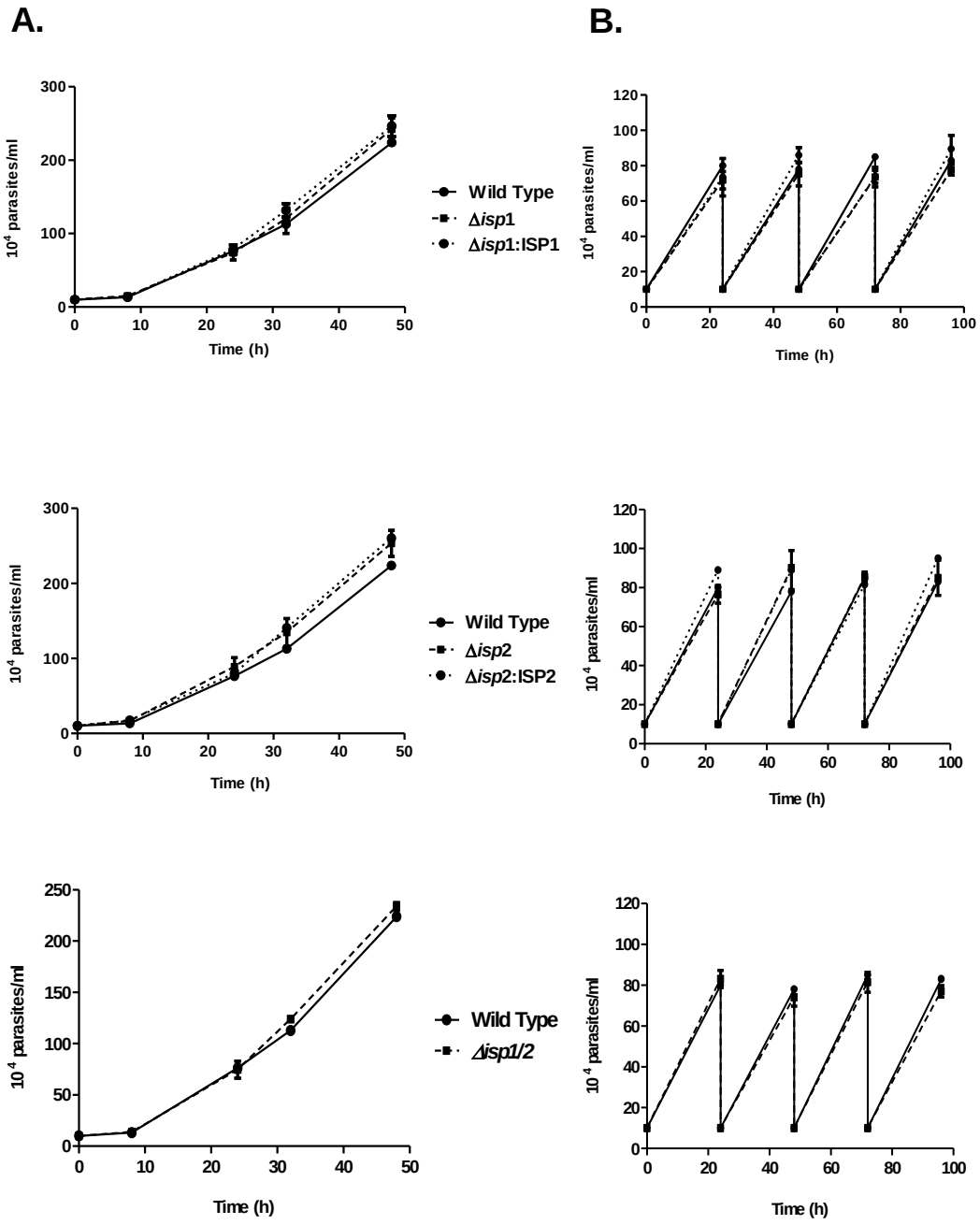

Figure – 3.24 *In vitro* growth analysis of ISP null mutant cell lines.

(A) Growth rate of Wild Type, Δ*isp1*, Δ*isp2* and Δ*isp1/2* cell lines was determined by haemocytometer cell counts at 8, 24, 32 and 48 hours after cell were seeded at 1×10^5 cells/ml **(B)** Cultures were diluted to 1×10^5 cells/ml every 24 hours and growth rates evaluated over a period of 4 days. All data are represented as mean ± SD of Δ*isp1*, Δ*isp2* and Δ*isp1/2* clones.

Wild type trypanosomes exhibit a distinctive bi-helical motion with the flagellum leading and driving the cell body towards its tip in a well-defined direction (Walker, 1961). In contrast, Δ*isp1/2* parasites barely move forward in a specific direction, spinning constantly without greatly altering their location.

The erratic movement displayed by Δ*isp1/2* parasites, although very distinct from the auger-like motion characteristic of wild type parasites, resembles the phenotype presented by trypanin knockdown mutants, which are also incapable of directional mobility (Hutchings *et al*., 2002).

3.3.4 *In vivo* analysis of null mutant cell lines

Given the apparent absence of serine peptidases sensitive to the action of ISP1 and ISP2 in the genome of *T. brucei* the function of these inhibitors are most likely associated with the infection of the host.

To investigate a potential role of ISP1 and ISP2 in the infection of mammalian hosts, the infection profile of Δ*isp1*, Δ*isp2* and Δ*isp1/2* in mice was compared to the wild type *T. brucei rhodesiense* IL1852 (Figure 3.25).

Groups of 4 ICR mice were injected intraperitoneally with 5×10^3 parasites from a donor mouse and parasitemia was monitored by haemocytometer counting of parasites in blood samples collected by tail prick.

All mice presenting severe clinical symptoms or parasitemia above 1×10^8 cells/ml were culled to ensure animal welfare.

Survival rates were determined (Figure 3.25) and results show that individual deletion of either *ISP1* or *ISP2* does not compromise *in vivo* infectivity, with Δ*isp1* and Δi*sp2* parasites displaying similar virulence to the wild type or Δ*isp1*:ISP1 in ICR mice.

No significant difference was observed in the course of infections and mice survival, with mean survival times of 17 days for mice infected with Δ*isp1* or Δi*sp2* parasites and 18 days for mice infected with wild type and Δ*isp1*:ISP1 cell lines (Figure 3.25A).

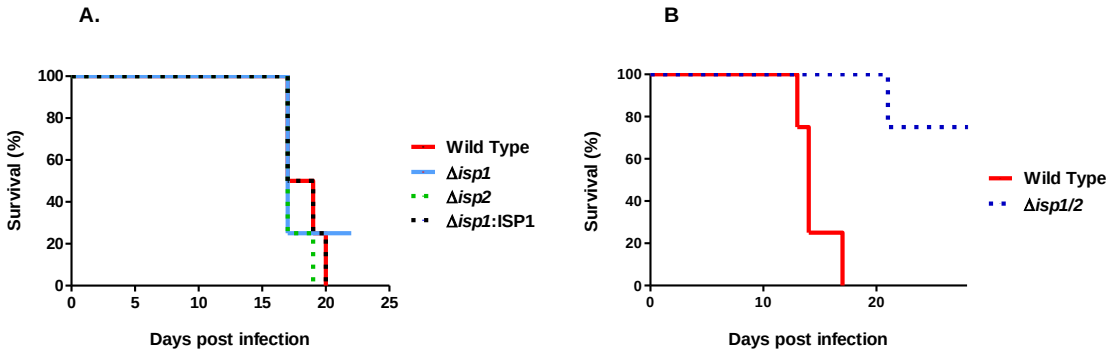

Figure 3.25 – Mouse survival rates.

Survival rates of infected ICR mice were determined and represented in a Kaplan-Meier survival curve. Two independent experiments were performed and survival rate was determined for **(A)** infection with wild type, Δ*isp1*, Δi*sp2* and Δ*isp1*:ISP1 parasites and **(B)** infection with wild type and Δ*isp1/2* parasites. Experiment performed in collaboration with Ms Alana Hamilton.

In contrast, Δ*isp1/2* parasites show reduced virulence *in vivo* with 75% of mouse survival 28 days post infection and a mean survival time of 15 days for the group infected with wild type parasites (Figure 3.25 B).

Wild type *T. brucei* strain 427 is extremely virulent in mice causing rapid increase of parasitemia and death within few days (Lanteri *et al*., 2006) and so the use of a less virulent strain for mice such as *T. brucei rhodesiense* strain IL 1852 in this study allows an extension to the time of the *in vivo* infection analysis.

Infection patterns of the groups infected with wild type, Δ*isp1*, Δi*sp2* and Δ*isp1*:ISP1 cell lines were very similar with peaks of parasitemia followed by time intermissions, where parasitemia falls below the detection limit. Furthermore, parasitemia levels registered during the peaks was not significantly different between groups. In all groups clearance occurred at day 5, two days after the first parasitemia peak. Recurrence arose between days 10 and 12 and the majority of mice never recovered from the cumulative levels of parasitemia, except for one Δ*isp1* infected mouse that was able to control the infection and survived the experiment without showing detectable levels of parasitemia and one Δ*isp2* infected mouse that peaked at day 7 and again at day 14 with no signs of parasitemia in between (Figure 3.26 A).

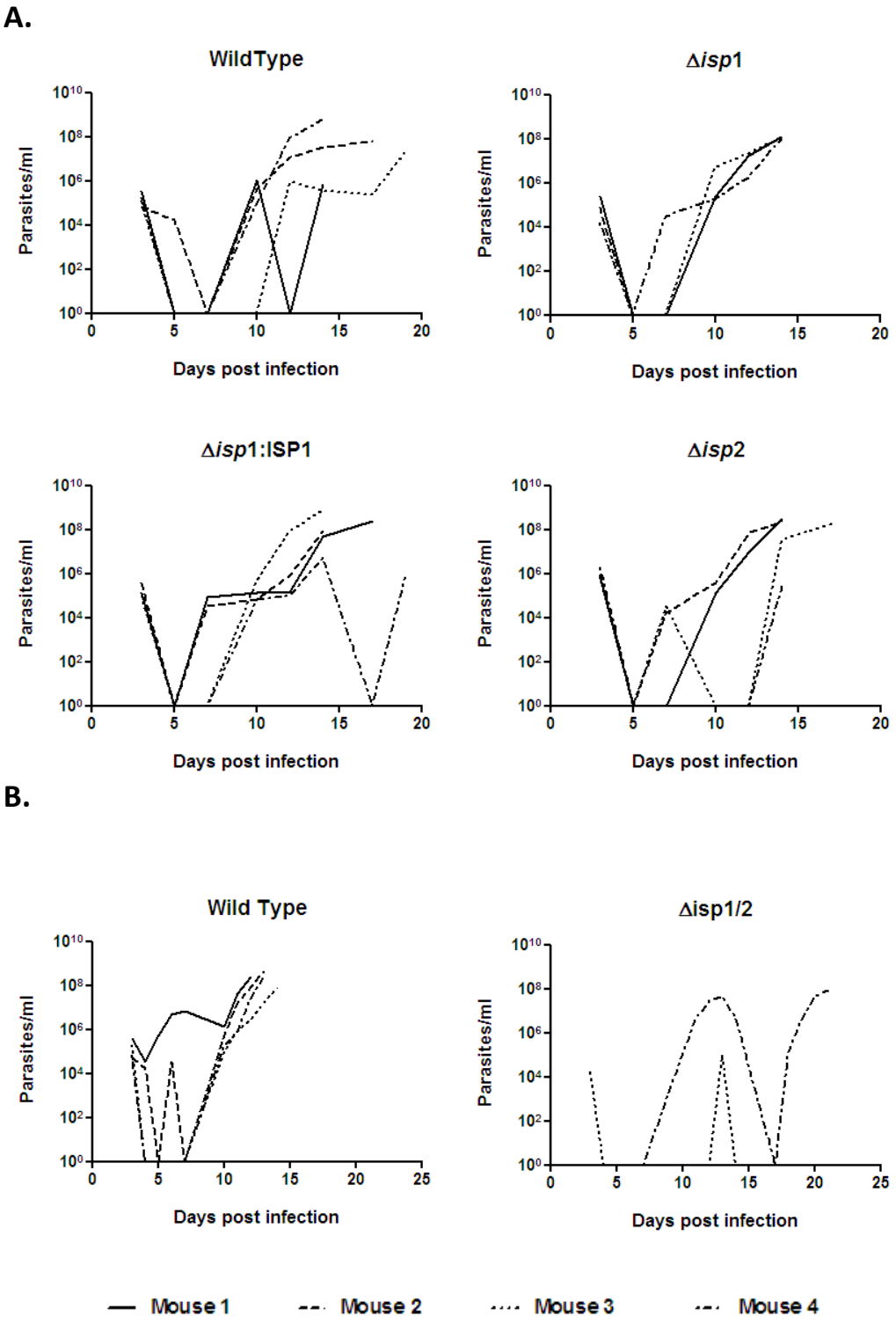

Figure 3.26 – Mouse infection profile.

Each mouse (labeled 1–4 in each group) was inoculated with 5×10^3 parasites from a specific donor mouse previously infected with wild type, Δ*isp*1, Δ*isp*2, Δ*isp1*:ISP1 and Δ*isp1*/2 cell lines. Parasitemia was monitored and registered individually within each group and mice presenting severe clinical symptoms or parasitemia above 1×10^8 cells/ml were culled. Experiment performed in collaboration with Ms Alana Hamilton.

In the second experiment wild type and Δ*isp1/2* infection profiles were compared and results show that 3 out of 4 mice in the group infected with Δ*isp1/2* parasites reached the end of the experiment without detectable levels of parasitemia and only 2 revealed the presence of parasites in the blood in the course of the experiment; one being able to overcome the infection after two parasitemia peaks (at day 3 and 13 post infection) and the other one being unable to recover after developing two later parasitemia peaks at days 13 and 18 post infection (Figure 3.26 B).

These results suggest that sequential deletion of ISP1 and ISP2 affects viability of BSF trypanosomes and both inhibitors are required for the development of infection in mice.

3.3.5 Electron Microscopy

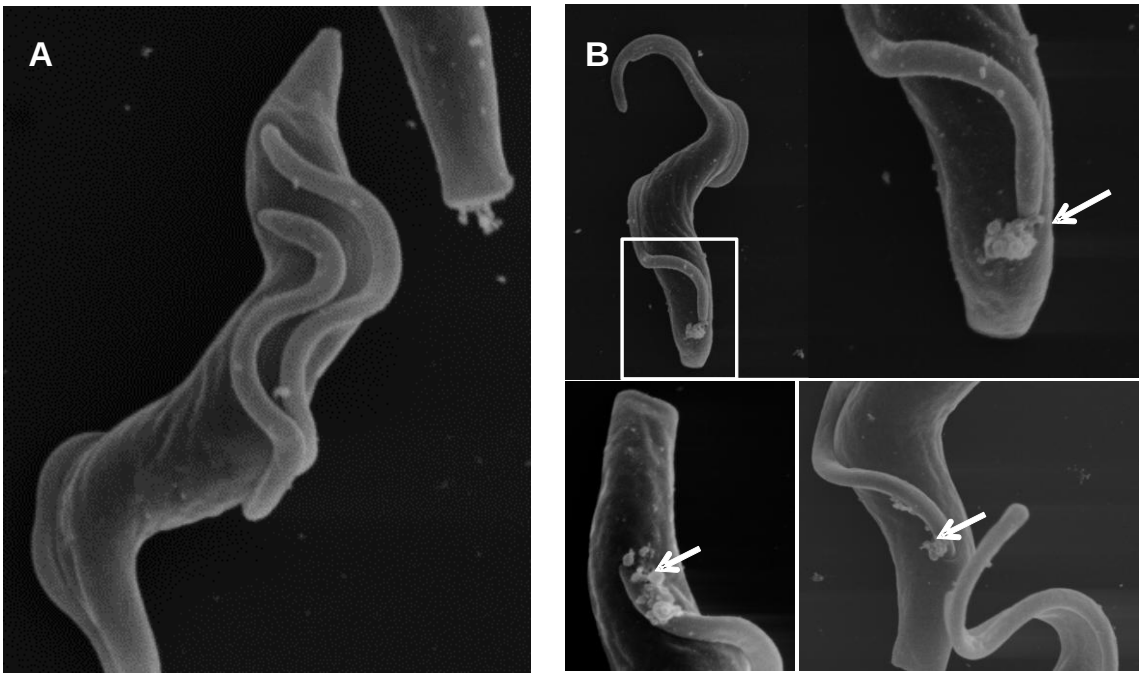

Figure 3.27 – Scanning Electron Microscopy analysis.

(A) BSF wild type parasites were used as a control in the analysis of **(B)** Δ*isp*1/2 parasites by SEM. White arrows show the accumulation of abnormal material outside the flagellar pocket. Experiment performed in collaboration with Dr Laurence Tetley (University of Glasgow).

Scanning Electron Microscopy (SEM) analysis of Δ*isp*1/2 parasites shows accumulation of small vesicles emerging from the flagellar pocket possibly corresponding to exosomes (Figure 3.27B).

The secreted vesicles seem to be restricted to the flagellar pocket and the presence of such material along the flagellum or throughout the cell body of Δ*isp1/2* parasites could not be detected. In wild type parasites the presence of vesicular material accumulated outside the flagellar pocket or any other cellular structure could not be detected (Figure 3.27A).

3.3.6 Expression of ISP1 is regulated by ISP2

The confirmation of the absence of protein expression in *ISP* null mutants by Western Blotting led to an unexpected observation. When using the anti-ISP1 antibody against Δ*isp2* whole cell lysates a protein with the expected size of 17 kDa was not detected (Figure 3.28 A). Similar result was obtained when using the anti-ISP2 antibody. The band corresponding to ISP1 could not be detected in the Δ*isp*1 whole cell lysates (Figure 3.28 B). Western Blotting was repeated to confirm that the result obtained is not an artifact.

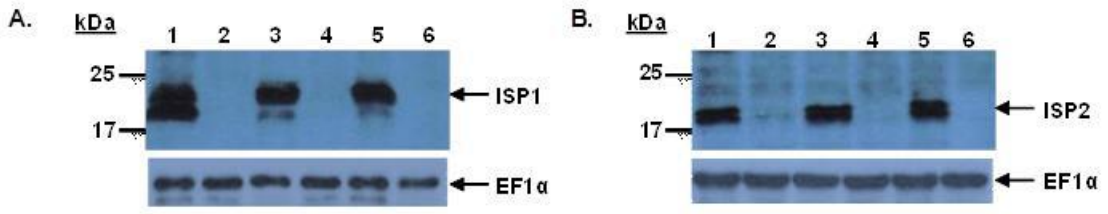

Figure 3.28 – Analysis of *T. brucei* ISP1 and ISP2 expression by Western Blotting.

Expression of ISP1 and ISP2 in Δ*isp*1 and Δ*isp*2 mutants was analysed by western blotting using (A) anti-ISP1 antibody and (B) anti-ISP2 antibody. Anti EF1-α antibody was used as loading control. Lane 1 – Wild Type *T. brucei rhodesiense* IL1852; Lane 2 – Δ*isp*1; Lane 3 – Δ*isp*1:ISP1; Lane 4 – Δ*isp*2; Lane 5 – Δ*isp*2:ISP2; Lane 6 – Δ*isp1/*2

PCR results using specific primers for the amplification of ISP ORFs show that *ISP2* ORF can be amplified in the Δ*isp1* cell lines as well as *ISP1* ORF can be amplified in the Δ*isp2* cell lines (results not shown).

Additionally, given the absence of expression of both ISPs in the Δ*isp1* and Δ*isp2* cell lines, it would be expected that the individual knock out cell lines developed similar phenotypes to the ones presented by the Δ*isp1/2*.

Such does not occur and individual knock out cell lines have normal motility when cultured (see Section 3.3.3) and normal survival and growth rates when used to infect mice, contrasting with the Δ*isp1/2* parasites (see Section 3.3.4). This result suggests that the expression of one ISP is regulated by the presence of the other ISP.

3.4 Growth Inhibition by Monoclonal Antibodies

3.4.1 *In vitro* growth inhibition assay

To determine if the presence of monoclonal antibodies generated against ISP1 and ISP2 has any effect on cultured parasites two different assays were performed.

A preliminary assay was conducted in 24 well plates. Trypanosomes were cultured at 1×10^4 cell/ml in 900 µl of HMI-9 medium and 100 µl of each supernatant previously selected (see section 3.1.2) were added to each well. To use as negative control, wild type BSF trypanosomes were cultured at the same density in 1 ml of HMI-9 medium (HMI-9 control) and in 1 ml of HMI-9 medium containing 10% of hybridoma culture medium (DMEM control).

The experiment was conducted for 96 hours and results showed that both antibodies against ISP1 and ISP2 have an effect on the parasite's growth rates. In the presence of antibody, cultures have significantly lower densities, at times 48, 72 and 96 hours. The difference of growth rates is statistically more significant in the presence of antibody anti-ISP1 3G8 and antibody anti-ISP2 4G7 (with $P<0.001$).

Parasites growing in HMI-9 medium containing 10% DMEM (DMEM control) also showed reduced growth at 96 hours but no significant difference was observed at the remaining time (results not shown).

A second experiment was conducted using the purified antibodies anti-ISP1 3G8 and anti-ISP2 4G7. 25 µg of each anti-ISP1 antibody and pre-immune affinity purified IgG were added to a 5 ml culture with a seeding density of 1×10^5 cells/ml. Cultures were maintained in HMI-9 for 3 days and cell density determined daily by haemocytometer counting (Figure 3.29).

The experiment was also performed with higher amounts of antibody (50 and 100 µg) but no reliable results were obtained once the added antibody solution exceeded 1% of the total culture volume and could affect cell growth.

Results showed that in the presence of both 50 and 100 µg of antibody cell growth was strongly inhibited after 24 hours and most parasites were dead after 48 hours. The use of 12.5 µg of antibody did not have any effect on the parasite's growth rates (results not shown).

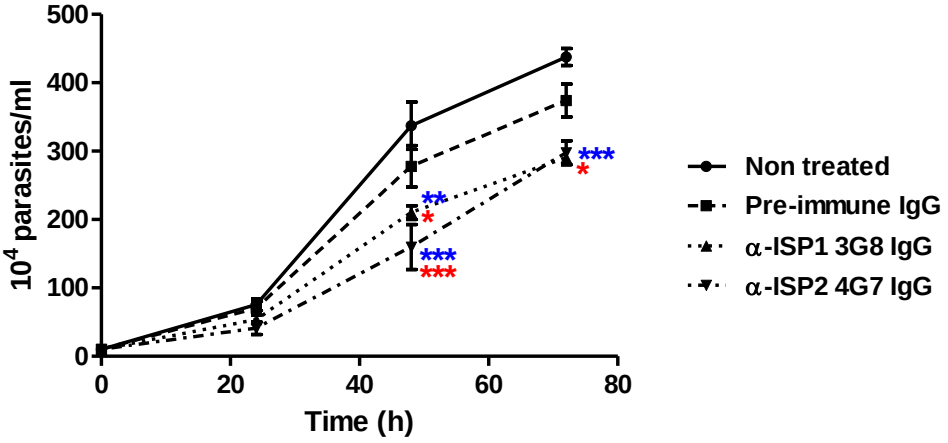

Figure 3.29 – *In vitro* growth analysis of *T. brucei*.

BSF parasites were seeded at 1×10^5 cells/ml and maintained for 72 hours in HMI-9 containing 25 µg of pre-immune IgG, anti-ISP1 3G8 IgG and anti-ISP2 4G7 IgG. Cell density was analysed daily by haemocytometer counting with data represented as the mean values ± SD of 3 independent experiments. Asterisks indicates statistical significance from non treated (blue) or pre-immune IgG treated parasites (red) at $P<0.05$ (∗), $P<0.01$ (∗∗) and $P<0.001$ (∗∗∗).

The use of 25 µg of antibody was sufficient to produce an effect on the parasite's growth rates. When compared to the non treated control, parasites treated with both anti-ISP1 and anti-ISP2 antibodies displayed significantly reduced growth. If we compare the growth of anti-ISPs IgG treated parasites with the ones treated with pre-immune IgG, the difference is less pronounced but still statistical significant (Figure 3.29).

Since there are no peptidases sensitive to the action of ISPs predicted in the genome of *T. brucei*, it is likely that these inhibitors exert their inhibitory role on the host's serine peptidases. This observation allied to the fact that ISP null mutant cell lines show no growth deffect in culture would suggest that the incubation of *T. brucei* cultures with anti-ISP antibodies didn't produce any effect on the parasite's growth rates.

However, results obtained are contradictory and the presence of anti-ISP antibodies results in slowly growing parasites after 48 hours that reach stationary phase at lower densitiy than non treated or pre-immune IgG treated parasites.

After 48 hours, parasites were diluted in fresh HMI-9 medium to the concentration of 1×10^4 cell/ml and normal growth was restored for both cultures treated with α-ISP1 and α-ISP2 antibodies (results not shown).

3.4.2 *In vivo* growth inhibition assay

To study the effect of monoclonal antibodies against ISP1 and ISP2 on experimental *T. brucei* infection, mice were divided in 4 different groups and injected intraperitoneally with PBS (control group), anti-ISP1 antibody (α-ISP1 3G8 IgG group), anti-ISP2 antibody (α-ISP2 4G7 IgG group) and both antibodies simultaneously (α-ISP1 3G8 IgG + α-ISP2 4G7 IgG group) one day before being challenged with 1×10^4 cultured *T. brucei* 427 and on days 0 and 2 post challenge.

Parasitemia was determined daily by haemocytometer counting after day 2 post challenge.

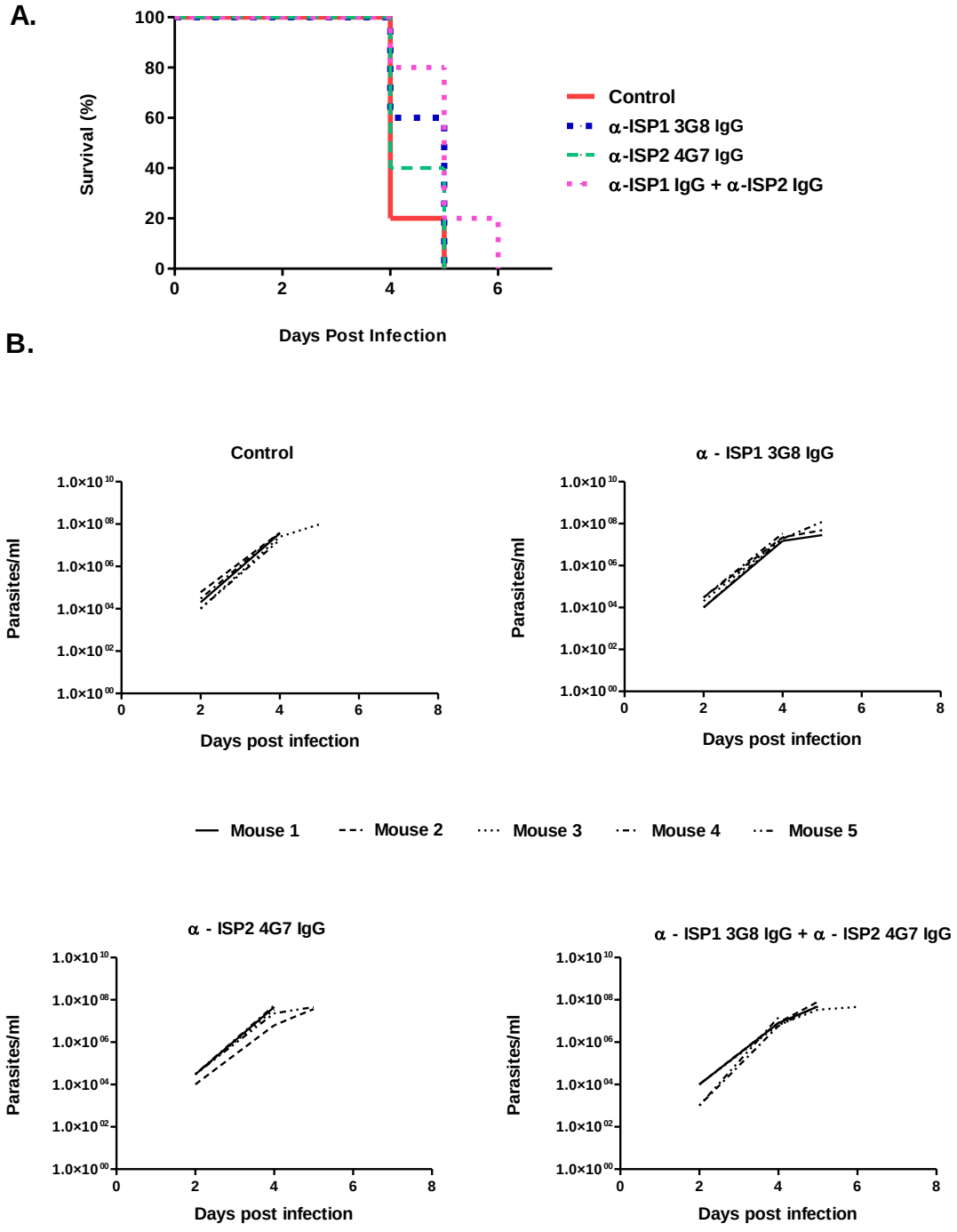

Figure – 3.30 Antibodies against ISP1 and ISP2 have no effect on *T. brucei* infection *in vivo*.

Groups of 4 mice were injected intraperitoneally with α-ISP1 Mab, α-ISP2 Mab and both α-ISP1 and α-ISP2 Mabs simultaneously at day –1, 0 and 2 and challenged with 1×10^4 parasites. (A) Mouse survival rates. Survival rates of infected mice were determined and represented in a Kaplan-Meier survival curve. (B) Mouse infection profile. Each mouse was labeled 1–5 and parasitemia was monitored and registered individually within each group and mice presenting severe clinical symptoms or parasitemia above 1×10^8 cells/ml were culled.

Given the results obtained in the growth inhibition assay of *T. brucei* in culture, it would be expected that antibodies against ISP1 and ISP2 had an inhibitory or neutralizing effect on the infection by *T. brucei* in mice.

However such effect could not be observed in any of the groups injected with anti-ISPs antibodies and the experiment was concluded on day 6 post challenge with the death of all mice.

No difference was observed between the survival rates of the groups injected with anti-ISP antibodies when compared to the control group. On day 4 post challenge 80% of the control group was dead with the remaining mouse dying on day 5. Higher percentages of survival were registered at day 4 post-infection in the α-ISP1 3G8 IgG group (60% survival) and α-ISP2 4G7 IgG group (40% survival). However, the outcome was similar to the control group with 100% of mice from both groups dying on day 5 post-infection. The α-ISP1 3G8 IgG + α-ISP2 4G7 IgG group had a slightly different course with 80% survival on day 4 post-infection but with similar mortality since no mice survived the day 6 post infection (Figure 3.30A).

The analysis of infection profiles revealed that the parasitemia patterns were similar in all groups with the number of parasites per ml of blood increasing consistently and rapidly as was expected for the control group, given the high level of virulence of *T. brucei* strain 427 in mice (Figure 3.30B) (Lanteri *et al*., 2006).

3.5 Immuno-protection assay

To determine if the immunization of mice with ISPs confers any protection to the infection with *T. brucei*, 4 groups consisting of 5 mice each were created. The ISP1 group was immunized with recombinant ISP1, ISP2 group was immunized with recombinant ISP2 and the ISP1 + ISP2 group was immunized with both inhibitors. Each group was immunized with 10 µg of recombinant combined with Freund's complete adjuvant at days 0, 15 and 30 and serum titer was determined by ELISA after the third injection.

Mice were infected with 1×10^4 cultured *T. brucei* 427 after receiving a final boost of the respective recombinants. Parasitemia was determined by haemocytometer cell counting as described previously. The control group, also composed by 5 mice, was injected with PBS and Freund's complete adjuvant, following the immunization scheme developed for the study groups.

Results show that the immunization with ISP1, ISP2 or both ISPs did not confer any kind of protection to the infection with *T. brucei* 427. Kaplan-Meyer curve analysis determined that no difference was observed in mice survival with mean survival times of 6.2 days for the control group, 7 days for the ISP1 group, 6.6 days for the ISP2 group and 7 days for the ISP1+ISP2 group (Figure 3.31A).

One single mouse from the ISP1+ISP2 group survived the experiment without presenting detectable levels of parasitemia or showing signs of clinical symptoms. Although not statistically relevant, this result could indicate that the combined immunization with ISP1 and ISP2 can confer protection to *T. brucei* infection in mice.

In fact, this mouse revealed higher serum titers than the rest of the group suggesting that the immune response was more effective in this animal justifying a possible protection against infection. It is also possible that during the inoculation no viable parasites were injected due to inadequate homogenization or some other manipulation inaccuracy.

The analysis of infection profiles showed no difference in the parasitemia patterns from the different groups. Consistent with the pattern characteristic of infection with wild type *T. brucei* 427, parasitemia was established 3 days after inoculation and increased drastically reaching values above 1×10^8 parasites/ml within 5 to 6 days (Figure 3.31B).

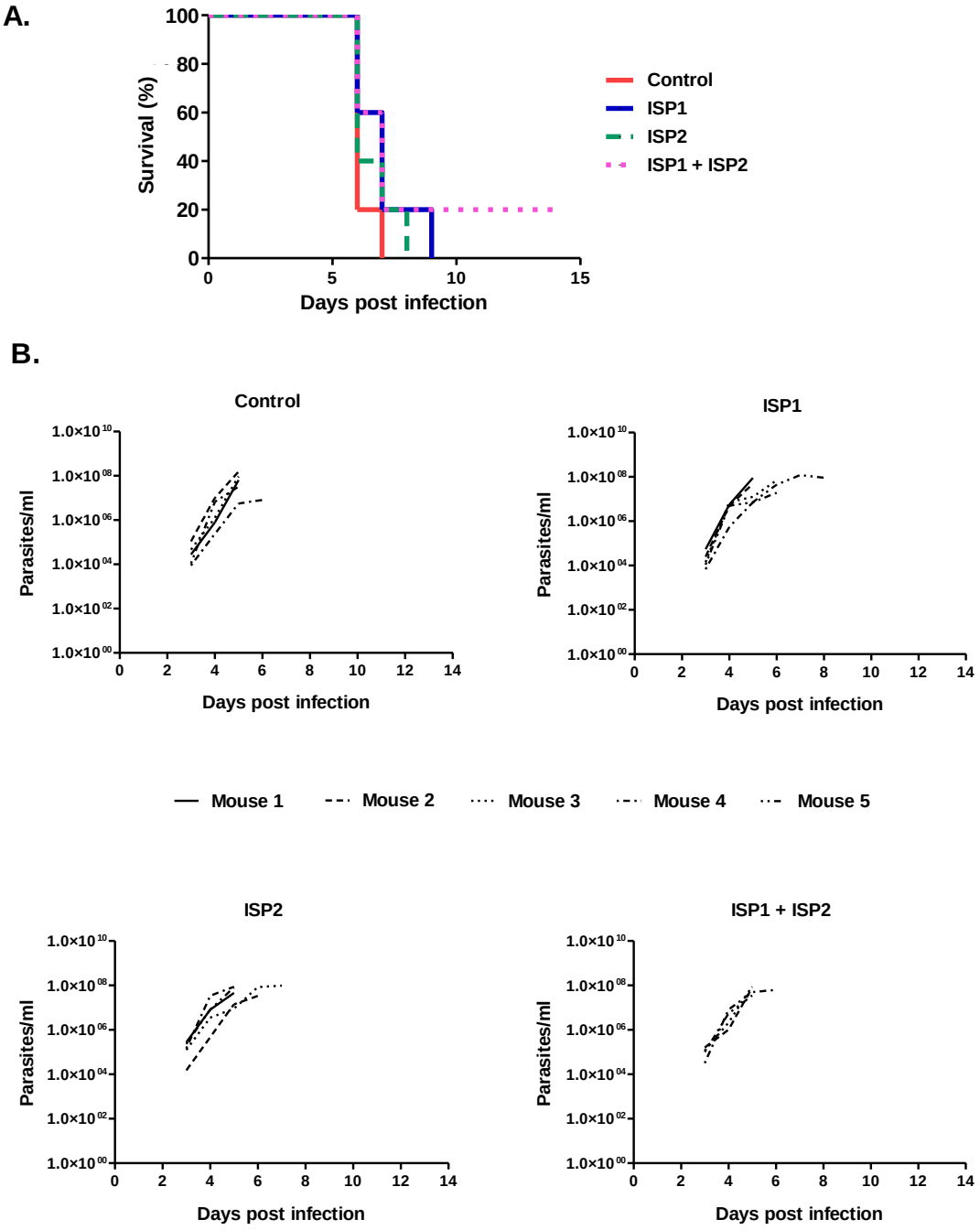

Figure 3.31 – Immunization of mice with ISP1 and ISP2 doesn't confer protection to *T. brucei* infection.

(A) Mouse survival rates. Groups of 4 mice were immunized with ISP1, ISP2 and ISP1 and ISP2 simultaneously and subsequently infected with 1×10^4 parasites. Survival rates of infected mice were determined and represented in a Kaplan-Meier survival curve. **(B) Mouse infection profile.** Each mouse was labeled 1–4 and parasitemia was monitored and registered individually within each group and mice presenting severe clinical symptoms or parasitemia above 1×10^8 cells/ml were culled

Chapter 4

Discussion and Conclusions

The genome of *T. brucei* encodes two putative inhibitors of serine peptidases (Berriman *et al*., 2005), belonging to the family of ecotin (I11) (Rawlings, 2010). Ecotin was first identified in the periplasmic space of *E. coli* and described as a dimeric low molecular weight protein capable of inhibiting trypsin-like peptidases belonging to the S1A family (Chung *et al*., 1983).

Since then, homologues of ecotin have been identified in related Gram-negative bacteria including *Pseudomonas, Salmonella* and *Yersinia* and in the trypanosomatid parasitic protozoa (Eschenlauer *et al.*, 2009).

The biological role of ecotin in *E. coli* and ecotin-like inhibitors in *T. brucei* remains unknown but the absence of S1A family peptidases from the genome of both organisms suggests that these inhibitors are most likely targeting the host's serine peptidases and protecting the cell from the exogenous peptidic activity (Eschenlauer *et al*., 2009).

The only published studies on ISPs from trypanosomatids relate to *Leishmania* and revealed some interesting insights of these inhibitors and their possible role on protecting the cell against the host's immune system (Faria *et al.*, 2011, Eschenlauer *et al*., 2009) and on the flagellar pocket dynamics and parasite's differentiation (Morrison *et al*., 2012).

In an attempt to understand the existence of ISP1 and ISP2 in *T. brucei* and what possible roles they may play in the parasite's biology or in the infection of the mammalian host, two different approaches were made.

First, monoclonal antibodies were generated against *T. brucei* ISP1 and ISP2 and used in Immunolocalization and immuno-protection studies. The second approach consisted of the use of reverse genetics to generate ISP null mutant cell lines and subsequent analysis of the respective phenotypes.

Although the possibility of *T. brucei* ISPs having a role within the insect vector was not discounted, this investigation was conducted only on BSF parasites and all the results obtained only apply to the mammalian infective form of the parasite.

4.1 ISP1 and ISP2 have an intracellular function associated with the flagellum and the flagellar pocket

The generation of ISP null mutant cell lines revealed some interesting features of *T. brucei* ISPs. The successful generation of Δ*isp1* and Δ*isp2* parasites viable in culture indicates that *ISP1* and *ISP2* are not essential genes for the BSF cell division and growth. Analysis of growth rates *in vitro* revealed normal growth of all clones from Δ*isp1* and Δ*isp2* cell lines when compared to the wild type *T. brucei rhodesiense* IL1852 cell line.

Additionally, no gross morphology defect could be detected among the Δ*isp1* and Δ*isp2* parasites by microscopic evaluation and comparison to the wild type parasites.

The two clones from the Δ*isp1/2* cell line also displayed normal growth and gross morphology but the microscopic observation of these parasites disclosed an interesting motility phenotype.

Instead of the bi-helilcal, cork-screw type movement with the flagellum leading the cell body in a well defined direction, that characterizes *T. brucei* (Walker, 1961), Δ*isp1/2* parasites present a disorganized and uncoordinated kind of movement, spinning constantly without being able to move themselves in a determined direction. This inability to move in a certain direction resembles the phenotype displayed by trypanin knockdown mutants described by (Hutchings *et al*., 2002).

Trypanin is a highly conserved protein among flagellated organisms that is associated with the flagellar fraction of the cytoskeleton in *T. brucei* (Hill *et al*., 2000). In PCF cells trypanin is localised along the length of the flagellum and represents part of the flagellar dynein regulatory complex.

RNAi knock down of trypanin in procyclic *T. brucei* resulted in a severe motility defect in which parasites, although not paralyzed, were incapable of directional cell motility, spinning and tumbling frantically, barely without changing their location and even moving backwards sometimes (Hutchings *et al*., 2002).

Like in typanin knock down mutants, Δ*isp1/2* cells retained a vigorously beating flagellum but have lost the ability to coordinate the flagellar beat and actively produce directional movement. This result strongly suggests that ISPs have a role within the parasite itself, possibly in the regulation of flagellar beat.

An association of *T. brucei* ISPs with a flagellar function is not at all a surprise, although the fact that they have an intracellular function *per se* can be a bit surprising given the apparent lack of S1A endogenous SPs. In fact, *T. brucei* ISP1 and ISP2 have been identified in the flagellar proteome in wild type *T. brucei* (Broadhead *et al*., 2006) and recent studies on leishmanial ISPs revealed that both ISP1 and ISP2 are essential for flagellum homeostasis (Morrison *et al*., 2012).

L. major Δ*isp1/2/3* parasites displayed several features that associate these inhibitors with an intrinsic function linked to the flagellum. Triple null mutant promastigotes developed a growth phenotype in culture, presenting reduced growth rates in mid-log phase and reaching stationary phase earlier and at half the density of wild type parasites. Additionally, these parasites showed abnormal morphology marked by an enlarged flagellar pocket region and a tendency to form unusually large aggregates. Finally, Δ*isp1/2/3* parasites have significantly longer flagella than wild type parasites in late-log phase and show reduced motility. These findings, allied to the fact that ISP1 and ISP2 are localised to the flagellar collar in haptomonad promastigotes, an intermediate stage in the differentiation of procyclic into infective metacyclic promastigotes, suggest that ISPs have a primary role in flagellum homeostasis and parasite differentiation (Morrison *et al*., 2012).

The immunofluorescence study done in *T. brucei* using the antibodies produced specifically against ISP1 and ISP2 has shown that both proteins are mainly cytosolic, presenting a punctate staining pattern. This localization is distinct from the localization along the flagellum observed for trypanin in PCF (Hutchings *et al*., 2002) or BSF trypanosomes (Ralston and Hill, 2006) and other flagellar proteins. Nevertheless, some of those punctate structures observed in the immunofluorescence assay appear to be extremely close to the kinetoplast and the flagellum and could represent a discrete localization of ISP1 and ISP2 in the flagellar pocket, which could be confirmed by co-staining with FM4-64 (Field *et al*., 2004).

Several other studies correlate the ablation of flagellar proteins with loss of flagellar motility in *T. brucei*. For example, the RNAi knock down of the two homologues of the parkin co-regulated gene product PACRG (PACRG-A and PACRG-B) simultaneous leads to defective motility while the individual knockdown of either PACRG-A or PACRG-B does not produce any effect on the cell's motility (Dawe *et al*., 2005). Also, the knockdown of the protofilament ribbon protein Rib 72 results in impaired motility (Baron *et al*., 2007b) and the depletion of outer arm dynein subunits LC1, IC78 and other axoneme proteins leads to the loss of tip-to-base beat, causing the cell to move backwards and other severe motility defects (Baron *et al*., 2007a, Branche *et al*., 2006). Common to all this studies is the use of procyclic trypanosomes and show that flagellar motility can be compromised without affecting the parasite's proliferation.

Similar studies have been conducted using BSF parasites instead of procyclics and phenotype consistency indicates that flagellar motility is essential for BSF parasite's viability. In an extensive study by Brodhead *et al*, five proteins identified as part of the flagellar proteome were studied by RNAi.

The knockdown of each one of the selected proteins revealed that all five proteins were essential for BSF *T. brucei*. Allied to severe motility phenotypes developed by RNAi knockdown mutants, it was observed that trypanosomes failed to complete cytokinesis but continued to progress through the cell cycle, continuing to replicate their organelles and leading to large distorted cells with multiple nuclei and kinetoplasts unable to proliferate (Broadhead *et al*., 2006).

Several other studies using BSF flagellar proteins have shown similar phenotypes including the silencing of MCA4 (Proto *et al*., 2011) or trypanin (Ralston and Hill, 2006) by RNAi.

This essentiality is not observed for ISP1 or ISP2 since the Δ*isp1/2* parasites have normal growth in culture. However, the use of a distinct genetic approach can be the responsible for this, once the genetic deletion of *ISP1* and *ISP2* was performed opposing to the RNAi silencing strategy common to all the studies mentioned above. Thus, it is possible that the lethal phenotypes described are associated with RNAi mutants in general (where the rapid depletion of a gene occurs without previous adaptation of the parasite) and not with the flagellar function itself.

Consistent with this explanation is the fact that *MCA4* could be successfully deleted from BSF *T. brucei* originating viable null mutants in culture despite the lethality observed in the RNAi silencing (Proto *et al*., 2011). It would be interesting to see if RNAi silencing of *ISP1* and *ISP2* results in a more severe phenotype similar the one observed for *MCA4* (Proto *et al*., 2011) and other flagellar proteins (Broadhead *et al*., 2006) therefore determining if the lethal phenotype is RNAi specific.

Also supporting the fact that motility defects and lethality phenotypes are not necessarily related is a study by Ralston *et al*. In this study, an inducible system was developed to allow the functional analysis of point mutations in flagellar proteins. A point mutation was identified in LC1 protein that compromises the motility of the parasites without affecting their viability, contrasting with the RNAi knockdown results obtained by Baron *et al*., suggesting that the lethal phenotype observed is not due to the motility defect and indicating for the first time that normal motility is not required for viability of BSF *T. brucei* (Ralston *et al*., 2011)

Despite its unusual localization for a flagellar protein and the lack of morphological or proliferation defects, it is possible that ISPs have an endogenous function associated with the flagellum. Whether that function is associated with one ISP or both is yet undetermined and further investigation on this subject is required.

The generation of Δ*isp1/2* cell lines re-expressing *ISP1*, *ISP2* and both *ISP*s would be extremely important in assessing to which ISP the motility phenotype is due. Furthermore, it would help to clarify the importance of existing two ISPs.

There are three ISP genes present in the *L. major* genome and while ISP1 and ISP2 are homologues to the two *T. brucei* ISPs, ISP3 is specific to *Leishmania* species and it seems to have arisen through the duplication of *ISP2* (Eschenlauer *et al*., 2009).

ISP1 and ISP2 from *L. major* have distinct roles and while *ISP2* is expressed throughout the parasite's life cycle with particular high levels in infective metacyclic promastigotes where it has an influence in the early macrophage infection and parasite's survival (Faria *et al*., 2011, Eschenlauer *et al*., 2009), *ISP1* expression is restricted to procyclic and metacyclic promastigotes and seems to be involved in flagellar homeostasis, flagellar pocket dynamics and promastigote differentiation (Morrison *et al*., 2012).

Although not confirmed in this study, both *T. brucei* ISP1 and ISP2 seem to be expressed in all life cycle stages of the parasite and individual RNAi knockdown reveals normal cell proliferation in BSF and PCF trypomastigotes (Alsford *et al*., 2011). The ISPs expression profile and the absence of any phenotype in the Δ*isp1* and Δ*isp2* but not in the Δ*isp1/2* cell lines may be indicatory of functional redundancy.

The phenomenon by which the deletion of one gene homologue produces no effect at all in the cells and the deletion of both homologues results in a distinct phenotype is not unique among trypanosomes. In PCF *T. brucei*, the RNAi knockdown of *PACRGA* and *PACRGB* individually has no visible effect on the cells while the ablation of both protein in simultaneous results in slow growing parasites and paralysis of the flagellum with severe effects on organelle positioning (Dawe *et al.*, 2005).

In BSF parasites occurrence was observed for PDEB1 and PDEB2, two very similar cAMP-specific phosphodiesterases. Individual RNAi knockdown analysis revealed that the enzymes can complement each other causing no phenotype on the induced cells while simultaneous ablation results in cell death (Oberholzer *et al*., 2007). In both cases, results suggest functional redundancy, with one protein complementing the other, despite the different localization of PDEB1 and PDEB2 in the second case (Luginbuehl *et al*., 2010, Dawe *et al*., 2005).

A curious finding arose almost accidentally during an experiment in which the specificity of the antibodies produced against ISP1 and ISP2 was assessed. In this experiment an antibody generated against ISP1 didn't recognize any protein in the whole cell lysate from Δ*isp2* parasites. A similar result was observed with the antibody produced against ISP2 that failed to recognize a protein in the whole cell lysate from Δ*isp1* cell line. Both antibodies recognized a protein of the predicted size in the WT and re-expressor cell lines.

This result was totally unpredicted and given the supposed functional redundancy of ISP1 and ISP2 in *T. brucei*, it was expected that the expression levels of ISP2 would be maintained or increased in the Δ*isp1* cell line to compensate the absence of ISP1. Besides, the absence of phenotype in the individual knockouts is inconsistent with such expression profile once the deletion of both ISPs results in distinctive phenotypes in the Δ*isp1/2* cell line.

A possible explanation for the absence of phenotype in the individual knockout cell lines is that the remaining gene is expressed at such a low level that the antibody can't detect the respective protein in the whole cell lysates but it still preserves its function giving rise to fully functional parasites. The reason why the expression decreases to such undetectable levels remains unknown. There seems to be some kind of interaction or co-regulation mechanism in which the absence of expression of one ISP affects the expression of the other. Ecotin is a dimeric inhibitor that binds to two peptidase molecules to form a hetero-tetramer establishing a unique peptidase-inhibitor interaction in which one ecotin monomer is in contact with another ecotin monomer and also with two peptidases. It is possible that ISP1 and ISP2 are forming heterodimers in *T. brucei*, explaining the downregulation of one when the other is absent.

Another interesting feature of the Δ*isp1/2* parasites is the accumulation of small vesicles emerging from the flagellar pocket. Similar phenotype was found in the *L. major* Δ*isp1/2/3* parasites (Morrison *et al*., 2012) and associated with the phenotype reported in *T. brucei* IFT mutants (Absalon *et al*., 2008a). In these studies, the accumulation of vesicles in the flagellar pocket region is visible by transmission electron microscopy and was linked with the disruption of IFT, abnormal shape of the flagellar pocket, abnormal flagella length and less efficient fluid-phase endocytosis in the case of IFT mutants. Such doesn't occur in the *T. brucei* Δ*isp1/2* parasites that display normal flagellar pocket and flagellar length and therefore are unlikely to present any disruption of the IFT.

Accumulated vesicles seem to be confined to the flagellar pocket and it is possible that they are linked to blockage in the endocytosis. Defects in endocytosis are frequently associated with an enlarged flagellar pocket, a phenotype called "Big Eye" first described in *T. brucei* BSF parasites subjected to RNAi against clathrin in which a blockage in receptor mediated endocytosis correlated with the enlargement of the flagellar pocket (Allen *et al.*, 2003). Δ*isp1/2* parasites don't show this phenotype so typical in cells with endocytosis defects. Likewise, the RNAi knock down of the enzyme myristoyl-CoA:proteinN-myristoyltransferase (NMT) results in the accumulation of vesicles around the flagellar pocket without showing the "Big Eye" phenotype indicating a defect in endocytic uptake that occurs after endocytic fusion (Price *et al.*, 2010).

To confirm whether the accumulation of vesicles in the flagellar pocket of Δ*isp1/2* cells is due to an endocytosis defect, an uptake assay for endocytosis could be done using either lectin concanavalinA (ConA), an excellent marker for membrane-bound endocytic activity (Brickman *et al*., 1995), FM4-64 to evaluate fluid phase endocytosis or AF594-transferrin to assess the integrity of receptor-linked endocytosis (Field *et al.*, 2004).

Alternatively, vesicles emerging from the flagellar pocket can represent an excessive secretion from the mutant parasites in the form of exosomes. Proteins involved in the endocytosis and exocytosis, such as clathrin, actin and Rab proteins have been identified as part of the *T. brucei* secretome in association with the budding of microvesicles from the plasma membrane and flagellum. These microvesicles resemble exosomes, and the correlation of the *T. brucei* secretome with different exosome proteomic studies available revealed 13 proteins in common suggesting the presence of an exosome-mediated secretory pathway (Geiger *et al*., 2010). Exosome secretion was also described in *Leishmania* (Silverman *et al*., 2008) and studies on the *Leishmania* exosomes when exposed to infection-like conditions revealed that the parasite is capable of modulating the exosome release and protein content in response to environmental conditions (Silverman *et al.*, 2010a). Another study by Silverman *et al*., has shown that *Leishmania* exosome secretion has the ability to modulate the immune response, making it permissive to infection and disease progression (Silverman *et al*., 2010b).

Whether exosomes have similar immunomodulatory properties in *T. brucei* has yet to be determined but evidences are that exosomes in general are important for the infection biology, either they are pathogen derived or released from infected mammalian cells (Silverman and Reiner, 2011) and it's possible that exosome secretion also plays an important role on the pathogenesis of *T. brucei*.

Given the hypothesis that *T. brucei* ISPs interact with host's serine peptidases and may be involved in the infection of the mammalian host through modulation of the immune response, it is possible that the absence of such inhibitors in Δ*isp1/2* parasites results in the upregulation of exosome secretion, leading to an accumulation of vesicles in the flagellar pocket.

Despite the unclear nature of this phenotype, the data obtained in this study suggest that ISPs have an endogenous function independent of serine peptidase inhibitory activity, possibly associated with a structural role or with the flagellar pocket dynamics. Whether that function is attributed to one or both inhibitors is not totally clear but it is most likely that ISP1 and ISP2 have, if not the same, at least an overlapping function with one protein compensating for the loss of the other whenever it's needed.

4.2 Δ*isp1/2* parasites have reduced virulence in mice

The absence of serine peptidases from family S1A encoded in the genome of *T. brucei* suggested a potential role for ISPs in mediating the infection of the mammalian host. To confirm this hypothesis, *ISP* deficient parasites were used to infect mice and the infection profile of Δ*isp1*, Δ*isp2* and Δ*isp1/2* was compared to the one of wild type parasites.

While the deletion of *ISP1* and *ISP2* individually didn't produce any effect on the parasite's infectivity, the deletion of both *ISP*s resulted in parasites severely compromised in their ability to infect mice.

Mice infected with wild type, Δ*isp1*, Δ*isp2* and Δ*isp1*:ISP1 revealed an infection pattern, typical of *T. brucei rhodesiense* IL1852, dying within a 20 day period, after one or two peaks of parasitemia, with high loads of parasites in the blood (Antoine-Moussiaux *et al.,* 2008).

Only one mouse (25%) infected with Δ*isp1/2* parasites died within the experiment period that ended after 28 days. The remaining mice reached the end of the experiment asymptomatic and with no detectable levels of parasitemia, strongly suggesting a role for ISP1 and ISP2 in the parasite's ability to infect the mammalian host. The infection pattern displayed by the Δisp1/2 parasites is similar to the infection pattern of *T. brucei gambiense*. Mice infected with *T. brucei gambiense* exhibit prolonged survival with sporadic parasitemias, suggesting that the absence of ISP1 and ISP2 may induce chronicity of the infection (Antoine-Moussiaux *et al.*, 2008).

The successful establishment of the infection in the mammalian host depends on the ability of *T. brucei* to circulate in the bloodstream and penetrate the blood vessels, spreading into connective tissues to ultimately cross the blood brain barrier, invading the central nervous system. The correct flagellar motility is essential for the parasite's migration through the host tissues and thus central to the pathogenesis and disease progression.

Indeed, other flagellar proteins have been associated with *T. brucei* virulence in mice. For example, calflagin-deficient parasites exhibit normal growth *in vitro* but reduced virulence in mice after 7 days of infection despite the absence of a motility defect (Emmer *et al.*, 2010). Also the deletion of GPI-PLC (Webb *et al.*, 1997) and, more recently, of MCA4 (Proto *et al.*, 2011) resulted in prolonged mouse survival. In all three cases, reduced virulence was accompanied by successive peaks of parasitemia followed by periods of undetectable parasite levels.

Other process that seems to be associated with *T. brucei* infectivity in mice is endocytosis. RNAi silencing of proteins resulting in defects of the endocytic system also has shown to influence parasitemia in mice. NMT RNAi knockdown parasites are unable to infect mice (Price *et al.*, 2010) and the parasites overexpressing a dominantly active Rab11 mutant have compromised growth in mice (Natesan *et al.*, 2011).

Although it is possible that the altered motility or the presumed endocytosis defect observed in the Δ*isp1/2* parasites *in vitro* can be correlated with their lack of virulence, it is also possible that the absence of inhibitory activity towards the host's serine peptidases can account for this phenomenon.

Among the possible targets for *T. brucei* ISPs inhibitory activity is neutrophil elastase (NE), a key effector molecule of the innate immune system secreted by neutrophils and macrophages, with potent antimicrobial activity (Eggers *et al.*, 2004).

It has been shown that neutrophils can secrete an extracellular fibril network called neutrophil extracellular trap (NET). This network can kill extracellular pathogens using antimicrobial proteins such as NE, while minimizing damages to the host cells. By providing a high concentration of antimicrobial agents locally, NETs can disarm and kill pathogens extracellularly without the need of phagocytic uptake.

Additionally, NETs may function as a physical barrier, preventing the dissemination of the pathogen (Brinkmann *et al*., 2004). More recently, it has also been shown that NETs are induced not only by bacteria, but also by pathogenic fungi such as *Candida albicans* (Urban *et al*., 2006) and *Leishmania amazonensis* (Guimarães-Costa *et al*., 2009).

Although no published study on the subject is available until now, it is possible that *T. brucei* also induces the neutrophils to secrete NETs and that during the infection with Δ*isp1/2* trypanosomes, in the absence of inhibition, NE may have a trypanocidal activity or modulate the host's immune system in a way that prevents the establishment of the infection in mice.

In *L. major*, the inhibition of NE by a specific NE inhibitor abolished leishmanicidal activity in macrophages and resulted in enhanced infectivity *in vivo*, suggesting a role for NE in the macrophage activation (Ribeiro-Gomes *et al*., 2004).

The first barrier against *T. brucei* infection of the mammalian host is the innate immune response, in which different host cells are activated initiating an acute inflammatory response. Macrophages are activated, via classical activation, leading to the secretion of pro-inflammatory molecules such as TNF and nitric oxide (NO) that are involved in the control of the first peak of parasitemia (type I inflammatory response).

The initial inflammatory process is beneficial for the host but sustained inflammation can cause pathology and so the host reduces inflammation by down-regulating the classical activation of macrophages and promoting the activation of anti-inflammatory type macrophages that are involved in a longer survival of the host (type II inflammatory response) (Baral, 2010, Sternberg, 2004).

In mice it has been shown that cytokine responses to VSGs associated with resistance against murine African trypanosomiasis are dependent on the infection stage, with type-I cytokine responses being critical in the early infection and type-II cytokine responses being more important in the chronic infection and the late stage disease (Namangala *et al*., 2009). However the influence of cytokines and their responses on the outcome of the infection is unclear and may be dependent on the parasite strain, the mouse model or both.

Given the extracellular nature of the parasite, a strong humoral response is expected during the course of infection with *T. brucei*. Murine trypanosomiasis is characterized by activation of polyclonal B-cells and although VSG-specific antibodies can be protective by promoting the clearance of parasites during the early stages of infection, a considerable amount of the antibodies produced is either poly-specific or auto-reactive (Baral, 2010, Sternberg, 2004).

Additionally, as the infection progresses, B-cells become suppressed or exhausted, resulting in the total absence of IgG responses and the extreme reduction of IgM responses (Hudson and Terry, 1979). Macrophages play a central role in this dramatic immunosupression, mediating the inhibition of both B- and T-cell proliferative responses by the release of nitric oxide, prostaglandin and TNF-α (Sternberg, 2004).

From the group infected with Δ*isp1/2* parasites three mice survived and only one revealed detected parasitemia along the study period. That mouse had a parasitemia peak at day 17 and didn't show any signs of parasites circulating in the blood during the rest of the experiment. It's possible that the other 2 mice also had at least one peak of parasitemia during the experiment. However parasite counting was not carried out every day and the peaks may have passed unnoticed.

Given the absence of successive peaks of parasitemia it is likely that the infection was controlled in its early stages during the macrophage activation phase promoting the alternative instead of the classical macrophage activation. Due to a possible modulation of the macrophage activation by and the respective cytokine release by NE, the suppression of humoral response may have also been inhibited and antibody-mediated parasite clearance may have occurred resulting in undetectable levels parasitemia or in the total eradication of *T. brucei* infection.

Apart from the control of infection mediated by the host's immune system, the initial setting of parasitemia levels is regulated by the parasite itself. African trypanosomes use antigenic variation as primary strategy to evade the mammalian host's immune system.

By constantly changing their VSG coat, the parasite is capable of escaping the immune system (Vickerman, 1978) and maintain a state of chronic infection in the host, characterized by ascending levels of parasitemia, where the majority of the population is

constituted by long slender dividing forms of the parasite expressing the same antigenic type (homotype), followed by a period in which parasitemia goes into remission due to the elimination of parasites of the major variable antigenic type (VAT) by the host's immune system. During this descendent phase the parasites expressing a new VSG are multiplying and become the new homotype.

Trypanosomes can be efficiently opsonized by mammalian anti-VSG antibodies but, to escape from complement-mediated elimination, trypanosomes developed a macromolecular trafficking mechanism by which VSG-antibody complexes are rapidly endocytosed, occurring antibody degradation and VSG recycling (Field *et al.*, 2009, Engstler *et al*., 2007).

It has been demonstrated that normal flagellar beat is needed for the VSG-antibody complexes uptake by the parasite implying that normal flagellar motility is required for the immune evasion and persistent infection of the mammalian host (Engstler *et al.*, 2007).

This trafficking mechanism makes it harder for the immune system to play its part in eliminating the parasites. So, even with the humoral immunity mechanisms being potentially unsuppressed, the VSG recycling would enable the parasites to avoid destruction by the host's immune system and maintain a state of chronic infection.

However, since no parasites could be detected in the blood of survivor mice, it is possible that the inability of Δ*isp1/2* parasites to infect mice is due to a combination of different factors that may include impaired flagellar motility, defective endocytic mechanism and lack of inhibition of the host's NE or other serine peptidase involved in the host's immune response.

Further studies are required to determine exactly which serine peptidases are the *T. brucei* ISPs targeting in the host and determine what mechanisms underlie the prolonged survival of the host infected with ISP null mutant parasites.

However the results obtained by reverse genetics indicate that *T. brucei* ISP1 and ISP2 could represent good targets for therapy.

4.3 Monoclonal antibodies against ISP1 and ISP2 do not confer protection against *T. brucei* infection *in vivo*

The eradication of the entire trypanosome reservoir from livestock and game population as a way to control African trypanosomiasis is not feasible with currently available control measures and so treatment is the strategy to follow. While the development of new drugs effective against HAT is the main research target, vaccination has raised some interest by investigators. However, the search for a suitable vaccine candidate has been unsuccessful so far (La Greca and Magez, 2011).

In the literature there are several references to immunization studies or monoclonal antibody therapy in different pathogens, such as *Plasmodium* (Reddy *et al*., 2012, Feng *et al*., 2012, Zhang *et al*., 2001), *Schistosoma* (Xu *et al.*, 2011, Zhang *et al.*, 2001), *Toxoplasma* (Costa-Silva *et al.*, 2008, Cha *et al.*, 2001), *Trichinella* (Wei *et al*., 2011), *Leishmania* (Zanin *et al.*, 2007, Bimal *et al*., 2001), *T. cruzi (Buschiazzo et al.*, 2012), and *Borrelia* (LaRocca *et al*., 2009, Kurtenbach *et al*., 1997) with relative success in terms of protection against infection.

However, the peculiarities of *T. brucei* cellular organization hamper the pursuit of target molecules to use as antigens in the development of an effective vaccine or antibody-based therapy. After abandoning the idea of creating an anti-VSG vaccine, several other molecules were considered as potential targets for the development of a vaccine. Flagellar pocket proteins were the first to be considered due to the importance of this structure in the parasite's virulence and immune evasion. In 1995 an immunization study of cattle with a flagellar pocket antigen from *T. brucei rhodesiense* showed development of partial protection to *Trypanosoma congolense* and *Trypanosoma vivax* after natural exposure in the field (Mkunza *et al*., 1995).

Structural proteins such as actin and tubulin have also been proposed as vaccination candidates. Two different studies by Li *et al*., suggested that immunization with recombinant actin and recombinant β-tubulin from *Trypanosoma evansi* induces protective immunity against *T. evansi, T. equiperdum* and *T. b. brucei* in mice (Li *et al.*, 2009, Li *et al*., 2007).

In a similar approach, the immunization of mice with a tubulin-rich preparation from *T. brucei* also revealed to confer protection against infection and further studies on this matter showed that anti-tubulin antibodies specifically inhibit *T. brucei* in culture (Lubega *et al*., 2002a, Lubega *et al.,* 2002b).

Other molecules were also addressed in immunization and antibody-mediated therapy studies, such as the plasma membrane component ganglioside (Uemura *et al.,* 2005, Tsujimura *et al*., 2005), trasns-sialidases (Silva *et al*., 2009), cation pumps (Ramey *et al.,* 2009), invariant surface glycoproteins (Lança *et al*., 2011) and lymphocyte triggering factor (TLTF) (Hamadien *et al.*, 1999, Bakhiet *et al*., 1993)

ISPs are kinetoplastid specific inhibitors with no homologues in mammals with an apparently important role in the host-parasite interaction and infection of the mammalian host. Their localization on the flagellar pocket region allied to their specificity makes them potential targets for immune-protection studies. Given the severity of the phenotype presented by Δ*isp1/2* parasites in the mouse infection experiment we sought to determine if the immunization with recombinant ISP1 and ISP2 would elicit an immune response strong enough to grant protection towards a challenge with a lethal dose of *T. brucei* in mice.

Four different study groups composed by 5 mice each received three boosts of 10 µg of recombinant protein by intraperitoneal injection with 15 days apart and were subsequently challenged with 1×10^4 cells. The control group received PBS emulsified with adjuvant and the other groups received either rISP1, rISP2 or both recombinant proteins. No difference could be detected in the survival or in the parasitemia levels of the groups with all mice dying with high parasite loads within a period of 7 days. Therefore, the immunization of mice with rISP1, rISP2 or rISP1 and rISP2 together doesn't confer any protection to *T. brucei* 427 infection in mice.

It was not expected that the immunization of mice with rISP1 or ISP2 alone would have any effect on the infection outcome since we had previously established that both ISPs are required for the normal function of the parasite and it was predicted that only the inhibition of both proteins would result in a immune-protective response against the infection.

However the group immunized with both recombinants didn't show the expected response and the infection was equally lethal for these mice. Several factors may have influenced the outcome of the experience.

Firstly, the amount of recombinant injected may have been insufficient to trigger an immune response strong enough to be protective against the infection. In similar studies mice were immunized with amounts ranging from 20 to 40 µg of recombinant (Li *et al*., 2009, Li *et al.*, 2007, Lubega *et al.*, 2002a) and this can be an important factor. Although the serum titer was determined before the challenge it is impossible to predict which serum titer would be high enough to grant protection against the infection.

A second factor is the use of a preparation containing two different proteins to inject the mice. The serum titer was determined for both ISP1 and ISP2 and revealed substantially lower values compared with the values obtained for the serum titer determination of ISP1 in the ISP1 group and ISP2 in the ISP2 group. This may reflect some kind of competitive response from the host's immune system that compromises the concentration of each antibody in the bloodstream. The strain used in this experiment may also be important. Mice were infected with *T. brucei* 427, a strain more virulent to mice than the strain used to generate the null mutants. Different strains can have different susceptibilities to the effect of the inhibition of ISPs activity and even though the absence of ISP 1 and ISP2 in *T. brucei rhodesiense* results in reduced infectivity in mice there is no certainty that the same would happen if the strain used to generate the knockouts was *T. brucei* 427.

Finally, the subcellular localization of *T. brucei* ISP1 and ISP2 may be the key factor influencing this experiment. Although ISP1 and ISP2 have been localized in the flagellar pocket region, their presence was also detected in the cytosol and therefore inaccessible to the circulating antibodies explaining why the immunization with ISP1 and ISP2 has no protective effect on mice.

In an immunization study it is impossible to determine the exact amount of antibodies being produced and released into the bloodstream in response to the antigen. Thus, antibodies generated against ISP1 and ISP2 were used to test their protective effect on *T. brucei* infection in mice.

The growth inhibition by anti-ISP1 and anti-ISP2 antibodies was first assessed in cultured parasites. Using different amounts of antibody it was determined that 25 µg of purified anti-ISP1 IgG and anti-ISP2 IgG was enough to inhibit the growth of *T. brucei* in culture. When compared to the non treated parasites or to the parasites treated with pre-immune IgG control, parasites treated with anti-ISP1 3G8 antibody and with anti-ISP2 4G7 antibody displayed significantly reduced growth after 48h.

Although an intracellular function for *T. brucei* ISPs has been proposed earlier in this study, this result is totally unexpected. The generation of individual ISP null mutant cell lines didn't reveal any growth phenotype *in vitro* suggesting that whatever intracellular function ISPs may have, it is independent of the parasite's growth.

These results show that the parasite's growth is in fact inhibited by the presence of the antibody, although the mechanism by which this inhibition occurs is far from clear. The only plausible explanation is adaptation, or the lack of it. As discussed earlier, the deletion of one gene ORF by targeted gene replacement of both alleles and the depletion of the same gene reveal distinct phenotypes that can be much more severe in the RNAi silencing. The sequential replacement of both alleles of a gene provides the parasite enough time for it to adjust to the levels of gene expression while the RNAi silencing results in the rapid depletion of the gene without previous adaptation of the parasite.

Likewise, in this experiment it is possible that the growth inhibition observed in the presence of anti-ISP1 and anti-ISP2 antibodies is due to a blockage of ISP1 and ISP2 occurring before the parasite has time to adapt to its new condition. The chemical balance of the culture medium can also interfere with the growth of the parasites. The parasites are well adapted to grow in culture medium with determined characteristics and composition. The addition of the antibodies to the culture medium can alter that composition and affect the environment, causing stress to the parasites and therefore interfere with the growth. To minimize this problem, solutions containing the antibodies represented less than 1% of the total volume of HMI-9 but still it was possible to see an effect on parasites treated with the pre-immune IgG that presented reduced growth when compared with the wild type parasites. Also, higher amounts of antibody resulted in dramatic inhibition of cell growth after 24 hours and lower amounts produced no

effect on the parasite's growth rates, suggesting that the change of the parasite's environment can account for the reduced growth of *T. brucei* in the presence of anti-ISP1 and anti-ISP2 antibodies.

The same antibodies were used in the *in vivo* assay. Four groups of 5 mice each were injected intraperitoneally with PBS (control group), 25 µg of anti- ISP1 antibody (α-ISP1 3G8 IgG group), 25 µg of anti-ISP2 antibody (α-ISP2 4G7 IgG group) and 25 µg of both antibodies in simultaneous (α-ISP1 3G8 IgG + α-ISP2 4G7 IgG group) on the day before being challenged with 1×10^4 cells. All groups received 2 additional injections of antibody on days 0 and 2 post challenge.

Results obtained were very similar to the ones obtained in the immune-protection study. All mice were dead on day 6 post-infection and no difference could be observed in the parasitemia levels of mice from different study groups, suggesting that the treatment of mice with antibodies against ISP1 and ISP2 doesn't have a protective effect o mice infected with *T. brucei* 427.

Again, it was not expected that the administration of anti-ISP1 or anti-ISP2 antibodies alone would have a protective or neutralizing effect, but we expected some visible effect on the animals injected with both antibodies together.

The analysis of these results is very analogous to the analysis of the results obtained in the immuno-protection assay. Even though a preliminary assay *in vitro* was done to determine the optimal amount of antibody to use in the present assay, it was not fully established that the reduced growth of the cultures *in vitro* was indeed a direct effect of the antibody blocking action and so, the amount of antibody used may have been insufficient to have a protective or neutralizing effect on mice.

Also, it was difficult to predict if the number of doses administrated would be the ideal or if a fourth dose would beneficial to the treatment.

The factors that affected the immuno-protective study have to be taken into consideration in the present assay. So, apart from the amount of antibodies administrated to the animals, the *T. brucei* strain used in the infection, the cytosolic localization of ISPs and the use of a mixture containing both antibodies may have influenced the outcome of the experiment.

4.4 Conclusions and final considerations

This is the first study on *T. brucei* ISPs and, although further analysis of these inhibitors and their role is required, some interesting findings resulted from this study. It is now clear that ISP1 and ISP2 have an intracellular function that is independent of the inhibition of serine peptidase activity. That function, not yet clear, seems to be associated with the flagellum, given the loss of normal motility by the Δ*isp1/2* parasites given the localization of ISP1 and ISP2 near the flagellar pocket region and the existence of possible endocytosis/exocytosis defect in the null mutant cell lines.

It has also become clear with this study that ISPs are associated with the immune evasion of the parasite since their loss results in reduced infectivity in mice. The mechanism by which the loss of ISP1 and ISP2 in the null mutant cell line has such a dramatic effect on the infection's outcome is unknown and new insights on this matter could be provided by the study of the inhibitory activity of ISP1 and ISP2. There are no studies performed on this subject and although it is predicted that *T. brucei* ISPs indeed inhibit serine peptidases from family S1A, we still don't know which enzymes they inhibit, if both inhibitors have the same targets or even if they have an inhibitory activity at all. The recent studies on *Leishmania* have revealed that ISP1 and ISP2 have different inhibitory properties and different biological roles as well with one being involved in the host's infection and immune evasion and the other involved in the flagellum homeostasis and flagellar pocket dynamics.

Contrasting with the findings of the *Leishmania* investigation, the present study reveals some functional redundancy of ISP1 and ISP2 in *T. brucei,* with both being required for the parasite to infect the mammalian host efficiently. Furthermore, results obtained revealed that the deletion of one *ISP* results in the down regulation of the other, through some mechanism that we were unable to determine.

Finally, immunization of mice with rISP1 and rISP2 didn't have any protective effect on mice infected with *T. brucei*. Similarly, the treatment of *T. brucei* infected mice with antibodies specific against ISP1 and ISP2 had no protective or neutralizing effect. Therefore, the immune-protective studies show that ISP1 and ISP2 are not good candidates for an anti-disease vaccine or for antibody base therapy.

Further studies are required on the ISPs and their biological roles. With the information provided by this study and the information of the proteomic studies available, new leads on their possible roles and the mechanisms by which they exert their function may arise. ISP1 and ISP2 have been identified in several sub-proteomes: they were identified in the flagellar proteome as previously referred (Broadhead *et al.*, 2006); in the plasma membrane subproteome (Bridges *et al.*, 2008); in the phosphoproteome of BSF *T. brucei* (Nett *et al.*, 2009); The identification of a phosphorylation site in ISP1, for example, may have an important biological significance and it may be worth exploring.

Protein phosphorylation by protein kinases is one of the most studied post-translational modifications in eukaryotic cells, mainly due to its significant role in the regulation of a wide range of cellular processes including enzyme activation, protein-protein interaction and protein degradation (Cohen, 2000). In *T. brucei* there are 170 conventional protein kinases and 12 atypical protein kinases (Nett *et al*., 2009) and most research has been focused on cell cycle regulating protein kinases (Hammarton, 2007, Naula *et al.*, 2005).

The unraveling of complex signaling pathways can be extremely difficult but the growing number of phosphoproteome studies have shed some light on the function of protein phosphorylation in several organisms (Nett *et al.*, 2009). Perhaps identifying the kinases involved in the phosphorylation of *T. brucei* ISP1 would be helpful in determining the exact role of this inhibitor.

Also, the identification of ISP1 and ISP2 in the secretion products of PCF trypanosome strains (Atyame Nten *et al*., 2010) and the prediction of a palmitoylation site also in procyclics (Emmer *et al.*, 2011) is suggestive of ISPs playing a role in the insect vector, a role possibly related to the protein trafficking, protein-protein interactions and host-parasite interaction by neutralization of serine peptidases present in the midgut of the tsetse fly. It would be interesting to determine if procyclic parasites deficient in ISPs would develop similar phenotypes to the BSF and thus if the absence of ISPs in PCF *T. brucei* would have any impact on the cell development and also in the infection of the insect host.

Finally, although it is possible that vaccination is the way forward in the eradication of the disease, not a single promising candidate has been validated to date. Perhaps the classical vaccination methods are inadequate to the parasite in question and different strategies must be defined. A recent study has revealed that the competition between co-infecting *T. brucei* strains enhances host survival (Balmer *et al*., 2009). Co-infection of mice with different strains resulted in a competitive suppression that alleviates the effects of the infection on the mammalian host. This mutual suppression is also verified in co-infection with less virulent strains with enhanced host survival as well (Balmer *et al*., 2009). Additionally, the infection of mice with an attenuated strain of *T. cruzi*, created by the monoallelic knockout of the *dhfr-ts* gene, confers protective immunity against a virulent strain (Perez Brandan *et al*., 2011).

It would be interesting to see if the same kind of protective immunity is conferred by the co-infection of mice with Δ*isp1/2* and wild type *T. brucei rhodesiense* IL1852.

References

ABDULLA, M. H., O'BRIEN, T., MACKEY, Z. B., SAJID, M., GRAB, D. J. & MCKERROW, J. H. 2008. RNA interference of *Trypanosoma brucei* cathepsin B and L affects disease progression in a mouse model. *PLoS Negl Trop Dis,* 2**,** e298.

ABSALON, S., BLISNICK, T., BONHIVERS, M., KOHL, L., CAYET, N., TOUTIRAIS, G., BUISSON, J., ROBINSON, D. & BASTIN, P. 2008a. Flagellum elongation is required for correct structure, orientation and function of the flagellar pocket in *Trypanosoma brucei*. *J Cell Sci,* 121**,** 3704-16.

ABSALON, S., BLISNICK, T., KOHL, L., TOUTIRAIS, G., DORÉ, G., JULKOWSKA, D., TAVENET, A. & BASTIN, P. 2008b. Intraflagellar transport and functional analysis of genes required for flagellum formation in trypanosomes. *Mol Biol Cell,* 19**,** 929-44.

ACKERS, J. P., DHIR, V. & FIELD, M. C. 2005. A bioinformatic analysis of the RAB genes of *Trypanosoma brucei*. *Mol Biochem Parasitol,* 141**,** 89-97.

ALLEN, C. L., GOULDING, D. & FIELD, M. C. 2003. Clathrin-mediated endocytosis is essential in *Trypanosoma brucei*. *EMBO J,* 22**,** 4991-5002.

ALSFORD, S., TURNER, D. J., OBADO, S. O., SANCHEZ-FLORES, A., GLOVER, L., BERRIMAN, M., HERTZ-FOWLER, C. & HORN, D. 2011. High-throughput phenotyping using parallel sequencing of RNA interference targets in the African trypanosome. *Genome Res,* 21**,** 915-24.

ANTOINE-MOUSSIAUX, N., BÜSCHER, P. & DESMECHT, D. 2009. Host-parasite interactions in trypanosomiasis: on the way to an antidisease strategy. *Infect Immun,* 77**,** 1276-84.

ANTOINE-MOUSSIAUX, N., MAGEZ, S. & DESMECHT, D. 2008. Contributions of experimental mouse models to the understanding of African trypanosomiasis. *Trends Parasitol,* 24**,** 411-8.

ATKINSON, H. J., BABBITT, P. C. & SAJID, M. 2009. The global cysteine peptidase landscape in parasites. *Trends Parasitol,* 25**,** 573-81.

ATYAME NTEN, C. M., SOMMERER, N., ROFIDAL, V., HIRTZ, C., ROSSIGNOL, M., CUNY, G., PELTIER, J. B. & GEIGER, A. 2010. Excreted/secreted proteins from trypanosome procyclic strains. *J Biomed Biotechnol,* 2010**,** 212817.

BAKHIET, M., OLSSON, T., EDLUND, C., HÖJEBERG, B., HOLMBERG, K., LORENTZEN, J. & KRISTENSSON, K. 1993. A *Trypanosoma brucei brucei*-derived factor that triggers CD8+ lymphocytes to interferon-gamma secretion: purification, characterization and protective effects *in vivo* by treatment with a monoclonal antibody against the factor. *Scand J Immunol,* 37**,** 165-78.

BALMER, O., STEARNS, S. C., SCHÖTZAU, A. & BRUN, R. 2009. Intraspecific competition between co-infecting parasite strains enhances host survival in African trypanosomes. *Ecology,* 90**,** 3367-78.

BARAL, T. N. 2010. Immunobiology of African trypanosomes: need of alternative interventions. *J Biomed Biotechnol,* 2010**,** 389153.

BARON, D. M., KABUTUTU, Z. P. & HILL, K. L. 2007a. Stuck in reverse: loss of LC1 in *Trypanosoma brucei* disrupts outer dynein arms and leads to reverse flagellar beat and backward movement. *J Cell Sci,* 120**,** 1513-20.

BARON, D. M., RALSTON, K. S., KABUTUTU, Z. P. & HILL, K. L. 2007b. Functional genomics in *Trypanosoma brucei* identifies evolutionarily conserved components of motile flagella. *J Cell Sci,* 120**,** 478-91.

BARRETT, A. J. & RAWLINGS, N. D. 1995. Families and clans of serine peptidases. *Arch Biochem Biophys,* 318**,** 247-50.

BARRETT, M. P. 1997. The pentose phosphate pathway and parasitic *protozoa*. *Parasitol Today,* 13**,** 11-6.

BARRETT, M. P. 2006. The rise and fall of sleeping sickness. *Lancet,* 367**,** 1377-8.

BARRETT, M. P., BURCHMORE, R. J., STICH, A., LAZZARI, J. O., FRASCH, A. C., CAZZULO, J. J. & KRISHNA, S. 2003. The trypanosomiases. *Lancet,* 362**,** 1469-80.

BASTIN, P., PULLEN, T. J., MOREIRA-LEITE, F. F. & GULL, K. 2000. Inside and outside of the trypanosome flagellum:a multifunctional organelle. *Microbes Infect,* 2**,** 1865-74.

BASTIN, P., SHERWIN, T. & GULL, K. 1998. Paraflagellar rod is vital for trypanosome motility. *Nature,* 391**,** 548.

BEATRIZ VERMELHO, A., GIOVANNI DE SIMONE, S., MASINI, D., AVILA-LEVY, C., LUIS SOUZA DO SANTOS, A., CRISTINA NOGUEIRA DE MELO, A., PAES SILVA, F., PINTO DA SILVA BON, E. & HELENA BRANQUINHA, M. 2007. *Trypanosomatidae* Peptidases: A Target for Drugs Development. *Current Enzyme Inhibition,* 3**,** 19-48.

BERRIMAN, M., GHEDIN, E., HERTZ-FOWLER, C., BLANDIN, G., RENAULD, H., BARTHOLOMEU, D. C., LENNARD, N. J., CALER, E., HAMLIN, N. E., HAAS, B., BÖHME, U., HANNICK, L., ASLETT, M. A., SHALLOM, J., MARCELLO, L., HOU, L., WICKSTEAD, B., ALSMARK, U. C., ARROWSMITH, C., ATKIN, R. J., BARRON, A. J., BRINGAUD, F., BROOKS, K., CARRINGTON, M., CHEREVACH, I., CHILLINGWORTH, T. J., CHURCHER, C., CLARK, L. N., CORTON, C. H., CRONIN, A., DAVIES, R. M., DOGGETT, J., DJIKENG, A.,

FELDBLYUM, T., FIELD, M. C., FRASER, A., GOODHEAD, I., HANCE, Z., HARPER, D., HARRIS, B. R., HAUSER, H., HOSTETLER, J., IVENS, A., JAGELS, K., JOHNSON, D., JOHNSON, J., JONES, K., KERHORNOU, A. X., KOO, H., LARKE, N., LANDFEAR, S., LARKIN, C., LEECH, V., LINE, A., LORD, A., MACLEOD, A., MOONEY, P. J., MOULE, S., MARTIN, D. M., MORGAN, G. W., MUNGALL, K., NORBERTCZAK, H., ORMOND, D., PAI, G., PEACOCK, C. S., PETERSON, J., QUAIL, M. A., RABBINOWITSCH, E., RAJANDREAM, M. A., REITTER, C., SALZBERG, S. L., SANDERS, M., SCHOBEL, S., SHARP, S., SIMMONDS, M., SIMPSON, A. J., TALLON, L., TURNER, C. M., TAIT, A., TIVEY, A. R., VAN AKEN, S., WALKER, D., WANLESS, D., WANG, S., WHITE, B., WHITE, O., WHITEHEAD, S., WOODWARD, J., WORTMAN, J., ADAMS, M. D., EMBLEY, T. M., GULL, K., ULLU, E., BARRY, J. D., FAIRLAMB, A. H., OPPERDOES, F., BARRELL, B. G., DONELSON, J. E., HALL, N., FRASER, C. M., *et al*. 2005. The genome of the African trypanosome *Trypanosoma brucei. Science,* 309**,** 416-22.

BESTEIRO, S., COOMBS, G. H. & MOTTRAM, J. C. 2004. A potential role for ICP, a Leishmanial inhibitor of cysteine peptidases, in the interaction between host and parasite. *Mol Microbiol,* 54**,** 1224-36.

BIMAL, S., BAGCHI, A. K., DAS, V., SINHA, P. K., LAL, C. S., RANJAN, A., GUPTA, A. K. & KAR, S. K. 2001. Effect of immunization with lipid associated polysaccharide antigen and anti CD-2 antibodies on class II MHC expression and cellular immune response in BALB/C mice infected with *Leishmania donovani*. *Indian J Exp Biol,* 39**,** 878-82.

BODE, W. & HUBER, R. 2000. Structural basis of the endoproteinase-protein inhibitor interaction. *Biochim Biophys Acta,* 1477**,** 241-52.

BRANCHE, C., KOHL, L., TOUTIRAIS, G., BUISSON, J., COSSON, J. & BASTIN, P. 2006. Conserved and specific functions of axoneme components in trypanosome motility. *J Cell Sci,* 119**,** 3443-55.

BRICKMAN, M. J., COOK, J. M. & BALBER, A. E. 1995. Low temperature reversibly inhibits transport from tubular endosomes to a perinuclear, acidic compartment in African trypanosomes. *J Cell Sci,* 108 (Pt 11)**,** 3611-21.

BRIDGES, D. J., PITT, A. R., HANRAHAN, O., BRENNAN, K., VOORHEIS, H. P., HERZYK, P., DE KONING, H. P. & BURCHMORE, R. J. 2008. Characterisation of the plasma membrane subproteome of bloodstream form *Trypanosoma brucei. Proteomics,* 8**,** 83-99.

BRIGGS, L. J., MCKEAN, P. G., BAINES, A., MOREIRA-LEITE, F., DAVIDGE, J., VAUGHAN, S. & GULL, K. 2004. The flagella connector of *Trypanosoma brucei*: an unusual mobile transmembrane junction. *J Cell Sci,* 117**,** 1641-51.

BRINKMANN, V., REICHARD, U., GOOSMANN, C., FAULER, B., UHLEMANN, Y., WEISS, D. S., WEINRAUCH, Y. & ZYCHLINSKY, A. 2004. Neutrophil extracellular traps kill bacteria. *Science,* 303**,** 1532-5.

BROADHEAD, R., DAWE, H. R., FARR, H., GRIFFITHS, S., HART, S. R., PORTMAN, N., SHAW, M. K., GINGER, M. L., GASKELL, S. J., MCKEAN, P. G. & GULL, K. 2006. Flagellar motility is required for the viability of the bloodstream trypanosome. *Nature,* 440**,** 224-7.

BRUN, R., BLUM, J., CHAPPUIS, F. & BURRI, C. 2010. Human African trypanosomiasis. *Lancet,* 375**,** 148-59.

BUCKNER, F. S., YOKOYAMA, K., NGUYEN, L., GREWAL, A., ERDJUMENT-BROMAGE, H., TEMPST, P., STRICKLAND, C. L., XIAO, L., VAN VOORHIS, W. C. & GELB, M. H. 2000. Cloning, heterologous expression, and distinct substrate specificity of protein farnesyltransferase from *Trypanosoma brucei*. *J Biol Chem,* 275**,** 21870-6.

BURLEIGH, B. A., CALER, E. V., WEBSTER, P. & ANDREWS, N. W. 1997. A cytosolic serine endopeptidase from *Trypanosoma cruzi* is required for the generation of Ca2+ signaling in mammalian cells. *J Cell Biol,* 136**,** 609-20.

BUSCHIAZZO, A., MUIÁ, R., LARRIEUX, N., PITCOVSKY, T., MUCCI, J. & CAMPETELLA, O. 2012. *Trypanosoma cruzi* trans-sialidase in complex with a neutralizing antibody: structure/function studies towards the rational design of inhibitors. *PLoS Pathog,* 8**,** e1002474.

CAFFREY, C. R., SCORY, S. & STEVERDING, D. 2000. Cysteine proteinases of trypanosome parasites: novel targets for chemotherapy. *Curr Drug Targets,* 1**,** 155-62.

CAFFREY, C. R. & STEVERDING, D. 2009. Kinetoplastid papain-like cysteine peptidases. *Mol Biochem Parasitol,* 167**,** 12-9.

CALER, E. V., VAENA DE AVALOS, S., HAYNES, P. A., ANDREWS, N. W. & BURLEIGH, B. A. 1998. Oligopeptidase B-dependent signaling mediates host cell invasion by *Trypanosoma cruzi*. *EMBO J,* 17**,** 4975-86.

CASTRO, H. C., MONTEIRO, R. Q., ASSAFIM, M., LOUREIRO, N. I., CRAIK, C. & ZINGALI, R. B. 2006. Ecotin modulates thrombin activity through exosite-2 interactions. *Int J Biochem Cell Biol,* 38**,** 1893-900.

CHA, D. Y., SONG, I. K., LEE, G. S., HWANG, O. S., NOH, H. J., YEO, S. D., SHIN, D. W. & LEE, Y. H. 2001. Effects of specific monoclonal antibodies to dense granular proteins on the invasion of *Toxoplasma gondii in vitro* and *in vivo*. *Korean J Parasitol,* 39**,** 233-40.

CHAPPUIS, F. 2007. Melarsoprol-free drug combinations for second-stage Gambian sleeping sickness: the way to go. *Clin Infect Dis,* 45**,** 1443-5.

CHAPPUIS, F., LOUTAN, L., SIMARRO, P., LEJON, V. & BÜSCHER, P. 2005. Options for field diagnosis of human african trypanosomiasis. *Clin Microbiol Rev,* 18**,** 133-46.

CHECCHI, F., FILIPE, J. A., HAYDON, D. T., CHANDRAMOHAN, D. & CHAPPUIS, F. 2008. Estimates of the duration of the early and late stage of gambiense sleeping sickness. *BMC Infect Dis,* 8**,** 16.

CHEN, J., RAUCH, C. A., WHITE, J. H., ENGLUND, P. T. & COZZARELLI, N. R. 1995. The topology of the kinetoplast DNA network. *Cell,* 80**,** 61-9.

CHUNG, C. H., IVES, H. E., ALMEDA, S. & GOLDBERG, A. L. 1983. Purification from *Escherichia coli* of a periplasmic protein that is a potent inhibitor of pancreatic proteases. *J Biol Chem,* 258**,** 11032-8.

CLAYTON, C. E., ESTÉVEZ, A. M., HARTMANN, C., ALIBU, V. P., FIELD, M. & HORN, D. 2005. Down-regulating gene expression by RNA interference in *Trypanosoma brucei. Methods Mol Biol,* 309**,** 39-60.

COETZER, T. H., GOLDRING, J. P. & HUSON, L. E. 2008. Oligopeptidase B: a processing peptidase involved in pathogenesis. *Biochimie,* 90**,** 336-44.

COHEN, P. 2000. The regulation of protein function by multisite phosphorylation--a 25 year update. *Trends Biochem Sci,* 25**,** 596-601.

COOMBS, G. H. & MOTTRAM, J. C. 1997. Parasite proteinases and amino acid metabolism: possibilities for chemotherapeutic exploitation. *Parasitology,* 114 Suppl**,** S61-80.

COSTA-SILVA, T. A., MEIRA, C. S., FERREIRA, I. M., HIRAMOTO, R. M. & PEREIRA-CHIOCCOLA, V. L. 2008. Evaluation of immunization with tachyzoite excreted-secreted proteins in a novel susceptible mouse model (A/Sn) for *Toxoplasma gondii*. *Exp Parasitol,* 120**,** 227-34.

CROSS, G. A. 1975. Identification, purification and properties of clone-specific glycoprotein antigens constituting the surface coat of Trypanosoma brucei. *Parasitology,* 71**,** 393-417.

DAVIDGE, J. A., CHAMBERS, E., DICKINSON, H. A., TOWERS, K., GINGER, M. L., MCKEAN, P. G. & GULL, K. 2006. Trypanosome IFT mutants provide insight into the motor location for mobility of the flagella connector and flagellar membrane formation. *J Cell Sci,* 119**,** 3935-43.

DAWE, H. R., FARR, H., PORTMAN, N., SHAW, M. K. & GULL, K. 2005. The Parkin co-regulated gene product, PACRG, is an evolutionarily conserved axonemal protein that functions in outer-doublet microtubule morphogenesis. *J Cell Sci,* 118**,** 5421-30.

DI CERA, E. 2009. Serine proteases. *IUBMB Life,* 61**,** 510-5.

DOCAMPO, R., ULRICH, P. & MORENO, S. N. 2010. Evolution of acidocalcisomes and their role in polyphosphate storage and osmoregulation in eukaryotic microbes. *Philos Trans R Soc Lond B Biol Sci,* 365**,** 775-84.

DOS REIS, F. C., SMITH, B. O., SANTOS, C. C., COSTA, T. F., SCHARFSTEIN, J., COOMBS, G. H., MOTTRAM, J. C. & LIMA, A. P. 2008. The role of conserved residues of chagasin in the inhibition of cysteine peptidases. *FEBS Lett,* 582**,** 485-90.

DOYLE, P. S., ZHOU, Y. M., ENGEL, J. C. & MCKERROW, J. H. 2007. A cysteine protease inhibitor cures Chagas' disease in an immunodeficient-mouse model of infection. *Antimicrob Agents Chemother,* 51**,** 3932-9.

EGGERS, C. T., MURRAY, I. A., DELMAR, V. A., DAY, A. G. & CRAIK, C. S. 2004. The periplasmic serine protease inhibitor ecotin protects bacteria against neutrophil elastase. *Biochem J,* 379**,** 107-18.

EGGERS, C. T., WANG, S. X., FLETTERICK, R. J. & CRAIK, C. S. 2001. The role of ecotin dimerization in protease inhibition. *J Mol Biol,* 308**,** 975-91.

EMMER, B. T., DANIELS, M. D., TAYLOR, J. M., EPTING, C. L. & ENGMAN, D. M. 2010. Calflagin inhibition prolongs host survival and suppresses parasitemia in *Trypanosoma brucei* infection. *Eukaryot Cell,* 9**,** 934-42.

EMMER, B. T., NAKAYASU, E. S., SOUTHER, C., CHOI, H., SOBREIRA, T. J., EPTING, C. L., NESVIZHSKII, A. I., ALMEIDA, I. C. & ENGMAN, D. M. 2011. Global analysis of protein palmitoylation in African trypanosomes. *Eukaryot Cell,* 10**,** 455-63.

ENGSTLER, M., PFOHL, T., HERMINGHAUS, S., BOSHART, M., WIEGERTJES, G., HEDDERGOTT, N. & OVERATH, P. 2007. Hydrodynamic Flow-Mediated Protein Sorting on the Cell Surface of Trypanosomes. *Cell,* 131**,** 505-515.

ESCHENLAUER, S. C., FARIA, M. S., MORRISON, L. S., BLAND, N., RIBEIRO-GOMES, F. L., DOSREIS, G. A., COOMBS, G. H., LIMA, A. P. & MOTTRAM, J. C. 2009. Influence of parasite encoded inhibitors of serine peptidases in early infection of macrophages with *Leishmania major*. *Cell Microbiol,* 11**,** 106-20.

FARIA, M. S., REIS, F. C., AZEVEDO-PEREIRA, R. L., MORRISON, L. S., MOTTRAM, J. C. & LIMA, A. P. 2011. *Leishmania* inhibitor of serine peptidase 2 prevents TLR4 activation by neutrophil elastase promoting parasite survival in murine macrophages. *J Immunol,* 186**,** 411-22.

FENG, H., ZHU, X. T., QI, Z. M., WANG, Q. H., WANG, G. G., PAN, Y. Y., LI, Y., ZHENG, L., JIANG, Y. J., SHANG, H., CUI, L. & CAO, Y. M. 2012. Transient attenuated Foxp3 expression on $CD4^+$ T cells treated with 7D4 mAb contributes to the control of parasite burden in DBA/2 mice infected with lethal *Plasmodium chabaudi chabaudi* AS. *Scand J Immunol,* 75**,** 46-53.

FENN, K. & MATTHEWS, K. R. 2007. The cell biology of *Trypanosoma brucei* differentiation. *Curr Opin Microbiol,* 10**,** 539-46.

FIELD, H., FARJAH, M., PAL, A., GULL, K. & FIELD, M. C. 1998. Complexity of trypanosomatid endocytosis pathways revealed by Rab4 and Rab5 isoforms in *Trypanosoma brucei*. *J Biol Chem,* 273**,** 32102-10.

FIELD, M. C., ALLEN, C. L., DHIR, V., GOULDING, D., HALL, B. S., MORGAN, G. W., VEAZEY, P. & ENGSTLER, M. 2004. New approaches to the microscopic imaging of *Trypanosoma brucei*. *Microsc Microanal,* 10**,** 621-36.

FIELD, M. C. & CARRINGTON, M. 2009. The trypanosome flagellar pocket. *Nat Rev Microbiol,* 7**,** 775-86.

FIELD, M. C., LUMB, J. H., ADUNG'A, V. O., JONES, N. G. & ENGSTLER, M. 2009. Macromolecular trafficking and immune evasion in african trypanosomes. *Int Rev Cell Mol Biol,* 278**,** 1-67.

GEIGER, A., HIRTZ, C., BÉCUE, T., BELLARD, E., CENTENO, D., GARGANI, D., ROSSIGNOL, M., CUNY, G. & PELTIER, J. B. 2010. Exocytosis and protein secretion in *Trypanosoma*. *BMC Microbiol,* 10**,** 20.

GILLMOR, S., MCGRATH, M. & FLETTERICK, R. 1995. Ecotin: A most adaptable protease inhibitor. *Persp Drug Disc Des,* 2**,** 475-482.

GLUSHAKOVA, S., MAZAR, J., HOHMANN-MARRIOTT, M. F., HAMA, E. & ZIMMERBERG, J. 2009. Irreversible effect of cysteine protease inhibitors on the release of malaria parasites from infected erythrocytes. *Cell Microbiol,* 11**,** 95-105.

GRIFFITHS, S., PORTMAN, N., TAYLOR, P. R., GORDON, S., GINGER, M. L. & GULL, K. 2007. RNA interference mutant induction *in vivo* demonstrates the essential nature of trypanosome flagellar function during mammalian infection. *Eukaryot Cell,* 6**,** 1248-50.

GRÜNFELDER, C. G., ENGSTLER, M., WEISE, F., SCHWARZ, H., STIERHOF, Y. D., MORGAN, G. W., FIELD, M. C. & OVERATH, P. 2003. Endocytosis of a glycosylphosphatidylinositol-anchored protein via clathrin-coated vesicles, sorting by default in endosomes, and exocytosis via RAB11-positive carriers. *Mol Biol Cell,* 14**,** 2029-40.

GUIMARÃES-COSTA, A. B., NASCIMENTO, M. T., FROMENT, G. S., SOARES, R. P., MORGADO, F. N., CONCEIÇÃO-SILVA, F. & SARAIVA, E. M. 2009. *Leishmania amazonensis* promastigotes induce and are killed by neutrophil extracellular traps. *Proc Natl Acad Sci U S A,* 106**,** 6748-53.

GULL, K. 1999. The cytoskeleton of trypanosomatid parasites. *Annu Rev Microbiol,* 53**,** 629-55.

GULL, K. 2001. The biology of kinetoplastid parasites: insights and challenges from genomics and post-genomics. *Int J Parasitol,* 31**,** 443-52.

GULL, K. 2003. Host-parasite interactions and trypanosome morphogenesis: a flagellar pocketful of goodies. *Curr Opin Microbiol,* 6**,** 365-70.

HAMADIEN, M., LYCKE, N. & BAKHIET, M. 1999. Induction of the trypanosome lymphocyte-triggering factor (TLTF) and neutralizing antibodies to the TLTF in experimental african trypanosomiasis. *Immunology,* 96**,** 606-11.

HAMMARTON, T. C. 2007. Cell cycle regulation in *Trypanosoma brucei. Mol Biochem Parasitol,* 153**,** 1-8.

HE, C. Y., HO, H. H., MALSAM, J., CHALOUNI, C., WEST, C. M., ULLU, E., TOOMRE, D. & WARREN, G. 2004. Golgi duplication in *Trypanosoma brucei*. *J Cell Biol,* 165**,** 313-21.

HELMS, M. J., AMBIT, A., APPLETON, P., TETLEY, L., COOMBS, G. H. & MOTTRAM, J. C. 2006. Bloodstream form *Trypanosoma brucei* depend upon multiple metacaspases associated with RAB11-positive endosomes. *J Cell Sci,* 119**,** 1105-17.

HILL, K. L., HUTCHINGS, N. R., GRANDGENETT, P. M. & DONELSON, J. E. 2000. T lymphocyte-triggering factor of african trypanosomes is associated with the flagellar fraction of the cytoskeleton and represents a new family of proteins that are present in several divergent eukaryotes. *J Biol Chem,* 275**,** 39369-78.

HOCHULI, E. 1988. Large-scale chromatography of recombinant proteins. *J Chromatogr,* 444**,** 293-302.

HOTEZ, P. J., MOLYNEUX, D. H., FENWICK, A., KUMARESAN, J., SACHS, S. E., SACHS, J. D. & SAVIOLI, L. 2007. Control of Neglected Tropical Diseases. *New England Journal of Medicine,* 357**,** 1018-1027.

HU, C. & AKSOY, S. 2006. Innate immune responses regulate trypanosome parasite infection of the tsetse fly *Glossina morsitans morsitans. Mol Microbiol,* 60**,** 1194-204.

HUDSON, K. M. & TERRY, R. J. 1979. Immunodepression and the course of infection of a chronic *Trypanosoma brucei* infection in mice. *Parasite Immunol,* 1**,** 317-26.

HUETE-PÉREZ, J. A., ENGEL, J. C., BRINEN, L. S., MOTTRAM, J. C. & MCKERROW, J. H. 1999. Protease trafficking in two primitive eukaryotes is mediated by a prodomain protein motif. *J Biol Chem,* 274**,** 16249-56.

HUTCHINGS, N. R., DONELSON, J. E. & HILL, K. L. 2002. Trypanin is a cytoskeletal linker protein and is required for cell motility in African trypanosomes. *J Cell Biol,* 156**,** 867-77.

IVENS, A. C., PEACOCK, C. S., WORTHEY, E. A., MURPHY, L., AGGARWAL, G., BERRIMAN, M., SISK, E., RAJANDREAM, M. A., ADLEM, E., AERT, R., ANUPAMA, A., APOSTOLOU, Z., ATTIPOE, P., BASON, N., BAUSER, C., BECK, A., BEVERLEY, S. M., BIANCHETTIN, G., BORZYM, K., BOTHE, G., BRUSCHI, C. V., COLLINS, M., CADAG, E., CIARLONI, L., CLAYTON, C., COULSON, R. M., CRONIN, A., CRUZ, A. K., DAVIES, R. M., DE GAUDENZI, J., DOBSON, D. E., DUESTERHOEFT, A., FAZELINA, G., FOSKER, N., FRASCH, A. C., FRASER, A., FUCHS, M., GABEL, C., GOBLE, A., GOFFEAU, A., HARRIS, D., HERTZ-FOWLER, C., HILBERT, H., HORN, D., HUANG, Y., KLAGES, S., KNIGHTS, A., KUBE, M., LARKE, N., LITVIN, L., LORD, A., LOUIE, T., MARRA, M., MASUY, D., MATTHEWS, K., MICHAELI, S., MOTTRAM, J. C., MÜLLER-AUER, S., MUNDEN, H., NELSON, S., NORBERTCZAK, H., OLIVER, K., O'NEIL, S., PENTONY, M., POHL, T. M., PRICE, C., PURNELLE, B., QUAIL, M. A., RABBINOWITSCH, E., REINHARDT, R., RIEGER, M., RINTA, J., ROBBEN, J., ROBERTSON, L., RUIZ, J. C., RUTTER, S., SAUNDERS, D., SCHÄFER, M., SCHEIN, J., SCHWARTZ, D. C., SEEGER, K., SEYLER, A., SHARP, S., SHIN, H., SIVAM, D., SQUARES, R., SQUARES, S., TOSATO, V., VOGT, C., VOLCKAERT, G., WAMBUTT, R., WARREN, T., WEDLER, H., WOODWARD, J., ZHOU, S., ZIMMERMANN, W., SMITH, D. F., BLACKWELL, J. M., STUART, K. D., BARRELL, B., *et al.* 2005. The genome of the kinetoplastid parasite, *Leishmania major*. *Science,* 309**,** 436-42.

KENNEDY, P. G. 2008. The continuing problem of human African trypanosomiasis (sleeping sickness). *Ann Neurol,* 64**,** 116-26.

KOHL, L. & BASTIN, P. 2005. The flagellum of trypanosomes. *Int Rev Cytol,* 244**,** 227-85.

KOHL, L. & GULL, K. 1998. Molecular architecture of the trypanosome cytoskeleton. *Mol Biochem Parasitol,* 93**,** 1-9.

KOHL, L., ROBINSON, D. & BASTIN, P. 2003. Novel roles for the flagellum in cell morphogenesis and cytokinesis of trypanosomes. *EMBO J,* 22**,** 5336-46.

KORDE, R., BHARDWAJ, A., SINGH, R., SRIVASTAVA, A., CHAUHAN, V. S., BHATNAGAR, R. K. & MALHOTRA, P. 2008. A prodomain peptide of *Plasmodium falciparum* cysteine protease (falcipain-2) inhibits malaria parasite development. *J Med Chem,* 51**,** 3116-23.

KURTENBACH, K., DIZIJ, A., VOET, P., HAUSER, P. & SIMON, M. M. 1997. Vaccination of natural reservoir hosts with recombinant lipidated OspA induces a transmission-blocking immunity against Lyme disease spirochaetes associated with high levels of LA-2 equivalent antibodies. *Vaccine,* 15**,** 1670-4.

LA GRECA, F. & MAGEZ, S. 2011. Vaccination against trypanosomiasis: can it be done or is the trypanosome truly the ultimate immune destroyer and escape artist? *Hum Vaccin,* 7**,** 1225-33.

LACOMBLE, S., VAUGHAN, S., GADELHA, C., MORPHEW, M. K., SHAW, M. K., MCINTOSH, J. R. & GULL, K. 2009. Three-dimensional cellular architecture of the flagellar pocket and associated cytoskeleton in trypanosomes revealed by electron microscope tomography. *J Cell Sci,* 122**,** 1081-90.

LANDFEAR, S. M. & IGNATUSHCHENKO, M. 2001. The flagellum and flagellar pocket of trypanosomatids. *Mol Biochem Parasitol,* 115**,** 1-17.

LANTERI, C. A., STEWART, M. L., BROCK, J. M., ALIBU, V. P., MESHNICK, S. R., TIDWELL, R. R. & BARRETT, M. P. 2006. Roles for the *Trypanosoma brucei* P2 transporter in DB75 uptake and resistance. *Mol Pharmacol,* 70**,** 1585-92.

LANÇA, A. S., DE SOUSA, K. P., ATOUGUIA, J., PRAZERES, D. M., MONTEIRO, G. A. & SILVA, M. S. 2011. *Trypanosoma brucei*: immunisation with plasmid DNA encoding invariant surface glycoprotein gene is able to induce partial protection in experimental African trypanosomiasis. *Exp Parasitol,* 127**,** 18-24.

LAROCCA, T. J., HOLTHAUSEN, D. J., HSIEH, C., RENKEN, C., MANNELLA, C. A. & BENACH, J. L. 2009. The bactericidal effect of a complement-independent antibody is osmolytic and specific to *Borrelia*. *Proc Natl Acad Sci U S A,* 106**,** 10752-7.

LI, S. Q., FUNG, M. C., REID, S. A., INOUE, N. & LUN, Z. R. 2007. Immunization with recombinant beta-tubulin from *Trypanosoma evansi* induced protection against *T. evansi, T. equiperdum* and *T. b. brucei* infection in mice. *Parasite Immunol,* 29**,** 191-9.

LI, S. Q., YANG, W. B., LUN, Z. R., MA, L. J., XI, S. M., CHEN, Q. L., SONG, X. W., KANG, J. & YANG, L. Z. 2009. Immunization with recombinant actin from *Trypanosoma evansi* induces protective immunity against T. *evansi, T. equiperdum* and *T. b. brucei* infection. *Parasitol Res,* 104**,** 429-35.

LIMA, A. P. C. & MOTTRAM, J. C. 2010. Trypanosomatid-encoded inhibitors of peptidases: unique structural features and possible roles as virulence factors. *Open Parasitology Journal,* 4**,** 132-138.

LUBEGA, G. W., BYARUGABA, D. K. & PRICHARD, R. K. 2002a. Immunization with a tubulin-rich preparation from *Trypanosoma brucei* confers broad protection against African trypanosomosis. *Exp Parasitol,* 102**,** 9-22.

LUBEGA, G. W., OCHOLA, D. O. & PRICHARD, R. K. 2002b. *Trypanosoma brucei*: anti-tubulin antibodies specifically inhibit trypanosome growth in culture. *Exp Parasitol,* 102**,** 134-42.

LUGINBUEHL, E., RYTER, D., SCHRANZ-ZUMKEHR, J., OBERHOLZER, M., KUNZ, S. & SEEBECK, T. 2010. The N terminus of phosphodiesterase TbrPDEB1 of *Trypanosoma brucei* contains the signal for integration into the flagellar skeleton. *Eukaryot Cell,* 9**,** 1466-75.

LÓPEZ-OTÍN, C. & BOND, J. S. 2008. Proteases: multifunctional enzymes in life and disease. *J Biol Chem,* 283**,** 30433-7.

MACKEY, Z. B., O'BRIEN, T. C., GREENBAUM, D. C., BLANK, R. B. & MCKERROW, J. H. 2004. A cathepsin B-like protease is required for host protein degradation in *Trypanosoma brucei*. *J Biol Chem,* 279**,** 48426-33.

MALLARI, J. P., SHELAT, A. A., KOSINSKI, A., CAFFREY, C. R., CONNELLY, M., ZHU, F., MCKERROW, J. H. & GUY, R. K. 2009. Structure-guided development of selective TbcatB inhibitors. *J Med Chem,* 52**,** 6489-93.

MALVY, D. & CHAPPUIS, F. 2011. Sleeping sickness. *Clin Microbiol Infect,* 17**,** 986-95.

MATTHEWS, K. R. 2005. The developmental cell biology of *Trypanosoma brucei*. *J Cell Sci,* 118**,** 283-90.

MATTHEWS, K. R. & GULL, K. 1994. Evidence for an interplay between cell cycle progression and the initiation of differentiation between life cycle forms of African trypanosomes. *J Cell Biol,* 125**,** 1147-56.

MCGRATH, M. E., GILLMOR, S. A. & FLETTERICK, R. J. 1995. Ecotin: lessons on survival in a protease-filled world. *Protein Sci,* 4**,** 141-8.

MCKEAN, P. G. 2003. Coordination of cell cycle and cytokinesis in *Trypanosoma brucei*. *Curr Opin Microbiol,* 6**,** 600-7.

MCKERROW, J. H., DOYLE, P. S., ENGEL, J. C., PODUST, L. M., ROBERTSON, S. A., FERREIRA, R., SAXTON, T., ARKIN, M., KERR, I. D., BRINEN, L. S. & CRAIK, C. S. 2009. Two approaches to discovering and developing new drugs for Chagas disease. *Mem Inst Oswaldo Cruz,* 104 Suppl 1**,** 263-9.

MICHELS, P. A., BRINGAUD, F., HERMAN, M. & HANNAERT, V. 2006. Metabolic functions of glycosomes in trypanosomatids. *Biochim Biophys Acta,* 1763**,** 1463-77.

MKUNZA, F., OLAHO, W. M. & POWELL, C. N. 1995. Partial protection against natural trypanosomiasis after vaccination with a flagellar pocket antigen from *Trypanosoma brucei rhodesiense*. *Vaccine,* 13**,** 151-4.

MONTEIRO, A. C., ABRAHAMSON, M., LIMA, A. P., VANNIER-SANTOS, M. A. & SCHARFSTEIN, J. 2001. Identification, characterization and localization of chagasin, a tight-binding cysteine protease inhibitor in *Trypanosoma cruzi*. *J Cell Sci,* 114**,** 3933-42.

MOREIRA-LEITE, F. F., SHERWIN, T., KOHL, L. & GULL, K. 2001. A trypanosome structure involved in transmitting cytoplasmic information during cell division. *Science,* 294**,** 610-2.

MORENO, S. N. & DOCAMPO, R. 2003. Calcium regulation in protozoan parasites. *Curr Opin Microbiol,* 6**,** 359-64.

MORGAN, G. W., HALL, B. S., DENNY, P. W., CARRINGTON, M. & FIELD, M. C. 2002a. The kinetoplastida endocytic apparatus. Part I: a dynamic system for nutrition and evasion of host defences. *Trends Parasitol,* 18**,** 491-6.

MORGAN, G. W., HALL, B. S., DENNY, P. W., FIELD, M. C. & CARRINGTON, M. 2002b. The endocytic apparatus of the kinetoplastida. Part II: machinery and components of the system. *Trends Parasitol,* 18**,** 540-6.

MORRISON, L. S., GOUNDRY, A., FARIA, M. S., TETLEY, L., ESCHENLAUER, S. C., WESTROP, G. D., DOSTALOVA, A., VOLF, P., COOMBS, G. H., LIMA, A. P. & MOTTRAM, J. C. 2012. Ecotin-like serine peptidase inhibitor ISP1 of *Leishmania major* plays a role in flagellar pocket dynamics and promastigote differentiation. *Cell Microbiol*.

MORTY, R. E., LONSDALE-ECCLES, J. D., MOREHEAD, J., CALER, E. V., MENTELE, R., AUERSWALD, E. A., COETZER, T. H., ANDREWS, N. W. & BURLEIGH, B. A. 1999. Oligopeptidase B from *Trypanosoma brucei*, a new member of an emerging subgroup of serine oligopeptidases. *J Biol Chem,* 274**,** 26149-56.

MOTTRAM, J. C., BROOKS, D. R. & COOMBS, G. H. 1998. Roles of cysteine proteinases of trypanosomes and *Leishmania* in host-parasite interactions. *Curr Opin Microbiol,* 1**,** 455-60.

MOTTRAM, J. C., COOMBS, G. H. & ALEXANDER, J. 2004. Cysteine peptidases as virulence factors of *Leishmania*. *Curr Opin Microbiol,* 7**,** 375-81.

MUNDAY, J. C., MCLUSKEY, K., BROWN, E., COOMBS, G. H. & MOTTRAM, J. C. 2011. Oligopeptidase B deficient mutants of *Leishmania major*. *Mol Biochem Parasitol,* 175**,** 49-57.

NAMANGALA, B., DE BAETSELIER, P. & BESCHIN, A. 2009. Both type-I and type-II responses contribute to murine trypanotolerance. *J Vet Med Sci,* 71**,** 313-8.

NATESAN, S. K., BLACK, A., MATTHEWS, K. R., MOTTRAM, J. C. & FIELD, M. C. 2011. *Trypanosoma brucei brucei*: endocytic recycling is important for mouse infectivity. *Exp Parasitol,* 127**,** 777-83.

NATESAN, S. K., PEACOCK, L., LEUNG, K. F., GIBSON, W. & FIELD, M. C. 2010. Evidence that low endocytic activity is not directly responsible for human serum resistance in the insect form of African trypanosomes. *BMC Res Notes,* 3**,** 63.

NATESAN, S. K., PEACOCK, L., MATTHEWS, K., GIBSON, W. & FIELD, M. C. 2007. Activation of endocytosis as an adaptation to the mammalian host by trypanosomes. *Eukaryot Cell,* 6**,** 2029-37.

NAULA, C., PARSONS, M. & MOTTRAM, J. C. 2005. Protein kinases as drug targets in trypanosomes and *Leishmania*. *Biochim Biophys Acta,* 1754**,** 151-9.

NETT, I. R., MARTIN, D. M., MIRANDA-SAAVEDRA, D., LAMONT, D., BARBER, J. D., MEHLERT, A. & FERGUSON, M. A. 2009. The phosphoproteome of bloodstream form *Trypanosoma brucei*, causative agent of African sleeping sickness. *Mol Cell Proteomics,* 8**,** 1527-38.

NGÔ, H., TSCHUDI, C., GULL, K. & ULLU, E. 1998. Double-stranded RNA induces mRNA degradation in *Trypanosoma brucei*. *Proc Natl Acad Sci U S A,* 95**,** 14687-92.

NIKOLSKAIA, O. V., DE A LIMA, A. P., KIM, Y. V., LONSDALE-ECCLES, J. D., FUKUMA, T., SCHARFSTEIN, J. & GRAB, D. J. 2006. Blood-brain barrier traversal by African trypanosomes requires calcium signaling induced by parasite cysteine protease. *J Clin Invest,* 116**,** 2739-47.

NORTH, M. J., MOTTRAM, J. C. & COOMBS, G. H. 1990. Cysteine proteinases of parasitic protozoa. *Parasitol Today,* 6**,** 270-5.

NOWICKI, M. W., TULLOCH, L. B., WORRALLL, L., MCNAE, I. W., HANNAERT, V., MICHELS, P. A., FOTHERGILL-GILMORE, L. A., WALKINSHAW, M. D. & TURNER, N. J. 2008. Design, synthesis and trypanocidal activity of lead compounds based on inhibitors of parasite glycolysis. *Bioorg Med Chem,* 16**,** 5050-61.

OBERHOLZER, M., MARTI, G., BARESIC, M., KUNZ, S., HEMPHILL, A. & SEEBECK, T. 2007. The *Trypanosoma brucei* cAMP phosphodiesterases TbrPDEB1 and TbrPDEB2: flagellar enzymes that are essential for parasite virulence. *FASEB J,* 21**,** 720-31.

ODIIT, M., KANSIIME, F. & ENYARU, J. C. 1997. Duration of symptoms and case fatality of sleeping sickness caused by *Trypanosoma brucei rhodesiense* in Tororo, Uganda. *East Afr Med J,* 74**,** 792-5.

OGBADOYI, E. O., ROBINSON, D. R. & GULL, K. 2003. A high-order trans-membrane structural linkage is responsible for mitochondrial genome positioning and segregation by flagellar basal bodies in trypanosomes. *Mol Biol Cell,* 14**,** 1769-79.

OTLEWSKI, J., KROWARSCH, D. & APOSTOLUK, W. 1999. Protein inhibitors of serine proteinases. *Acta Biochim Pol,* 46**,** 531-65.

PAGE, M. J. & DI CERA, E. 2008. Serine peptidases: classification, structure and function. *Cell Mol Life Sci,* 65**,** 1220-36.

PAL, A., HALL, B. S., JEFFRIES, T. R. & FIELD, M. C. 2003. Rab5 and Rab11 mediate transferrin and anti-variant surface glycoprotein antibody recycling in *Trypanosoma brucei*. *Biochem J,* 374**,** 443-51.

PAL, A., HALL, B. S., NESBETH, D. N., FIELD, H. I. & FIELD, M. C. 2002. Differential endocytic functions of *Trypanosoma brucei* Rab5 isoforms reveal a glycosylphosphatidylinositol-specific endosomal pathway. *J Biol Chem,* 277**,** 9529-39.

PARSONS, M. 2004. Glycosomes: parasites and the divergence of peroxisomal purpose. *Mol Microbiol,* 53**,** 717-24.

PAUL, K. S., JIANG, D., MORITA, Y. S. & ENGLUND, P. T. 2001. Fatty acid synthesis in African trypanosomes: a solution to the myristate mystery. *Trends Parasitol,* 17**,** 381-7.

PEREZ BRANDAN, C., PADILLA, A. M., XU, D., TARLETON, R. L. & BASOMBRIO, M. A. 2011. Knockout of the dhfr-ts gene in *Trypanosoma cruzi* generates attenuated parasites able to confer protection against a virulent challenge. *PLoS Negl Trop Dis,* 5**,** e1418.

PLOUBIDOU, A., ROBINSON, D. R., DOCHERTY, R. C., OGBADOYI, E. O. & GULL, K. 1999. Evidence for novel cell cycle checkpoints in trypanosomes:

kinetoplast segregation and cytokinesis in the absence of mitosis. *J Cell Sci,* 112 (Pt 24)**,** 4641-50.

POLGÁR, L. 2005. The catalytic triad of serine peptidases. *Cell Mol Life Sci,* 62**,** 2161-72.

PORATH, J., CARLSSON, J., OLSSON, I. & BELFRAGE, G. 1975. Metal chelate affinity chromatography, a new approach to protein fractionation. *Nature,* 258**,** 598-9.

PORTMAN, N. & GULL, K. 2010. The paraflagellar rod of kinetoplastid parasites: from structure to components and function. *Int J Parasitol,* 40**,** 135-48.

PRICE, H. P., GÜTHER, M. L., FERGUSON, M. A. & SMITH, D. F. 2010. Myristoyl-CoA:protein N-myristoyltransferase depletion in trypanosomes causes avirulence and endocytic defects. *Mol Biochem Parasitol,* 169**,** 55-8.

PRIEST, J. W. & HAJDUK, S. L. 1994. Developmental regulation of mitochondrial biogenesis in *Trypanosoma brucei*. *J Bioenerg Biomembr,* 26**,** 179-91.

PRIOTTO, G., KASPARIAN, S., MUTOMBO, W., NGOUAMA, D., GHORASHIAN, S., ARNOLD, U., GHABRI, S., BAUDIN, E., BUARD, V., KAZADI-KYANZA, S., ILUNGA, M., MUTANGALA, W., POHLIG, G., SCHMID, C., KARUNAKARA, U., TORREELE, E. & KANDE, V. 2009. Nifurtimox-eflornithine combination therapy for second-stage African *Trypanosoma brucei gambiense* trypanosomiasis: a multicentre, randomised, phase III, non-inferiority trial. *Lancet,* 374**,** 56-64.

PRIOTTO, G., KASPARIAN, S., NGOUAMA, D., GHORASHIAN, S., ARNOLD, U., GHABRI, S. & KARUNAKARA, U. 2007. Nifurtimox-eflornithine combination therapy for second-stage *Trypanosoma brucei gambiense* sleeping sickness: a randomized clinical trial in Congo. *Clin Infect Dis,* 45**,** 1435-42.

PROTO, W. R., CASTANYS-MUNOZ, E., BLACK, A., TETLEY, L., MOSS, C. X., JULIANO, L., COOMBS, G. H. & MOTTRAM, J. C. 2011. *Trypanosoma brucei* metacaspase 4 is a pseudopeptidase and a virulence factor. *J Biol Chem,* 286**,** 39914-25.

PUENTE, X. S., SÁNCHEZ, L. M., OVERALL, C. M. & LÓPEZ-OTÍN, C. 2003. Human and mouse proteases: a comparative genomic approach. *Nat Rev Genet,* 4**,** 544-58.

QUESADA, V., ORDÓÑEZ, G. R., SÁNCHEZ, L. M., PUENTE, X. S. & LÓPEZ-OTÍN, C. 2009. The Degradome database: mammalian proteases and diseases of proteolysis. *Nucleic Acids Res,* 37**,** D239-43.

RALSTON, K. S. & HILL, K. L. 2006. Trypanin, a component of the flagellar Dynein regulatory complex, is essential in bloodstream form African trypanosomes. *PLoS Pathog,* 2**,** e101.

RALSTON, K. S. & HILL, K. L. 2008. The flagellum of *Trypanosoma brucei:* new tricks from an old dog. *Int J Parasitol,* 38**,** 869-84.

RALSTON, K. S., KABUTUTU, Z. P., MELEHANI, J. H., OBERHOLZER, M. & HILL, K. L. 2009. The *Trypanosoma brucei* flagellum: moving parasites in new directions. *Annu Rev Microbiol,* 63**,** 335-62.

RALSTON, K. S., KISALU, N. K. & HILL, K. L. 2011. Structure-function analysis of dynein light chain 1 identifies viable motility mutants in bloodstream-form *Trypanosoma brucei*. *Eukaryot Cell,* 10**,** 884-94.

RALSTON, K. S., LERNER, A. G., DIENER, D. R. & HILL, K. L. 2006. Flagellar motility contributes to cytokinesis in *Trypanosoma brucei* and is modulated by an evolutionarily conserved dynein regulatory system. *Eukaryot Cell,* 5**,** 696-711.

RAMEY, K., EKO, F. O., THOMPSON, W. E., ARMAH, H., IGIETSEME, J. U. & STILES, J. K. 2009. Immunolocalization and challenge studies using a

recombinant Vibrio cholerae ghost expressing *Trypanosoma brucei* Ca(2+) ATPase (TBCA2) antigen. *Am J Trop Med Hyg,* 81**,** 407-15.

RAWLINGS, N. D. 2010. Peptidase inhibitors in the MEROPS database. *Biochimie,* 92**,** 1463-83.

RAWLINGS, N. D., BARRETT, A. J. & BATEMAN, A. 2010. MEROPS: the peptidase database. *Nucleic Acids Res,* 38**,** D227-33.

RAWLINGS, N. D., TOLLE, D. P. & BARRETT, A. J. 2004. Evolutionary families of peptidase inhibitors. *Biochem J,* 378**,** 705-16.

REDDY, S. B., ANDERS, R. F., BEESON, J. G., FÄRNERT, A., KIRONDE, F., BERENZON, S. K., WAHLGREN, M., LINSE, S. & PERSSON, K. E. 2012. High affinity antibodies to *Plasmodium falciparum* merozoite antigens are associated with protection from malaria. *PLoS One,* 7**,** e32242.

RIBEIRO-GOMES, F. L., OTERO, A. C., GOMES, N. A., MONIZ-DE-SOUZA, M. C., CYSNE-FINKELSTEIN, L., ARNHOLDT, A. C., CALICH, V. L., COUTINHO, S. G., LOPES, M. F. & DOSREIS, G. A. 2004. Macrophage interactions with neutrophils regulate *Leishmania major* infection. *J Immunol,* 172**,** 4454-62.

RIGDEN, D. J., MONTEIRO, A. C. & GROSSI DE SÁ, M. F. 2001. The protease inhibitor chagasin of *Trypanosoma cruzi* adopts an immunoglobulin-type fold and may have arisen by horizontal gene transfer. *FEBS Lett,* 504**,** 41-4.

RIGDEN, D. J., MOSOLOV, V. V. & GALPERIN, M. Y. 2002. Sequence conservation in the chagasin family suggests a common trend in cysteine proteinase binding by unrelated protein inhibitors. *Protein Sci,* 11**,** 1971-7.

RODITI, I. & LEHANE, M. J. 2008. Interactions between trypanosomes and tsetse flies. *Curr Opin Microbiol,* 11**,** 345-51.

ROSENTHAL, P. J. 1999. Proteases of protozoan parasites. *Adv Parasitol,* 43**,** 105-59.

SAJID, M. & MCKERROW, J. H. 2002. Cysteine proteases of parasitic organisms. *Mol Biochem Parasitol,* 120**,** 1-21.

SALMON, D., DO AIDO-MACHADO, R., DIEHL, A., LEIDERT, M., SCHMETZER, O., DE A LIMA, A. P., SCHARFSTEIN, J., OSCHKINAT, H. & PIRES, J. R. 2006. Solution structure and backbone dynamics of the *Trypanosoma cruzi* cysteine protease inhibitor chagasin. *J Mol Biol,* 357**,** 1511-21.

SANDERSON, S. J., WESTROP, G. D., SCHARFSTEIN, J., MOTTRAM, J. C. & COOMBS, G. H. 2003. Functional conservation of a natural cysteine peptidase inhibitor in protozoan and bacterial pathogens. *FEBS Lett,* 542**,** 12-6.

SANTOS, C. C., COOMBS, G. H., LIMA, A. P. & MOTTRAM, J. C. 2007. Role of the *Trypanosoma brucei* natural cysteine peptidase inhibitor ICP in differentiation and virulence. *Mol Microbiol,* 66**,** 991-1002.

SANTOS, C. C., SANT'ANNA, C., TERRES, A., CUNHA-E-SILVA, N. L., SCHARFSTEIN, J. & DE A LIMA, A. P. 2005. Chagasin, the endogenous cysteine-protease inhibitor of *Trypanosoma cruzi*, modulates parasite differentiation and invasion of mammalian cells. *J Cell Sci,* 118**,** 901-15.

SCHLECKER, T., SCHMIDT, A., DIRDJAJA, N., VONCKEN, F., CLAYTON, C. & KRAUTH-SIEGEL, R. L. 2005. Substrate specificity, localization, and essential role of the glutathione peroxidase-type tryparedoxin peroxidases in *Trypanosoma brucei*. *J Biol Chem,* 280**,** 14385-94.

SCHMIDT, A. & KRAUTH-SIEGEL, R. L. 2002. Enzymes of the trypanothione metabolism as targets for antitrypanosomal drug development. *Curr Top Med Chem,* 2**,** 1239-59.

SCORY, S., CAFFREY, C. R., STIERHOF, Y. D., RUPPEL, A. & STEVERDING, D. 1999. *Trypanosoma brucei*: killing of bloodstream forms *in vitro* and *in vivo* by the cysteine proteinase inhibitor Z-phe-ala-CHN2. *Exp Parasitol,* 91**,** 327-33.

SHAPIRO, T. A. & ENGLUND, P. T. 1995. The structure and replication of kinetoplast DNA. *Annu Rev Microbiol,* 49**,** 117-43.

SHERWIN, T. & GULL, K. 1989. The cell division cycle of *Trypanosoma brucei brucei:* timing of event markers and cytoskeletal modulations. *Philos Trans R Soc Lond B Biol Sci,* 323**,** 573-88.

SILVA, M. S., PRAZERES, D. M., LANÇA, A., ATOUGUIA, J. & MONTEIRO, G. A. 2009. Trans-sialidase from *Trypanosoma brucei* as a potential target for DNA vaccine development against African trypanosomiasis. *Parasitol Res,* 105**,** 1223-9.

SILVERMAN, J. M., CHAN, S. K., ROBINSON, D. P., DWYER, D. M., NANDAN, D., FOSTER, L. J. & REINER, N. E. 2008. Proteomic analysis of the secretome of *Leishmania donovani*. *Genome Biol,* 9**,** R35.

SILVERMAN, J. M., CLOS, J., DE'OLIVEIRA, C. C., SHIRVANI, O., FANG, Y., WANG, C., FOSTER, L. J. & REINER, N. E. 2010a. An exosome-based secretion pathway is responsible for protein export from *Leishmania* and communication with macrophages. *J Cell Sci,* 123**,** 842-52.

SILVERMAN, J. M., CLOS, J., HORAKOVA, E., WANG, A. Y., WIESGIGL, M., KELLY, I., LYNN, M. A., MCMASTER, W. R., FOSTER, L. J., LEVINGS, M. K. & REINER, N. E. 2010b. *Leishmania* exosomes modulate innate and adaptive immune responses through effects on monocytes and dendritic cells. *J Immunol,* 185**,** 5011-22.

SILVERMAN, J. M. & REINER, N. E. 2011. Exosomes and other microvesicles in infection biology: organelles with unanticipated phenotypes. *Cell Microbiol,* 13**,** 1-9.

SIMARRO, P. P., DIARRA, A., RUIZ POSTIGO, J. A., FRANCO, J. R. & JANNIN, J. G. 2011. The human African trypanosomiasis control and surveillance programme of the World Health Organization 2000-2009: the way forward. *PLoS Negl Trop Dis,* 5**,** e1007.

STERNBERG, J. M. 2004. Human African trypanosomiasis: clinical presentation and immune response. *Parasite Immunol,* 26**,** 469-76.

STEVERDING, D. 2008. The history of African trypanosomiasis. *Parasit Vectors,* 1**,** 3.

STUART, K., BRUN, R., CROFT, S., FAIRLAMB, A., GÜRTLER, R. E., MCKERROW, J., REED, S. & TARLETON, R. 2008. Kinetoplastids: related protozoan pathogens, different diseases. *J Clin Invest,* 118**,** 1301-10.

STUART, K. D., SCHNAUFER, A., ERNST, N. L. & PANIGRAHI, A. K. 2005. Complex management: RNA editing in trypanosomes. *Trends Biochem Sci,* 30**,** 97-105.

TROEBERG, L., MORTY, R. E., PIKE, R. N., LONSDALE-ECCLES, J. D., PALMER, J. T., MCKERROW, J. H. & COETZER, T. H. 1999. Cysteine proteinase inhibitors kill cultured bloodstream forms of *Trypanosoma brucei brucei. Exp Parasitol,* 91**,** 349-55.

TROEBERG, L., PIKE, R. N., MORTY, R. E., BERRY, R. K., COETZER, T. H. & LONSDALE-ECCLES, J. D. 1996. Proteases from *Trypanosoma brucei brucei.* Purification, characterisation and interactions with host regulatory molecules. *Eur J Biochem,* 238**,** 728-36.

TSUJIMURA, Y., WATARAI, S., UEMURA, A., OHNISHI, Y. & KODAMA, H. 2005. Effect of anti-ganglioside antibody in experimental *Trypanosoma brucei* infection in mice. *Res Vet Sci,* 78**,** 245-7.

UEMURA, A., WATARAI, S., OHNISHI, Y. & KODAMA, H. 2005. Protective effect of antiganglioside antibodies against experimental *Trypanosoma brucei* infection in mice. *J Parasitol,* 91**,** 73-8.

ULMER, J. S., LINDQUIST, R. N., DENNIS, M. S. & LAZARUS, R. A. 1995. Ecotin is a potent inhibitor of the contact system proteases factor XIIa and plasma kallikrein. *FEBS Lett,* 365**,** 159-63.

URBAN, C. F., REICHARD, U., BRINKMANN, V. & ZYCHLINSKY, A. 2006. Neutrophil extracellular traps capture and kill *Candida albicans* yeast and hyphal forms. *Cell Microbiol,* 8**,** 668-76.

VAN DEN ABBEELE, J., CLAES, Y., VAN BOCKSTAELE, D., LE RAY, D. & COOSEMANS, M. 1999. *Trypanosoma brucei spp*. development in the tsetse fly: characterization of the post-mesocyclic stages in the foregut and proboscis. *Parasitology,* 118 (Pt 5)**,** 469-78.

VASSELLA, E., REUNER, B., YUTZY, B. & BOSHART, M. 1997. Differentiation of African trypanosomes is controlled by a density sensing mechanism which signals cell cycle arrest via the cAMP pathway. *J Cell Sci,* 110 (Pt 21)**,** 2661-71.

VAUGHAN, S. 2010. Assembly of the flagellum and its role in cell morphogenesis in *Trypanosoma brucei*. *Curr Opin Microbiol,* 13**,** 453-8.

VERLINDE, C. L., HANNAERT, V., BLONSKI, C., WILLSON, M., PÉRIÉ, J. J., FOTHERGILL-GILMORE, L. A., OPPERDOES, F. R., GELB, M. H., HOL, W. G. & MICHELS, P. A. 2001. Glycolysis as a target for the design of new anti-trypanosome drugs. *Drug Resist Updat,* 4**,** 50-65.

VICKERMAN, K. 1978. Antigenic variation in trypanosomes. *Nature,* 273**,** 613-7.

VICKERMAN, K. 1985. Developmental cycles and biology of pathogenic trypanosomes. *Br Med Bull,* 41**,** 105-14.

WALKER, P. J. 1961. Organization of Function in Trypanosome Flagella. *Nature,* 189**,** 1017-1018.

WEBB, H., CARNALL, N., VANHAMME, L., ROLIN, S., VAN DEN ABBEELE, J., WELBURN, S., PAYS, E. & CARRINGTON, M. 1997. The GPI-phospholipase C of *Trypanosoma brucei* is nonessential but influences parasitemia in mice. *J Cell Biol,* 139**,** 103-14.

WEI, J., GU, Y., YANG, J., YANG, Y., WANG, S., CUI, S. & ZHU, X. 2011. Identification and characterization of protective epitope of *Trichinella spiralis* paramyosin. *Vaccine,* 29**,** 3162-8.

WELBURN, S. C. & ODIIT, M. 2002. Recent developments in human African trypanosomiasis. *Curr Opin Infect Dis,* 15**,** 477-84.

WELBURN, S. C., PICOZZI, K., FÈVRE, E. M., COLEMAN, P. G., ODIIT, M., CARRINGTON, M. & MAUDLIN, I. 2001. Identification of human-infective trypanosomes in animal reservoir of sleeping sickness in Uganda by means of serum-resistance-associated (SRA) gene. *Lancet,* 358**,** 2017-9.

WOODWARD, R. & GULL, K. 1990. Timing of nuclear and kinetoplast DNA replication and early morphological events in the cell cycle of *Trypanosoma brucei*. *J Cell Sci,* 95 (Pt 1)**,** 49-57.

XU, J., ZHU, X. J., LI, Y. H., DAI, Y., ZHU, Y. C., ZHENG, J., FENG, Z. Q. & GUAN, X. H. 2011. Expression, characterization and therapeutic efficacy of chimeric Fab of anti-idiotypic antibody NP30 against *Schistosoma japonicum*. *Acta Trop,* 118**,** 159-64.

YANG, S. Q., WANG, C. I., GILLMOR, S. A., FLETTERICK, R. J. & CRAIK, C. S. 1998. Ecotin: a serine protease inhibitor with two distinct and interacting binding sites. *J Mol Biol*, 279**,** 945-57.

YOKOYAMA, K., TROBRIDGE, P., BUCKNER, F. S., SCHOLTEN, J., STUART, K. D., VAN VOORHIS, W. C. & GELB, M. H. 1998. The effects of protein farnesyltransferase inhibitors on trypanosomatids: inhibition of protein farnesylation and cell growth. *Mol Biochem Parasitol*, 94**,** 87-97.

ZANIN, F. H., COELHO, E. A., TAVARES, C. A., MARQUES-DA-SILVA, E. A., SILVA COSTA, M. M., REZENDE, S. A., GAZZINELLI, R. T. & FERNANDES, A. P. 2007. Evaluation of immune responses and protection induced by A2 and nucleoside hydrolase (NH) DNA vaccines against *Leishmania chagasi* and *Leishmania amazonensis* experimental infections. *Microbes Infect*, 9**,** 1070-7.

ZHANG, R., YOSHIDA, A., KUMAGAI, T., KAWAGUCHI, H., MARUYAMA, H., SUZUKI, T., ITOH, M., EL-MALKY, M. & OHTA, N. 2001. Vaccination with calpain induces a Th1-biased protective immune response against *Schistosoma japonicum*. *Infect Immun*, 69**,** 386-91.

ZIEGELBAUER, K., QUINTEN, M., SCHWARZ, H., PEARSON, T. W. & OVERATH, P. 1990. Synchronous differentiation of *Trypanosoma brucei* from bloodstream to procyclic forms *in vitro*. *Eur J Biochem*, 192**,** 373-8.